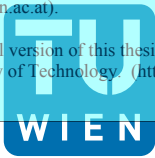


Die approbierte Originalversion dieser Dissertation ist an der Hauptbibliothek der Technischen Universität Wien aufgestellt und zugänglich (<http://www.ub.tuwien.ac.at>).

The approved original version of this thesis is available at the main library of the Vienna University of Technology (<http://www.ub.tuwien.ac.at>).



TECHNISCHE  
UNIVERSITÄT  
WIEN

Vienna University of Technology



universität  
wien

## DISSERTATION

# **The flow field around a flying blowfly: Characteristics and guidance of spider prey capture behavior**

ausgeführt zum Zwecke der Erlangung des akademischen Grades eines  
Doktors der technischen Wissenschaften unter der Leitung von

Univ.-Prof. Dipl.-Phys. Dr.rer.nat. H. C. Kuhlmann

E322 - Institut für Strömungsmechanik und Wärmeübertragung, TU Wien

o.Univ.-Prof. Dr.rer.nat. F. G. Barth

Department für Neurobiologie, Universität Wien

eingereicht an der Technischen Universität Wien  
bei der Fakultät für Maschinenwesen und Betriebswissenschaften

von

Dipl.-Ing. (FH) Christian Klopsch

Matrikelnummer: 0626934

Geschwandnergasse 42/7, 1170 Wien

Wien, im Februar 2010

## KURZFASSUNG

Die Wanderspinne *Cupiennius salei*, ein Lauerjäger überwiegend beheimatet in Zentralamerika, fängt fliegende Beute direkt aus der Luft durch einen gezielten Beutefangsprung. Offensichtlich ist die Spinne dabei in der Lage, die Beute dabei zu detektieren, zu erkennen, zu lokalisieren und sie mit einem räumlich und zeitlich präzisen Sprung zu fangen.

Verhaltensversuche, bei denen optische und vibratorische Reizungen ausgeschlossen wurden, zeigen, dass cuticulare Fadenhaare (Trichobothrien), welche sowohl Luftströmungen als auch Luftschall detektieren, der einzige Sinneskanal sind, der für einen Beutefangsprung nötig ist (mit Ausnahme der propriorezeptiven Rückkoppelung für die korrekte Durchführung des komplexen motorischen Programms, das dem Sprung zugrunde liegt). Gemäß vorher bestimmten Schwellenwerten (Barth and Höller 1999) ist die Schallschnelle, erzeugt durch eine fliegende Schmeißfliege, jedoch nicht stark genug, um die Trichobothrien überschwellig zu reizen. Sowohl die Schwellenwerte für die Winkelauslenkung ( $0,2^\circ$ ) als auch die Winkelgeschwindigkeit ( $250^\circ \text{ s}^{-1}$ ) können durch die tatsächliche Trichobothriumschwingung, ausgelöst durch den Luftschall einer Fliege, nicht erreicht werden (nur 6 % bzw. 8 % der Schwellenwerte).

Die Digitale Particle Image Velocimetry (DPIV) Analyse wurde angewandt, um die von einer frei fliegenden Schmeißfliege erzeugten Luftströmungsgeschwindigkeiten mit hoher zeitlicher und räumlicher Auflösung in der Nähe der Strömungssensoren von *Cupiennius salei* zu untersuchen. Die Strömung weist ein charakteristisches Intensitätsmuster und einen aus 3 Phasen bestehenden zeitlichen Verlauf (i-iii) auf.

(i) Die Schmeißfliege induziert bei Annäherung ein exponentiell ansteigendes Strömungssignal (maximale Strömungsgeschwindigkeit:  $0,164 \text{ m s}^{-1} \pm 0,051 \text{ m s}^{-1}$ ) an den Sensoren der Spinne mit verhältnismäßig geringer Fluktuation von  $0.013 \text{ m s}^{-1} \pm 0.006 \text{ m s}^{-1}$  (Phase I). Die Spinne **detektiert** diese Strömung, wenn die Fliege noch  $38.4 \text{ mm} \pm 5.6 \text{ mm}$  entfernt ist. Die Schwankung der Luftströmung während der Phase I nimmt zwischen  $0.004 \text{ m s}^{-1}$  to  $0.037 \text{ m s}^{-1}$  linear mit der **Flughöhe** der Fliege zu. Unterschiede in der Ankunftszeit und Intensität des Fliegensignals an den verschiedenen Beinen informieren die Spinne voraussichtlich über die **Richtung**, aus der die Fliege sich nähert. (ii) Zu dem Zeitpunkt, zu dem sich die Fliege direkt über dem Sensor befindet, geht das Luftströmungssignal schlagartig von Phase I in die deutlich mehr fluktuierende Phase II über (Fluktuationen:  $0.114 \text{ m s}^{-1} \pm 0.050 \text{ m s}^{-1}$ ). Die Phase II ist charakterisiert durch die Nachlaufströmung der Fliege. Die Strömung der Phase II signalisiert der Spinne, dass die Fliege sich innerhalb ihrer Reichweite befindet und **löst den Sprung aus**. Anhand der Hinweise, die in der Luftströmung enthalten sind, müsste die Spinne theoretisch in der Lage sein, die **Position** der Fliege und den

richtigen Zeitpunkt für ihren Absprung zu bestimmen. Die **horizontale Geschwindigkeit** der nahenden Fliege wird sowohl durch die Ankunftszeitunterschiede des Signals (erstrecken sich von 0.038 s bis 0.108 s) an den verschiedenen Beinen als auch durch die Steilheit des exponentiellen Geschwindigkeitsanstiegs in Phase I (Exponentenkoeffizient:  $16\text{-}79\text{ s}^{-1}$ ) ausgedrückt. (iii) Die Luftströmungsgeschwindigkeit klingt wieder ab, wenn die Fliege die Spinne passiert hat (Phase III).

Verhaltensversuche, in denen verschiedene Komponenten und Eigenschaften der Luftströmung der Fliege artifiziell erzeugt und gezielt als Reiz benutzt wurden, zeigen, dass Phase I verantwortlich für die Detektion, Lokalisation und möglicherweise für die Erkennung der Fliege ist, wohingegen der Beginn von Phase II den Beutefangsprung auslöst.

## ABSTRACT

The wandering spider *Cupiennius salei*, a sit-and-wait predator mainly living in Central America, catches flying prey directly out of the air by precisely jumping towards it. Obviously the spider is able to detect, recognize and localize the prey and to catch it with a spatial and temporal precise jump.

Behavioral experiments that exclude optical and vibrational stimulation show that the only sensory channel needed for the predatory jump (except proprioceptive feedback for the proper execution of the complex motor program underlying the jump) are cuticular filiform hairs (trichobothria) detecting air flow and airborne sound. According to previously determined thresholds (Barth and Höller 1999), however, the sound particle velocity generated by a blowfly (*Calliphora erythrocephala*) in flight is not strong enough to excite the trichobothria. Both the angular deflection and angular velocity thresholds of  $0.2^\circ$  and  $250^\circ \text{ s}^{-1}$ , respectively, are not reached (only 8 % and 6 % of these values) by the actual movement of the trichobothria due to airborne sound.

Digital particle image velocimetry (DPIV) analysis was applied to investigate with high temporal and spatial resolution the air flow velocities generated by a freely flying blowfly close to the flow sensors of *Cupiennius salei*. The flow shows a characteristic intensity pattern and time course composed of three phases (i-iii).

(i) When approaching, the blowfly induces an exponentially increasing airflow signal (maximum flow velocity:  $0.164 \text{ m s}^{-1} \pm 0.051 \text{ m s}^{-1}$ ) with comparatively little fluctuation of  $0.013 \text{ m s}^{-1} \pm 0.006 \text{ m s}^{-1}$  (phase I). The spider **detects** this flow while the fly is still  $38.4 \text{ mm} \pm 5.6 \text{ mm}$  away. The fluctuation of the phase I airflow above the sensors of the spider increases linearly from  $0.004 \text{ m s}^{-1}$  to  $0.037 \text{ m s}^{-1}$  with the fly's **altitude**. Differences in the time of arrival of the fly signal and intensity differences at its different legs likely inform the spider about the **direction** to the prey. (ii) Phase I of the airflow is abruptly followed by the much more fluctuating phase II (fluctuations:  $0.114 \text{ m s}^{-1} \pm 0.050 \text{ m s}^{-1}$ ) which starts when the fly is directly above the sensor. It corresponds to the wake below and behind the fly. Phase II flow indicates to the spider that its prey is now within reach and actually **triggers the jump**. In theory then the spider should be able to derive information on the fly's **position** and the proper timing of its jump from the clues contained in the airflow. The **horizontal velocity** of the approaching fly is reflected by the time of arrival differences (ranging from 0.038 s to 0.108 s) of the signal at different legs and also by the steepness of the exponential increase of velocity in phase I (exponential coefficient:  $16\text{-}79 \text{ s}^{-1}$ ). (iii) The air flow velocity decays again when the fly has passed the spider (phase III).

Behavioral experiments in which different components and characteristic features of the air flow of the fly were artificially generated and selectively used as stimuli demonstrate



that phase I is responsible for the detection, localisation and possibly for the recognition of the fly whereas the start of phase II elicits the prey capture jump.

## DANKSAGUNGEN

Ich möchte mich zunächst bei Herrn Prof. Dr. Friedrich G. Barth für die Bereitstellung des Themas, die Betreuung sowie die dreijährige Finanzierung der Arbeit und für die Ermöglichung der Teilnahme an diversen Tagungen sehr herzlich bedanken. Des Weiteren bedanke ich mich für die ständige Diskussionsbereitschaft und die mehrmalige Korrektur der hier vorliegenden Dissertation.

Ebenso gilt mein Dank Herrn Prof. Dr. Hendrik C. Kuhlmann für die Betreuung der Arbeit von Seiten der TU sowie für die ständige Diskussionsbereitschaft und Einladungen zu diversen Tagungen. Darüber hinaus möchte ich mich für das herzliche Klima in seiner Gruppe bedanken sodass ich mich, trotz der räumlichen Trennung, stets willkommen fühlte.

Beim Sekretariat der Neurobiologie (Frau Maria Wieser und Frau Margit Kainerstorfer) bedanke ich mich für die stete Hilfsbereitschaft bei jeglichen organisatorischen Fragen.

Ich danke Herrn Walter Witek für die Unterstützung in mechanischen und Herrn Ing. Andreas Szpetkowski für die Unterstützung in elektronischen Fragen beim Auf- und Umbau der Versuchsstände.

Bei allen weiteren Mitgliedern des Departments Neurobiologie bedanke ich mich für das einmalige Arbeitsklima und die immerwährende Gesprächsbereitschaft. Allen voran möchte ich Mag. Clemens Schaber für seine stetige Hilfsbereitschaft in allerlei biologischen Fragen danken, die mir unter anderem zu einem schnellen Einstieg in das interdisziplinäre Thema verhalfen.

Mein besonderer Dank gilt Thomas Hoinkes für die großartige Unterstützung bei der Durchführung der Sound- und Vibrationsmessungen sowie der Verhaltensversuche.

Ganz besonders danke ich meinen Eltern, Ernst und Ursula Klopsch, die mir eine wunderschöne Kindheit sowie eine akademische Ausbildung ermöglichten. Ganz besonders danke ich meinen Eltern für die komplette Finanzierung der Dissertation im 4. Jahr. Bei meiner Mutter möchte ich mich zusätzlich für die Unterstützung bei der grafischen Bearbeitung der Videobilder der Verhaltensversuche bedanken.

Nicht zuletzt gilt mein ganz besonderer Dank meiner Freundin Charlotte Schelander für die immense und ausdauernde Unterstützung sowie ihre Nachsicht mit jeglicher körperlicher und geistiger Abwesenheit ihres Partners während dieser Zeit. Du bist der wichtigste Mensch in meinem Leben!

Ich widme diese Arbeit meinem Großvater Franz Ansorg, der es leider nicht mehr miterleben konnte dass sein Enkelsohn in seine beruflichen Fußstapfen tritt.

# TABLE OF CONTENTS

<b>I. Introduction .....</b>	<b>1</b>
<b>II. Materials and methods.....</b>	<b>4</b>
<b>1. Experimental animals .....</b>	<b>4</b>
1.1 Spider ( <i>Cupiennius salei</i> ).....	4
1.2 Blowfly ( <i>Calliphora erythrocephala</i> ).....	5
<b>2. Airborne sound .....</b>	<b>5</b>
2.1 Sound pressure .....	6
2.2 Laser-Doppler-vibrometry (LDV) .....	7
<b>3. Digital particle image velocimetry (DPIV).....</b>	<b>7</b>
3.1 Tethered flying blowfly: stationary and experimentally moved.....	9
3.1.1 Flow around stationary blowfly.....	11
3.1.2 Flow around <i>Cupiennius</i> .....	12
3.2 Freely flying blowfly .....	13
<b>4. Synthetic fly-like air flow .....</b>	<b>15</b>
4.1 Complete flow signal .....	15
4.2 On the significance of phase I.....	18
<b>5. Behavioral experiments.....</b>	<b>19</b>
<b>6. Statistical tests.....</b>	<b>21</b>
<b>III. Results .....</b>	<b>22</b>
<b>1. Prey capture behavior induced by flying prey: reaction to an         experimentally moved humming blowfly .....</b>	<b>22</b>
<b>2. On the multimodality of natural stimuli .....</b>	<b>25</b>
2.1 Visual stimulus.....	25
2.2 Substrate vibration .....	25

2.3 Airborne sound.....	29
2.3.1 Sound pressure.....	29
2.3.2 Movement of trichobothrium due to sound .....	31
2.4 Air flow .....	34
<b>3. Flow field around the blowfly and above the spider .....</b>	<b>34</b>
3.1 Stationary tethered blowfly.....	34
3.1.1 Flow field around stationarily flying blowfly .....	35
3.1.2 Flow field around <i>Cupiennius</i> .....	37
3.2 Tethered flying blowfly moved forward.....	40
3.3 Freely flying blowfly .....	42
3.3.1 Flow field around freely flying fly .....	42
3.3.2 Flow signal generated by fly above spider legs.....	43
<b>4. Prey capture behavior induced by synthetic air flows .....</b>	<b>52</b>
4.1 Complete signal .....	52
4.2 On the significance of phase I.....	55
4.3 Control experiment .....	59
<b>IV. Discussion.....</b>	<b>61</b>
<b>1. Influence of the substrate on the capture of flying prey .....</b>	<b>61</b>
<b>2. Influence of the number of repeated identical sessions on the spider's willingness to jump.....</b>	<b>62</b>
<b>3. Differences between the sound pressure fields around <i>Calliphora erythrocephala</i> and <i>Lucilia sericata</i> .....</b>	<b>62</b>
<b>4. Differences between the flow fields generated by a stationary tethered, a manually moved and a freely flying blowfly .....</b>	<b>63</b>
<b>5. Detection of the blowfly.....</b>	<b>65</b>
5.1 Detection of a stationary humming blowfly .....	65
5.2 Detection of a freely flying blowfly.....	66
<b>6. Recognition of the blowfly .....</b>	<b>67</b>

---

<b>7. Localization of the flying blowfly .....</b>	<b>70</b>
7.1 Position .....	70
7.1.1 Horizontal distance .....	70
7.1.2 Direction .....	71
7.1.3 Altitude .....	73
7.2 Horizontal fly velocity .....	73
<b>8. Prey capture: Triggering the jump .....</b>	<b>74</b>
<b>References .....</b>	<b>76</b>

# I. INTRODUCTION

Arthropods such as crustaceans, insects and arachnids possess a wide range of specialized sensory organs by means of which they perceive and interact with their environments. These include sensors sensitive to light, odor, touch, substrate vibration and air or water medium displacement. In spiders, the sensors responding to air flow are used to detect and localize prey and predators. Individual sensilla usually form arrays. These have evolved under natural selection pressures over millions of years to perform adequately. As a consequence, they often display extreme sensitivity and selectivity with regard to the behaviorally relevant signals they detect (Barth 2002).

Here we report on experimental work with the airflow-sensing filiform hairs, or trichobothria, of spiders, in particular those of the wandering spider *Cupiennius salei*. Fig. 1 shows such hair sensilla on the metatarsal segment of a spider leg. Each of the spider's eight legs has about 100 filiform hairs; in addition there are ca. 50 trichobothria on each of the two pedipalps. The total of 900 hairs is arranged in specific clusters or arrays (Fig. 1). Different clusters contain between 2 and 24 hairs which range in diameter from 10  $\mu\text{m}$  at the base to 2  $\mu\text{m}$  at the tip and are from 100 to 1400  $\mu\text{m}$  long, depending on their location on the leg (Barth et al. 1993). Earlier work (Barth et al. 1993) showed that the range of hair lengths in a cluster works to extend the effective frequency range as compared to that of an individual hair. According to theoretical studies (Humphrey et al. 1993, 1998, 2003, review: Humphrey and Barth 2008) and experiments using controlled laboratory flows (Barth et al. 1993, 1995; Barth and Höller 1999) the trichobothria of *Cupiennius* respond to extremely low velocity oscillations (p-p amplitudes as small as 0.15  $\text{mm s}^{-1}$ ) and are mechanically tuned to stimulus frequencies between about 40 Hz and 600 Hz. Using natural stimuli like the air flow generated by a flying insect, prey capture behavior is elicited in the spider (Barth et al. 1995, Brittinger 1998). The flow in the wake of a fly is highly three dimensional, unsteady and vortical and, as a result, it is very rich in its spectral content (Barth and Höller 1999).

The wandering spider *Cupiennius salei* is able to catch flying insect prey like flies by jumping into the air towards them. This behavior is a remarkable achievement which relies on the detection, recognition and localization of an airborne moving object and the jump towards it. After the ablation of the trichobothria it cannot be elicited anymore (Brittinger 1998). The main questions of this investigation are:

*Which cues potentially contained in the airflow eliciting its behavioral reaction does *Cupiennius salei* use to **detect**, **recognize** and **localize** flying prey and how is the **jump** towards it **triggered**? Do other additional sensory modalities play a role and which are the properties of the stimulus patterns they respond to?*

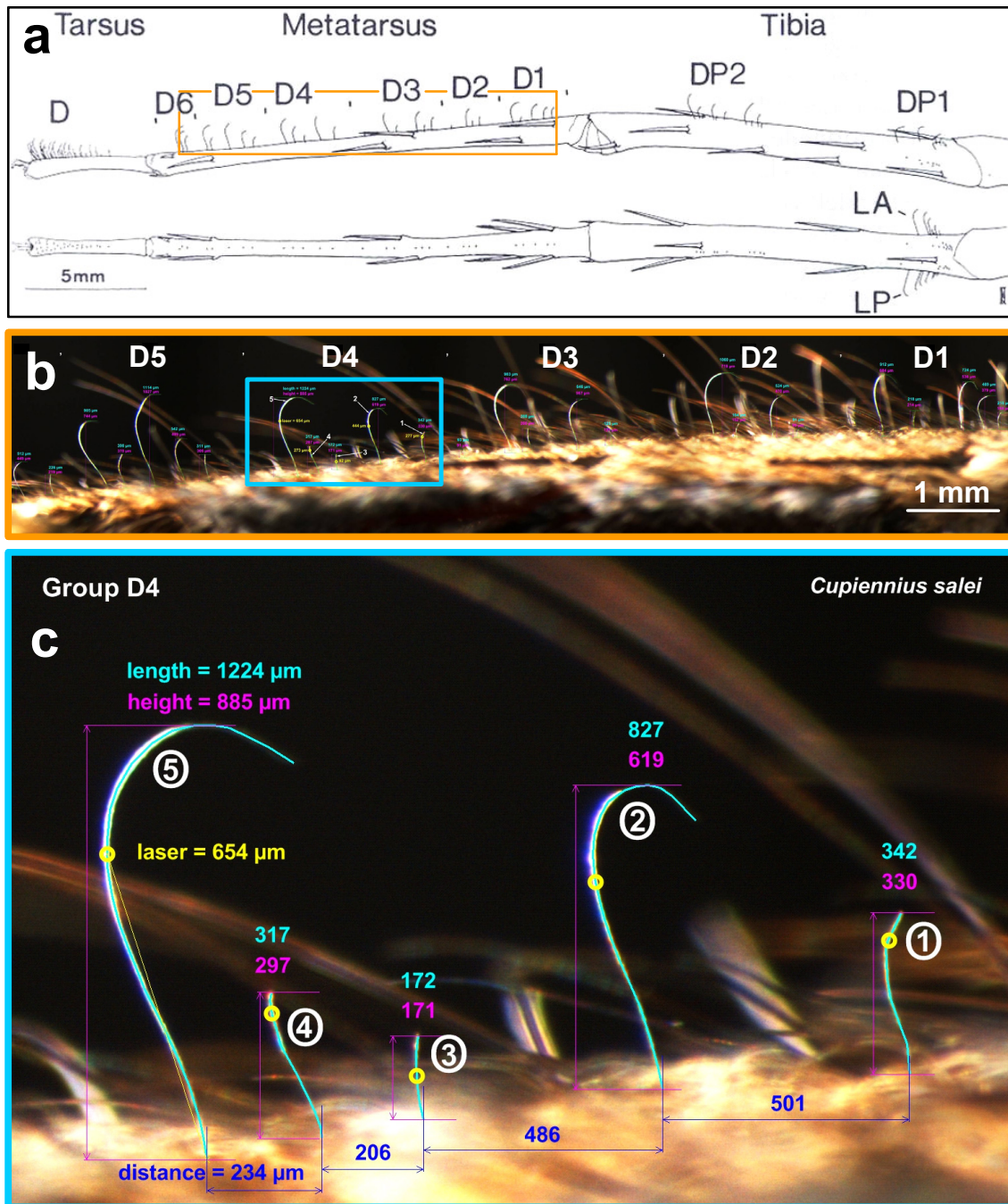


**Fig. 1** Wind sensitive filiform hairs (trichobothria) of the wandering spider *Cupiennius salei*. **a** Side and top view of the first three segments of the leg where the trichobothria are found (adapted from Barth et al. 1993). The labels identify groups of hairs. **b** Metatarsus of the leg of *Cupiennius*. **c** Enlargement of b takes group D4 as an example to show the length and height of each hair and the distances between the hairs.

Accordingly, the present study addresses three issues. (i) Behavioral experiments were performed to evaluate the potential relevance of different sensory modalities. (ii) Using digital particle image velocimetry (DPIV) the air flow patterns generated by a fly were analyzed and shown to guide the spider to its prey. (iii) Finally, artificial flow patterns

imitating characteristic features of the natural flows were selectively applied to see which flow parameters are indeed used by the spider to guide its behavior.

In contrast to the huge amount of the existing literature on the flight kinematics and the air flow around the flapping wings which produces aerodynamic forces (e.g. Vogel 1966, 1967a and b; Brodsky 1994; Ellington et al. 1996; Dickinson et al. 1999; Nachtigall 2003; Sane 2003; Birch et al. 2004; Lehmann et al. 2005; Bomphrey et al. 2005) the present work describes the entire flow field around the flying blowfly. Its focus is on the flows near the spider when the fly passes by and signals its presence by stimulating the airflow sensors.



## II. MATERIALS AND METHODS

### 1. Experimental animals

#### 1.1 Spider (*Cupiennius salei*)

All spiders used in this work were *Cupiennius salei* bred in our department in Vienna. Only female juvenile and subadult spiders were used. At this age the females in particular show more reliable willingness to hunt (Brittinger 1998).

For the DPIV measurements small subadult females (leg span between 7 cm and 8 cm) were selected to ensure that they completely fit into the image section of the DPIV-camera. The animals were sacrificed and prepared onto a polystyrene plate in hunting position using insect pins (Barth 2002). Therefore their body was lifted by ca. 0.5 cm above the ground and the legs placed symmetrically around and slightly pulled towards the body. After drying the spider for about 1 week the needles were removed and the spider remained in the desired position.

For behavioral experiments five females were used. At the time of the experiments they were between 5 and 12 months of age (juvenile and subadult).

The following endogenous and exogenous factors affect the responsiveness and therefore must be considered for the behavioral experiments (Rehner 1978; Hergenröder 1982; Brittinger 1998; Ungersböck 2004).

#### Endogenous factors

- *Cupiennius* is night active. To accomplish the experiments during daytime the day and night activity rhythm of the animals was reversed with the light on from 9 pm to 9 am and off from 9 am to 9 pm. After 48 hours the animals were adjusted to the new day and night rhythm (Seyfarth 1980).
- Prey capture is only expected for hungry animals (Melchers 1967). Following Brittinger (1998) and Ungersböck (2004) the spiders were fed twice every week with only one fly after the experiment to keep their reactivity high.
- Spiders close to a molt were not used because of their inactivity (Melchers 1963).

### Exogenous factors

- The spiders were kept separately in glass jars (capacity 3 liters) with peat on the floor. To provide sufficient humidity (ca. 85 %) the peat was kept wet and a bowl of water was placed on the floor. The temperature was kept between 22 °C and 24 °C.
- During the behavioral experiments vibrations and airflows were avoided as much as possible in order to keep *Cupiennius* alert and motivated to react to prey generated stimuli.
- To record the behavioral experiments with a video camera a weak light source emitting red light with a wavelength larger than 585 nm was used. The spider's relative sensitivity to this wavelength is reduced to less than 20 % compared to the spectral peaks of the green and blue cells (Walla et al. 1996). For the experiments the spider's eyes were in addition covered with a mixture of wax, colophony and carbon to render them unfunctional. With their eyes covered the spiders were much calmer than before and appeared more concentrated on the hunt.

### 1.2 Blowfly (*Calliphora erythrocephala*)

For experiments using the natural stimulus the common blowfly (*Calliphora erythrocephala*) served as a source of airflow. The larvae were bought from a commercial dealer and kept in our department till the flies hatched from the pupae. After eclosure they were kept in a cubical cage ( $40 \times 40 \times 60 \text{ cm}^3$ ) and fed with water and sugar.

In experiments with tethered flies a strap of paper (Fig. 2) gave the fly enough freedom to move its thorax naturally. Direct attachment of the fly to the rod would affect thorax constriction and the flapping motion. The long axis of the tethered fly formed an angle of c.  $20^\circ$  with the horizontal. This angle was also measured in a fly flying freely and horizontally (see also section II.3.2).



**Fig. 2** *Calliphora* mounted with a strap of paper to the fly support (see chapter II.3.1). The paper was waxed to the tergum of the fly using a mixture of bees wax and colophony.

## 2. Airborne sound

The airborne sound emitted by a humming blowfly was measured in two ways. First the sound pressure was directly recorded with a probe microphone (Brüel & Kjaer Type 4182) and second the motions of the trichobothria due to the sound were measured with

a laser-Doppler vibrometer (LDV) (Polytec PDV-100). In both cases a tethered blowfly took various defined positions with regard to the probe (that is the spider or the microphone) so that the sound field around the fly could be determined.

In addition to being stationary the humming fly should also be moved over the spider in a next step. In general, the emitted sound of a moving object differs from that of stationary object regarding its frequency which is shifted, depending on the velocity of the moving object, to higher (approaching object) or lower (departing object) values due to the Doppler effect. As the maximum velocity of a blowfly is about  $1.2 \text{ m s}^{-1}$  (Schilstra and van Hateren 1999) the maximum frequency shift using a moving instead of a stationary tethered fly would be 0.35 %. As the frequency variations between individual flies were up to 35 % (see chapter III.2.3), and therefore 100 times larger than the maximum frequency variation caused by moving the fly, we assume the sound measurements of the fixed fly also valid for the moved fly.

## 2.1 Sound pressure

The acoustic measurements were performed with a Brüel & Kjaer Probe Microphone Type 4182 connected to a Brüel & Kjaer measuring amplifier (Type 2610). The analog signal was digitalized with a Cambridge Electronic Design Limited (CED) A/D board (Type 1401) and transferred to a Pentium 4 PC. With the software Spike2 (Version 6.10) by CED the acoustic data was recorded with a temporal resolution of 20 kHz and afterwards analyzed (fast Fourier transform and sonogram). Both the fast Fourier transform (FFT) and the sonogram were calculated by using a Hanning window of 4096 points (= 0.2 s). This frame length led to a frequency resolution of 4.88 Hz. The grey scale of the sonogram ranged from 0 dB (white) to 96 dB (darkest grey).

For the determination of sound pressure field around a blowfly the microphone was positioned in the vertical symmetry plane (x-z) and in two horizontal planes (x-y) 10 mm and 50 mm below the fly's thorax (Fig. 25 and Fig. 26). The vertical plane was measured using a 5 by 5 grid with the z-positions at 0 mm, 10 mm, 30 mm, 50 mm and 70 mm and the x-positions at 0 mm, 25 mm, 50 mm, 75 mm and 100 mm (see Fig. 25a and Fig. 26a). The measurement point in the origin of the coordinate system ( $x = 0$ ,  $y = 0$ ,  $z = 0$ , Fig. 25 and Fig. 26) was excluded because the fly was located at this position. The horizontal planes each contain 25 grid points forming a 5 by 5 grid ranging with the step size of 25 mm from  $x = 0 \text{ mm}$  to  $x = 100 \text{ mm}$  and from  $y = -50 \text{ mm}$  to  $y = +50 \text{ mm}$ .

The pressure field of the harmonics of the wing beat frequency around the fly was calculated in dB SPL (re  $20 \mu\text{Pa}$ ). To this end the bin of the spectrum containing the frequency peak and in addition both bins on each side were taken for the evaluation as the

harmonics spread over more than one bin width. This procedure was performed in accordance to the manual of CED (2004).

## 2.2 Laser-Doppler-vibrometry (LDV)

A laser-Doppler vibrometer (Polytec PDV-100) was used to measure the angular deflection and the angular velocity of trichobothria upon exposure to the airborne sound generated by a flying blowfly. A living spider was mounted on a support in hunting position and immobilized to ensure that only the motion of the trichobothria was measured (Fig. 3). The trichobothria on the spider's tarsus are the focus of our investigations because of their importance. On one hand they are the most numerous group with the highest density of hairs and on the other hand they are the ones receiving the signal of an approaching fly first due to their most peripheral location.

The analog signal was also digitalized with the CED Type 1401 A/D board and both the angular deflection and angular velocity analyzed in the same way as described for the sound pressure measurement (see chapter II.2.1).

Additionally, the LDV was used to document the presence or absence of vertical and lateral vibrations of the bromeliad leaf and to check for vertical vibrations in the metal plate during the behavioral experiments (see chapter II.5).

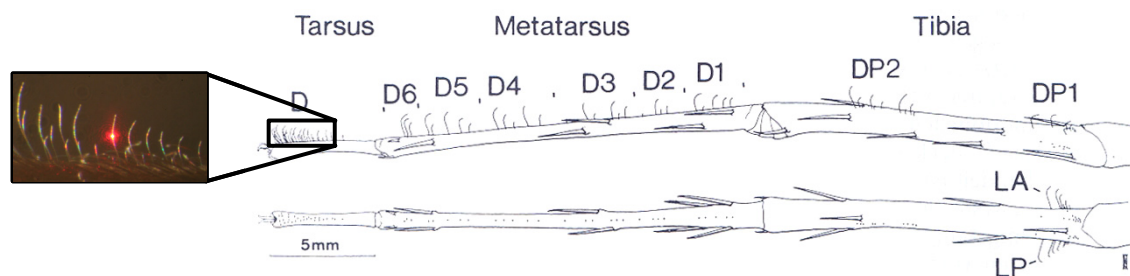


**Fig. 3** All trichobothria on a leg of an adult *Cupiennius*. Trichobothria on the tarsus are enlarged and the investigated trichobothrium is highlighted by the red dot of the LDV (adapted from Barth et al 1993).

## 3. Digital particle image velocimetry (DPIV)

A DPIV system (Dantec Dynamics A/S, Skovlunde, Denmark) was used to measure the air flow velocity vectors. The system consisted of two Nd:YAG lasers (3 W/532 nm wavelength, Mercury series, New Wave Research Inc., Fremont, USA) coupled to a dual laser unit. The laser optics (80 × 60 series, Dantec Dynamics A/S) generated a pulsed light sheet of 2 mm waist thickness at its focal point. The repetition rate of laser pulses was up to 100 kHz. A digital high-speed camera (iNanoSense MkIII revision 3E,

Integrated Design Tools Inc., Tallahassee, USA) with a CMOS chip allowed a temporal resolution of up to 1000 pictures per second (single frame) at its highest spatial resolution of  $1280 \times 1024$  pixels. It featured a special light intensifier allowing high quality measurements with reduced laser power so as not to damage the animals. The camera was equipped with an internal flash memory of 4096 MB allowing to save up to 3272 pictures at highest resolution during one measurement. A Nikon AF Nikkor 85 mm f/1.8D lens was used with a 12 mm spacer ring (Soligor GmbH, Leinfelden-Echterdingen, Germany). The laser and the camera were synchronized with the a Timing Hub (X-Stream series, Integrated Design Tools Inc.) which was connected via USB to a Dell Precision PWS670 PC (Intel Xeon 3.6 GHz, 3 GB of RAM). Data acquisition and post processing were performed using the current version (from 1.30 to 2.21) of the DynamicStudio software (Dantec Dynamics A/S). The pictures were acquired in single frame mode i.e. the time between the pictures was kept constant allowing to correlate picture 1 and 2, 2 and 3 and so on. Adaptive Correlation (Cross Correlation with Moving Average Validation and Interrogation Area Offset) was used to calculate the two dimensional velocity vector plots. Each velocity vector is composed of a horizontal ( $U_x$ ) and a vertical ( $U_y$ ) component and its length, defined as  $U = \sqrt{U_x^2 + U_y^2}$ , is referred to as velocity magnitude. The interrogation area size varies from  $32 \times 32$  pixels to  $64 \times 64$  pixels with 50 % overlap depending on the experiment. The size and the overlap of the interrogation areas was chosen to render uncertainties due to out-of-plane particle displacement negligible. The origin of the DPIV (x-y/  $U_x$ - $U_y$ ) system of coordinates is at the bottom, left-hand corner of the image.

When the fly had started to fly and generated airflow above a threshold level of  $8.1 \text{ cm s}^{-1}$ , the DPIV system was triggered using a Constant Temperature Anemometer (CTA) (Multichannel CTA 54N81, Dantec Dynamics A/S) with a one-dimensional fiber film probe (55R01 series, Dantec Dynamics A/S). The trigger delay was 0.001 s. The system offered the option to save pictures prior to reaching threshold. The ratio of the total number of pictures saved before and after the offset of the trigger could be variably determined.

Seed particles (nominal diameter  $2 \mu\text{m}$ ) were produced by means of a fog generator (Flow Tracker 700 CE, Dantec Dynamics A/S) using a special fog fluid (Inside Fog Fluid Super, Safex-Chemie GmbH, Schenefeld, Germany). The particles did not affect the performance of the CTA.

The error regarding the movement of the inert seeding particles with the air flow increases with its raising frequency content (Dring 1982). The maximum frequency contained in the air motion caused by a tethered flying fly is less than 600 Hz (Barth and Höller 1999). At the worst case (600 Hz) the velocity magnitude of a  $2 \mu\text{m}$  seed particle is at least 99.9 % of that of the air motion it tracks, and its phase lag with respect to the

air is  $0.09^\circ$ , approximately (Dring 1982). Additionally the maximal error regarding exponential acceleration is 1 % (Dring 1982). Therefore, possible errors due to the seeding agent not tracking the air flow are negligible.

By saving pre trigger images at the beginning of each measurement the degree of disturbance of the flow was checked. A sample is shown in Fig. 4. In case of any unwanted disturbance the acquisition was rejected.

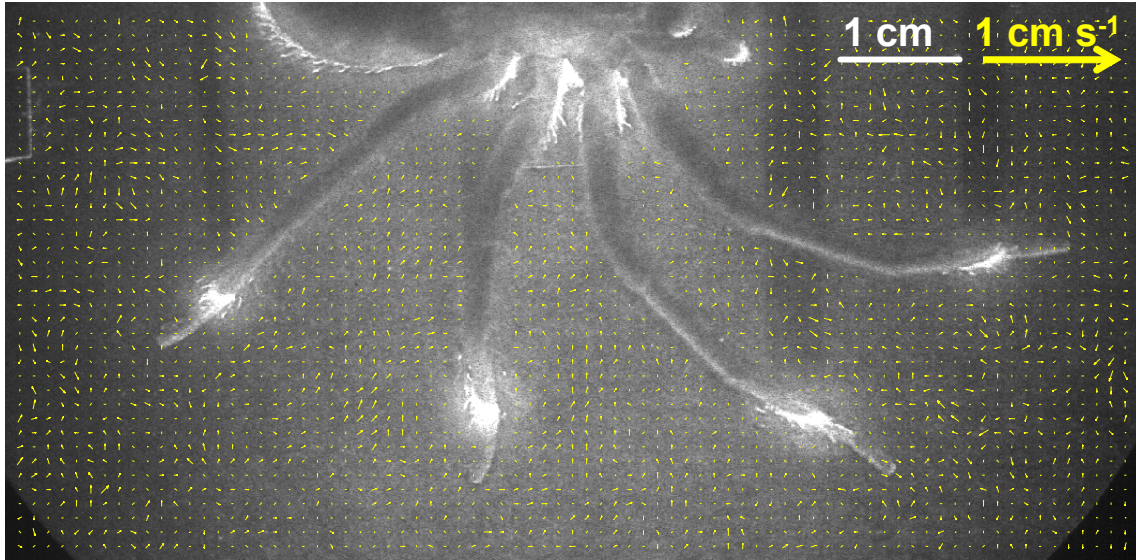


**Fig. 4** Typical flow field around spider prior to the actual experiment visualized in order to exclude any disturbances from outside during the data acquisition. In the given case the mean flow velocity was  $0.204 \text{ mm s}^{-1}$  and the maximum velocity was  $0.812 \text{ mm s}^{-1}$ . These values were typical for all flow fields prior to the actual measurement done in this work.

### 3.1 Tethered flying blowfly: stationary and experimentally moved

The fly-spider system was kept in a Perspex box ( $55 \times 30 \times 30 \text{ cm}^3$ ) (Fig. 5) to shield the flow generated by the fly from external perturbations and to keep the DPIV seeding agent confined to the measurement volume. The seed particles were introduced through a closeable opening in the box (see Fig. 5). To damp possible backflow from the walls which were orientated perpendicular to the main flow direction rubber foam was used to cover those walls (Fig. 5).

The spider, prepared as described in chapter II.1.1, was placed in the center of a flat rectangular Perspex substrate ( $15 \times 30 \text{ cm}^2$ ). The origin of the three dimensional (x, y, z) coordinate system was defined to be in the center of the Perspex substrate with the x-axis pointing towards the spider's anterior, the y-axis normal to the x-axis in the same plane, and the z-axis vertically upwards (Fig. 5).

The blowfly was prepared as shown in chapter II.1.2. The paper strip was then clamped to the fly support (Fig. 5) which consisted of two rotatable units, the holder itself and a small plate used to provide contact for the legs of the fly. The fly started flying when this plate is rotated away and thus the tarsal contact of the fly removed (tarsal reflex). The fly support itself was moveable mounted (in x-direction) to the Perspex box (see Fig. 5) and arrested at the desired positions (see Fig. 6).

The hot-wire of the trigger device was attached to the support and arranged 2 cm behind and 0.5 cm above the fly in order not to influence the flow of interest behind and below the fly.

When the blowfly was experimentally moved the setup shown in Fig. 5 was used as well but the fly support was not fastened to the Perspex box. Instead it remained loose and could be moved in x-direction at various velocities. In a first step the support was pulled by a thread attached to it by hand in a pilot experiment to check whether the natural flow field around the fly was significantly influenced by the pulling.



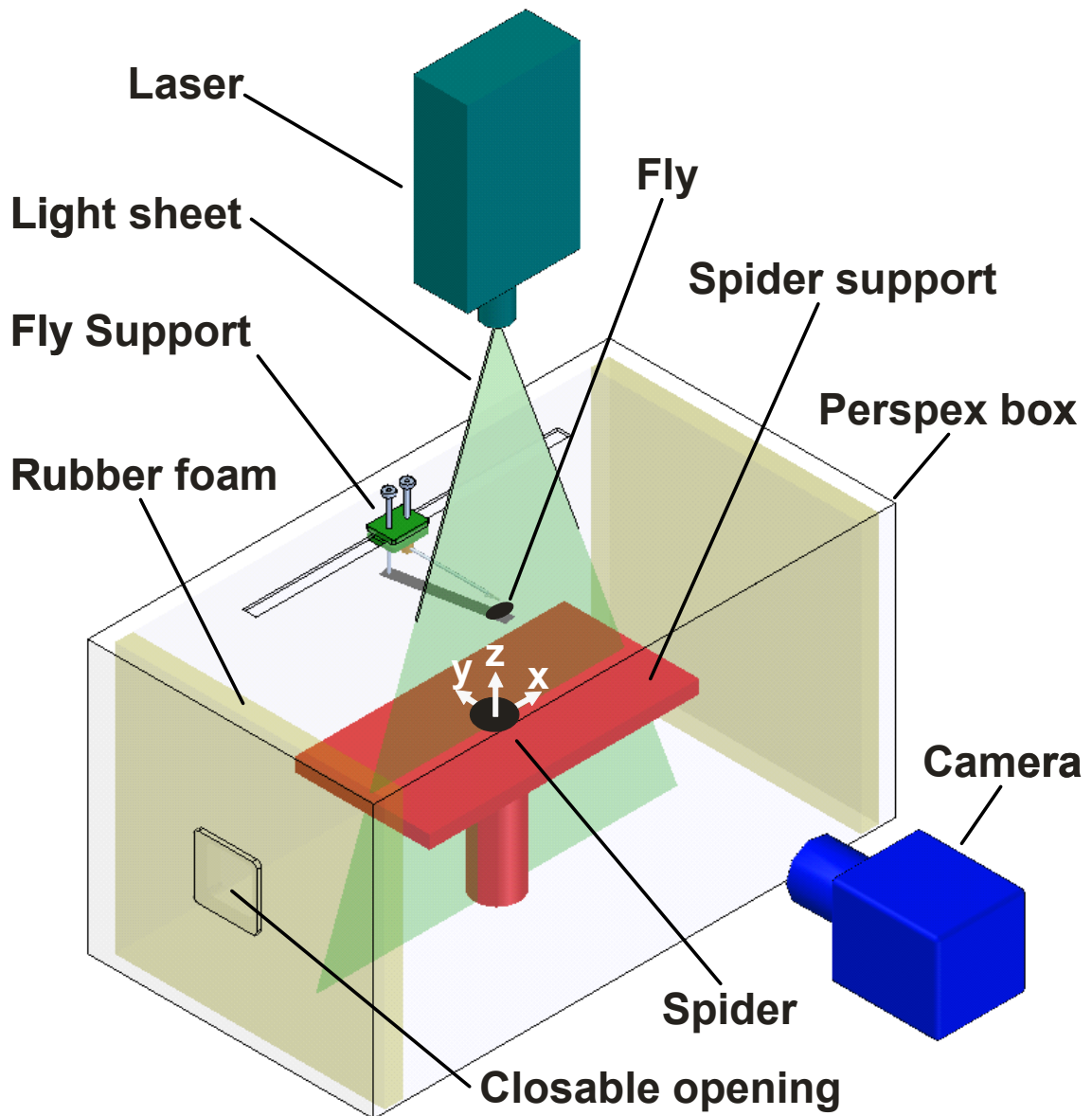


**Fig. 5** Test section showing the location of the spider on a horizontal Perspex substrate. The tethered blowfly was mounted onto a support that could be moved relative to the spider. The camera and the laser of the DPIV system were arranged as shown for the evaluation of a vertical measurement plane. For analyzing the horizontal components of the flow the positions of the laser and the camera were switched (Camera above and laser on the side of the Perspex box). The long hole in the box served to place the fly support in various x-positions (stationary) as well as a guide to move the fly at various horizontal velocities above the spider.

### 3.1.1 Flow around stationary blowfly

The fly was kept at one fixed position ( $x = 0$  cm,  $y = 0$  cm,  $z = 5$  cm) 5 cm above the Perspex plate (spider support) without a spider on it. Experiments were performed with the laser plane orientated vertically or horizontally. With the vertical setting the measurement plane lay in the symmetry plane of the fly (x-z-plane) as indicated in Fig. 5. When the light sheet was orientated horizontally (x-y-plane) the camera was located



above and the laser on the side of the Perspex box. The horizontal light sheet was positioned 5 mm below the attachment point of the wings to the fly's body.

The full image size of  $1280 \times 1024$  pixels was used for an image section of  $7.8 \times 6.2 \text{ cm}^2$  (vertical sheet) and  $4.9 \times 3.9 \text{ cm}^2$  (horizontal plane). Single frames were recorded at 1000 Hz with an interrogation area of  $32 \times 32$  pixels with 50 % overlap. These settings covered the entire velocity range from some  $\text{mm s}^{-1}$  to  $1 \text{ m s}^{-1}$ . 100 pre-trigger images were recorded. 150 individual velocity fields were taken for the analysis of the mean vector map.

### 3.1.2 Flow around *Cupiennius*

To analyze the flow generated by a tethered flying blowfly the camera was arranged above the Perspex box and focused on the horizontal light sheet at the level of the spider's legs (Fig. 6). Specifically the fly was located in the x-z-plane 10 cm above the substrate on which the spider sat ( $z = 10$ ). Measurements were taken at five different x-positions (Fig. 6). The laser sheet was positioned as shown in Fig. 6 to make the analysis of the air flow responsible for the deflection of the trichobothria on the tarsi of each leg possible. These are likely to be particularly important sensors for the capture of flying prey for two reasons. On the one hand those trichobothria receive the signal from the approaching fly first and on the other hand they form the largest group with the highest density of neighboring sensors.

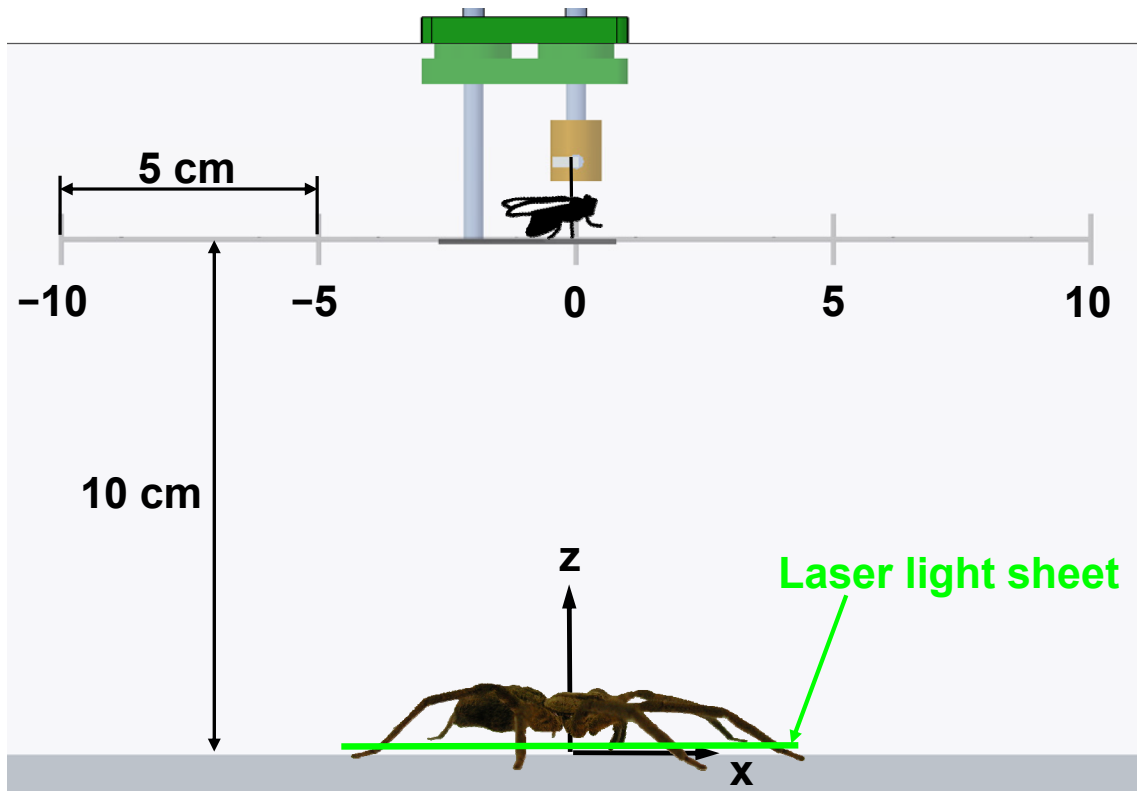


**Fig. 6** Measurement of airflow above spider legs with the fly at position ( $x = 0$  cm,  $y = 0$  cm,  $z = 10$  cm). Other fly positions at  $x = -10$  cm,  $-5$  cm,  $+5$  cm,  $+10$  cm are indicated by grey scale. The horizontal laser sheet (green line) of 2 mm waist thickness was aligned with its vertical position being such that it just “touched” the upper side of the tarsi (around 2 mm above the substrate).

The DPIV image size was  $1280 \times 630$  pixels and large enough to photograph the flow around the right half of the spider ( $9.8 \times 4.8$  cm<sup>2</sup>, Fig. 4). At positions  $x = -10$  cm and  $-5$  cm single frames were recorded at a rate of 25 Hz whereas the frame rate at the other positions was 100 Hz taking into account the higher velocities occurring when the fly was at these positions. Ten images were saved prior to the trigger set off by the hot-wire anemometer. Best results in calculating the vector maps from correlations between the single frames were achieved with an interrogation area of  $32 \times 32$  pixels with 50 % overlap.

### 3.2 Freely flying blowfly

To analyze the flow field around a freely flying blowfly a fly was released inside the Perspex box. The hot-wire trigger was positioned on one end of the spider support (Fig. 7) and 1 cm above it at position ( $-15$  cm,  $0$  cm,  $1$  cm). This site was chosen after pre-experiments with the hot-wire in different positions and at variable velocity thresholds to achieve both of the following goals. To exclude disturbances of the flow field generated by the freely flying blowfly the hot-wire must be positioned far enough away from the measurement area but still close enough to only to trigger the start of a DPIV meas-

urement when the fly is flying close to the image section of the camera. In these pre-experiments backflow reflected from the wall was observed so that the setup had to be changed to that shown in Fig. 7. The tube openings were positioned so that they came to lie in a plane above that of the top of the Perspex box to keep the seeding particles inside. Single frames were recorded with a temporal resolution of 1000 Hz. With a spatial resolution of  $1280 \times 1024$  pixels an image size of  $7.7 \times 6.2 \text{ cm}^2$  could be analyzed. The interrogation area was enlarged to  $64 \times 64$  pixels with 50 % overlap. This was necessary to compensate for variable seeding densities as the start of the measurement could not be timed by the experimenter.

In addition experiments done in the previous setup (Fig. 5) were repeated using the new configuration (Fig. 7) to judge the potential influence of the sidewalls on the former measurements. The results from both setups were qualitatively and quantitatively identical.

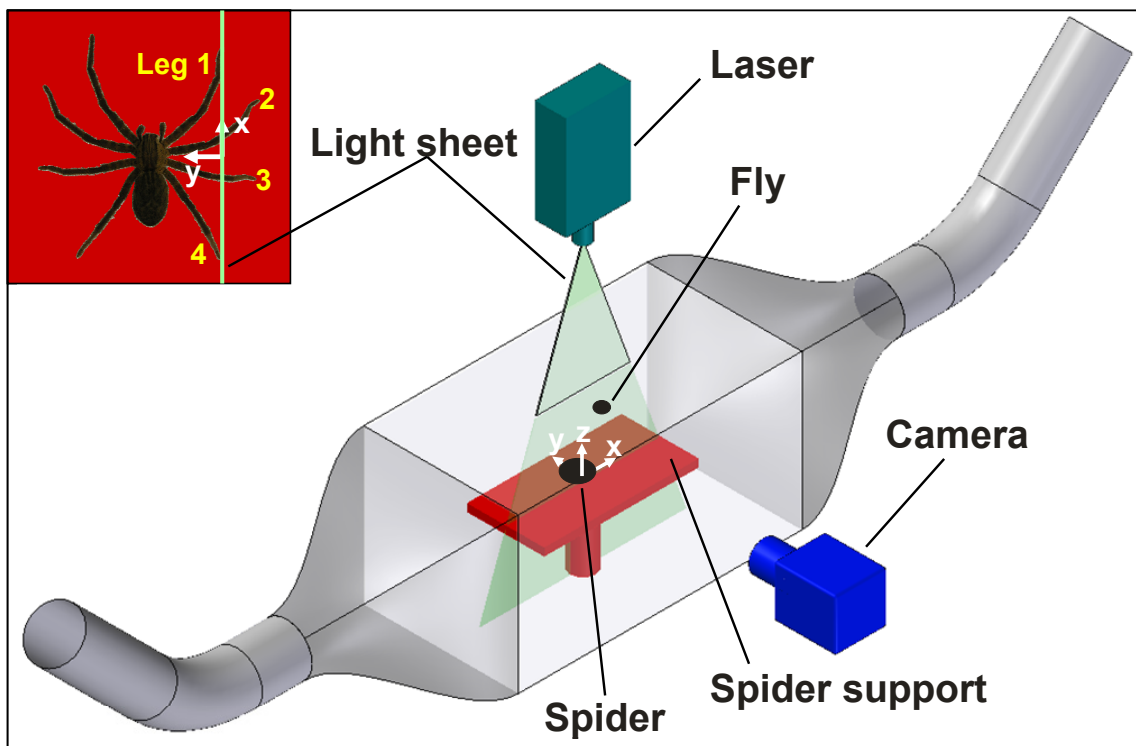


**Fig. 7** Setup used to measure the airflow generated by a fly flying freely inside the Perspex box. Due to backflow from the sidewalls these were replaced by open tubes. The laser generated a vertical light sheet cutting all four legs on the right side of the spider (see inset at top left and Fig. 36). Leg 1 and 4 were cut at the tarsus and leg 2 and 3 at the tibia.

## 4. Synthetic fly-like air flow

### 4.1 Complete flow signal

To reproduce the flow velocity signal generated by a freely flying blowfly close to the spider's trichobothria a particular mechanical device was developed (Fig. 8). From the approaching blowfly, which induces a circulating flow field around itself, the spider first receives a mostly horizontal velocity signal with its vectors pointing in flight direction and increasing exponentially with time (phase I, Fig. 36, Fig. 37a). A cylinder, rotating at 66 revolutions per minute, produced a rotational flow field (Fig. 9) inducing a horizontal flow around the spider (Fig. 10). In the original fly signal phase I is followed by the much more fluctuating phase II caused by the fly's wake pointing backwards and downwards (Fig. 36, Fig. 37a). A fender above the rotating cylinder served to collect the flow from the cylinder's upper side and to tunnel it downwards from the rear of the cylinder to generate a synthetic vertical wake (Fig. 11). When the cylinder was moved horizontally at fly-like velocities, the horizontal vectors of phase I increased exponentially and the wake's angle decreased from  $90^\circ$  to around  $45^\circ$  (Fig. 12). The resulting synthetic flow field was similar to that generated by a freely flying blowfly as seen in Fig. 36.

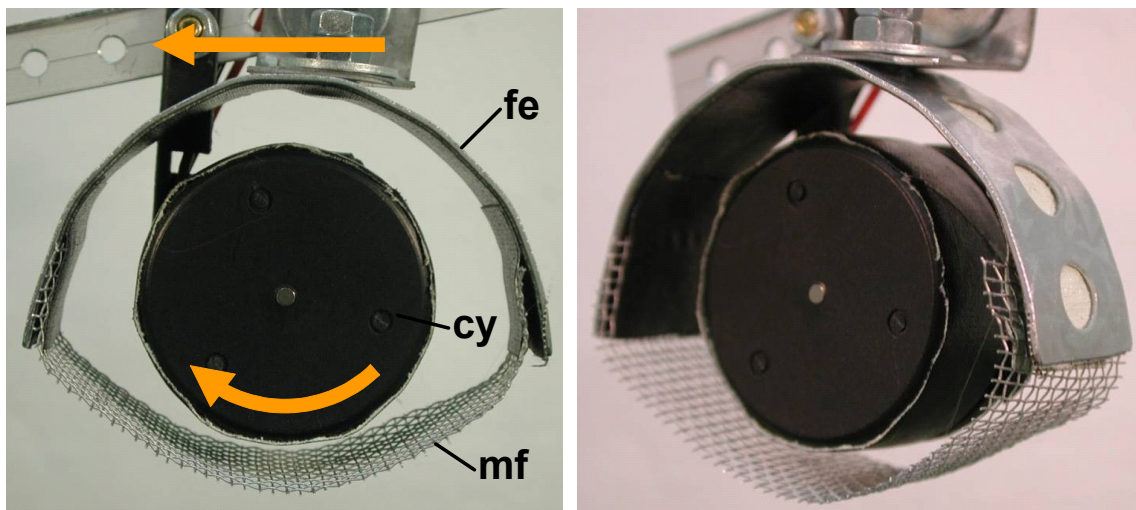


**Fig. 8** Device developed to artificially generate the flow field measured around a fly: A rotating cylinder (cy) with a fender (fe) covering the top  $180^\circ$  of the cylinder. A close meshed fence (mf) fixed to the edges of the fender covered the bottom of the cylinder to avoid that the spider jumping onto the cylinder gets caught between the rotating cylinder and fender.



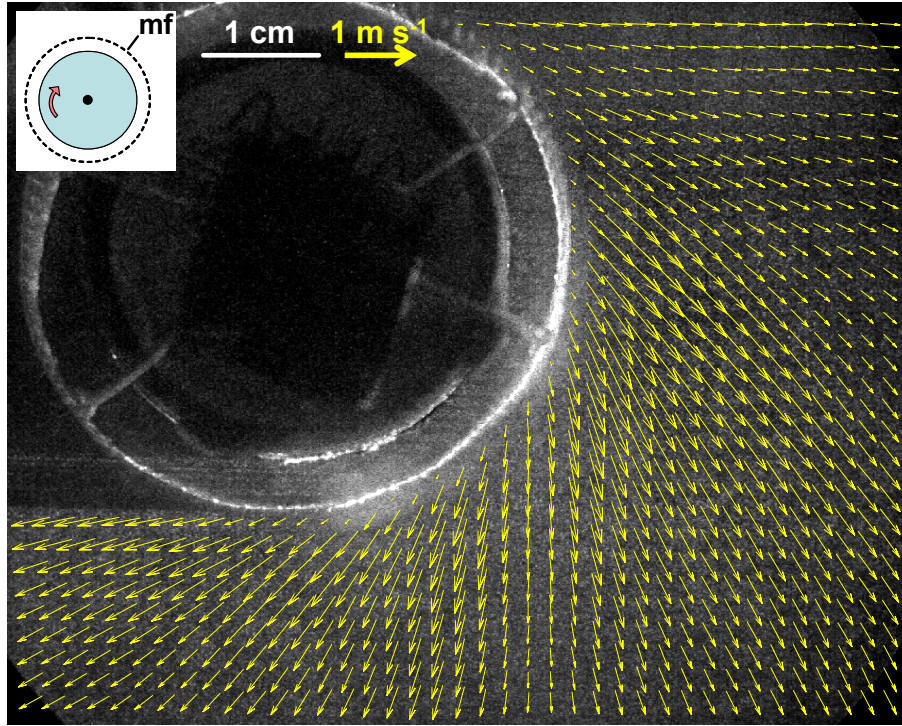


**Fig. 9** DPIV vector map of the flow field generated by clockwise rotating cylinder without fender. A meshed fence (mf) was placed 360° around the cylinder to protect the spider.

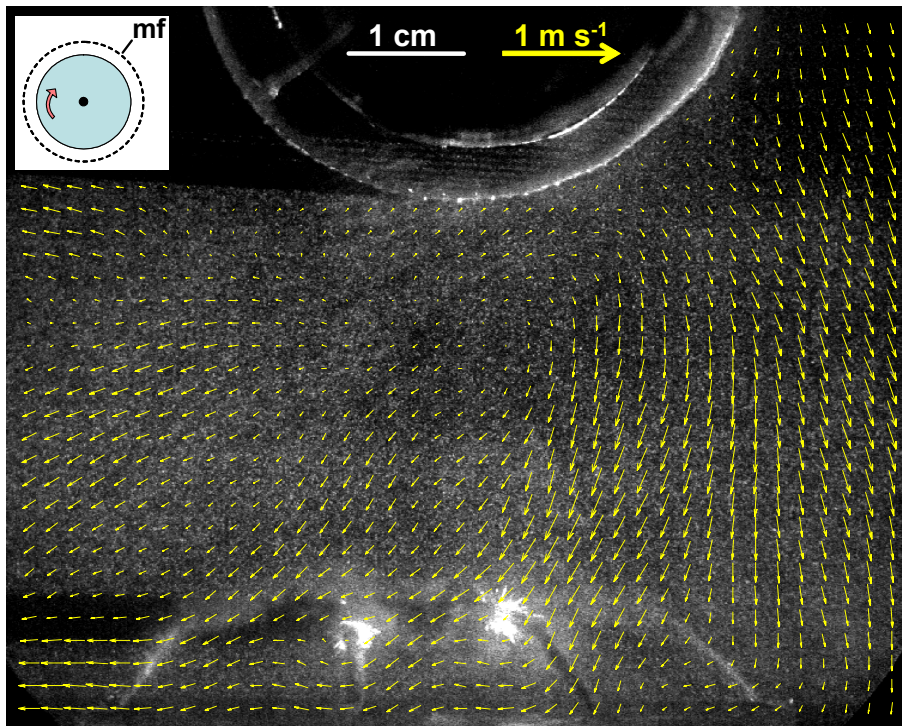


**Fig. 10** Clockwise rotating cylinder from Fig. 9 placed above the spider support with spider on it. With the presence of the horizontal Perspex plate the rotational flow field of the rotating cylinder forms a horizontal flow above the surface around the spider. *mf* meshed fence.



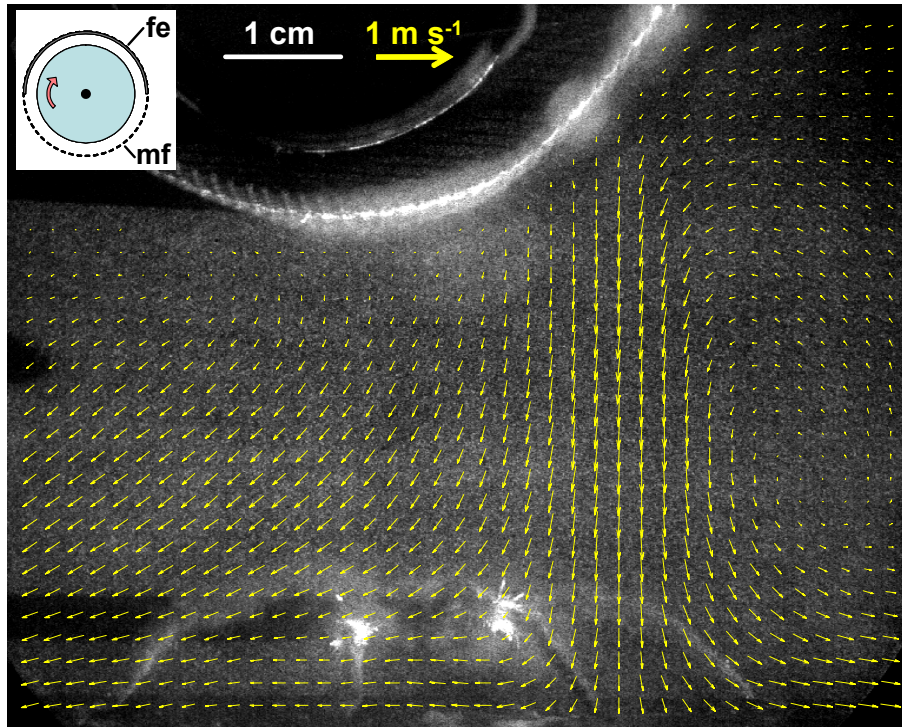


**Fig. 11** A fender (fe) around the upper half of the clockwise rotating cylinder collects the air flow from above and generates a wake pointing downwards. The horizontal flow below the cylinder (due to the rotational flow field of the cylinder itself) is still present around the spider.

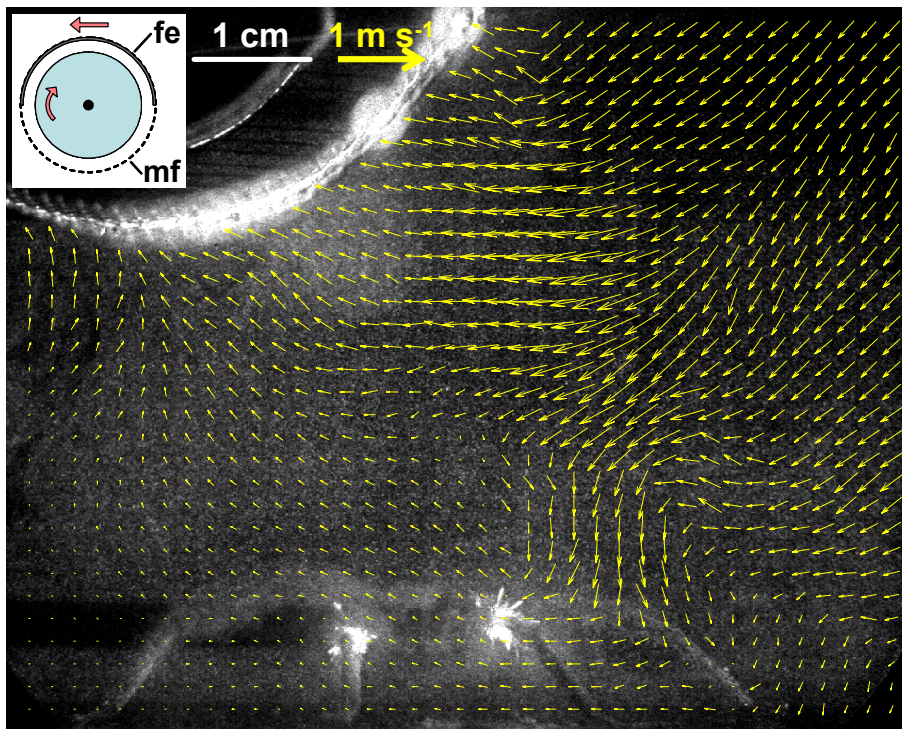


**Fig. 12** The flow field generated by the cylinder (rotating clockwise) in combination with the fender (Fig. 8 and Fig. 11) and moving from right to left. The flow field is similar to that generated by a freely flying blowfly (Fig. 36).

## 4.2 On the significance of phase I

Results described in chapter III.1 and III.3.3.2 suggested that the spider uses the flow signal of phase I to detect, recognize and localize the flying prey whereas the fluctuating phase II triggers the prey capture jump. To decide on this hypothesis we investigated the reaction of the spider towards a stimulus simulating only phase I of the fly signal. Therefore the fluctuations of phase II were eliminated by mounting a deflector to the rear of the cylinder which funnels the wake away from the cylinder, leaving only phase I of the fly signal for the spider (Fig. 13 and Fig. 14).

The same setup as for the freely flying blowfly (Fig. 7) was used for the DPIV measurements to adjust the synthetic airflows to the actual fly flow by empirical selection of the speeds of rotation of the cylinder and the velocity of the horizontal movement of the device.

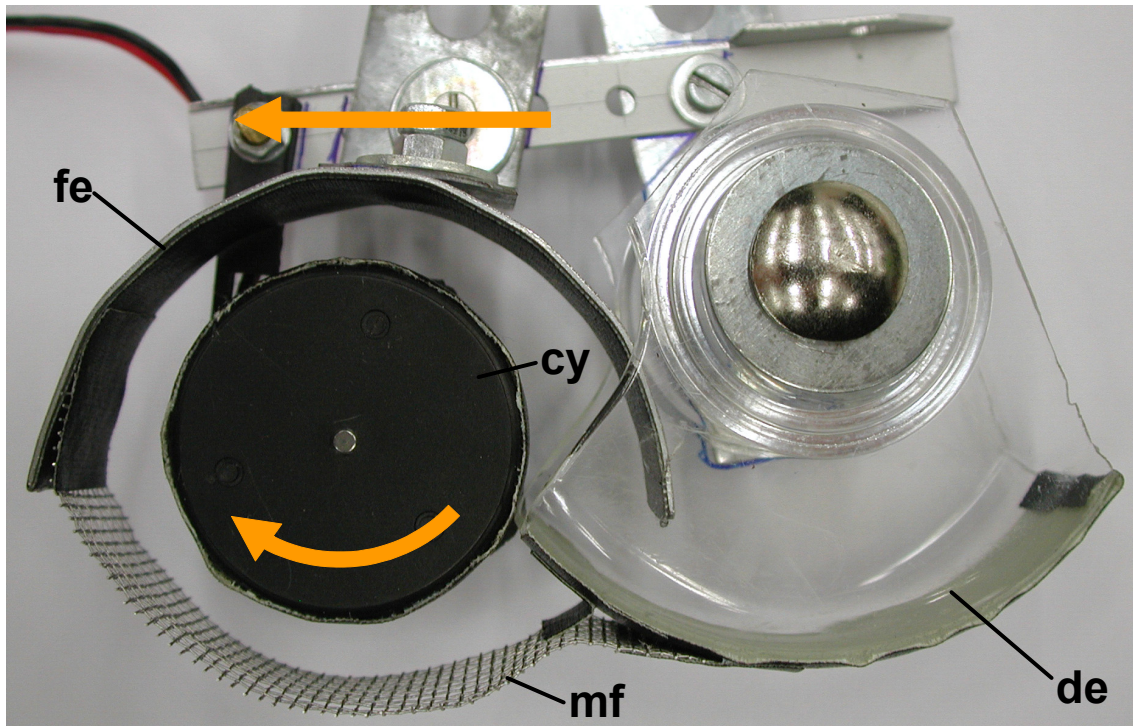


**Fig. 13** Combination of rotating cylinder (cy), fender (fe) and meshed fence (mf) as shown in Fig. 8 with additional deflector (de) to exclude the fluctuating phase II from the flow signal.



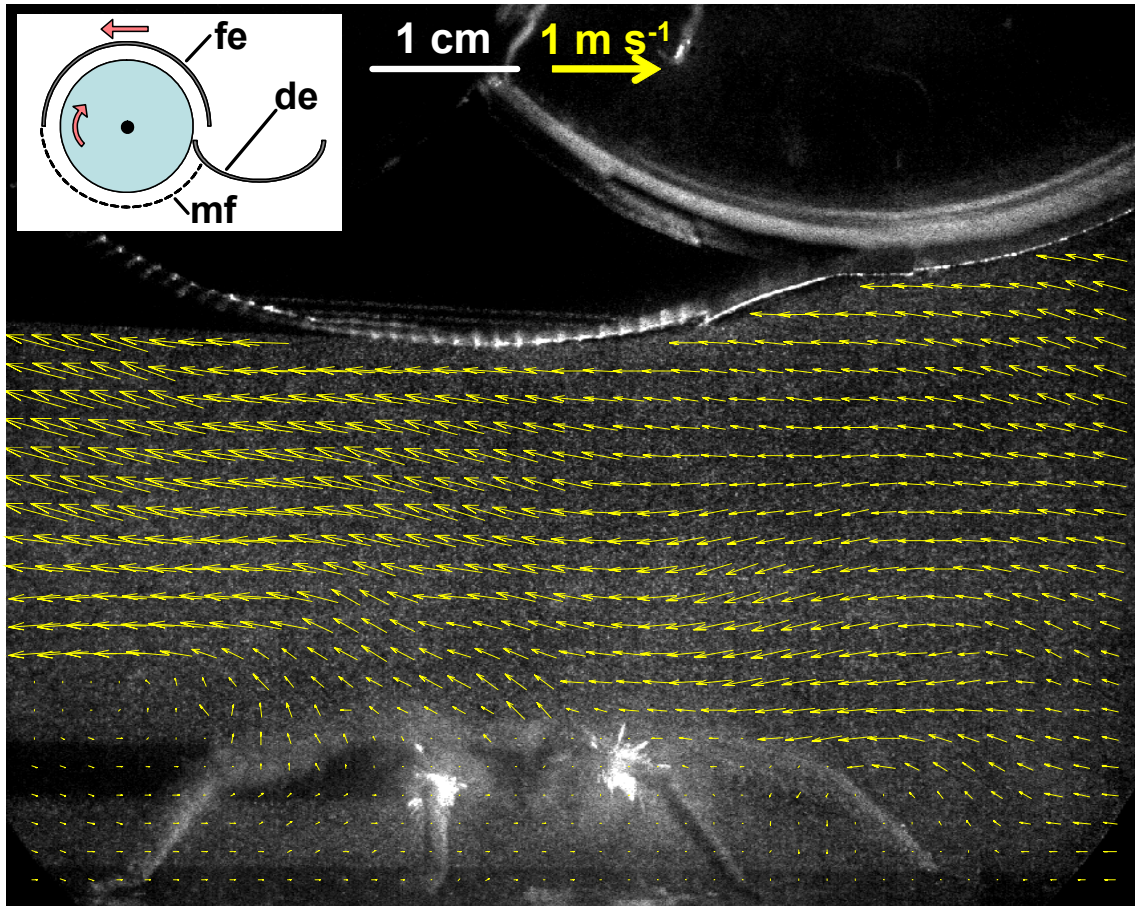


**Fig. 14** Flow field around spider generated by the device shown in Fig. 13. The flow generator was moved from right to left and the cylinder was rotating clockwise. Only horizontal flow components, pointing in the direction of the device's movement, are left as the wake is deflected.

## 5. Behavioral experiments

After having analyzed the natural and artificial fly stimuli the spider was exposed to these different signals in behavioral experiments.

The following experiments were carried out:

- Tethered flying fly moved above spider sitting on a bromeliad leaf (chapter III.1)
- Tethered flying fly moved above spider sitting on a stiff substrate (chapter III.2.2)
- Synthetic fly-like airflow moved above spider sitting on a stiff substrate (chapter III.4.1)
- Only phase I of the artificial fly flow moved above spider sitting on stiff substrate (chapter III.4.2)



- Control experiment with device shown in Fig. 8 moved above spider sitting on stiff substrate. For this experiment the rotating cylinder was turned off to explore the influence of the moved device itself when it is not generating the characteristic fly-like flow patterns. (chapter III.4.3).

The general setup was the same for all behavioral experiments (Fig. 15). The signal source, either a blowfly (chapter III.1 and III.2.2) or the synthetic fly-flow generator (see chapter III.4.1, III.4.2 and III.4.3), was fixed to the rod (see Fig. 15) and moved above the spider 5 cm above the substrate. The experiments on a stiff and heavy substrate (see chapter III.2.2, III.4.1, III.4.2 and III.4.3) were performed with the spider released directly on the metal plate (see Fig. 15) whereas during the experiment described in chapter III.1 the spider was released on a bromeliad. The bromeliad was thereby placed as well on the metal plate of the setup described in Fig. 15 to ensure a similar disconnection from vibrations of the building. In both cases a laser-Doppler vibrometer was used to document the oscillations of the bromeliad leaf and to check for vibrations in the metal plate. With its working range down to theoretically 0.04 nm (200 Hz, 0 dB signal to noise ratio) the LDV is able to resolve vibrations smaller than the spider vibration sensor (metatarsal organ) can detect at fly relevant frequencies up to 200 Hz. The lowest threshold occurs at 200 Hz at slit 6 (tarsus loosely coupled to the vibrator and vertically displaced) and is around 50 nm (Barth and Geethabali 1982).

Five spiders were used for the behavioral experiments. Each individual was tested in about 15 sessions. During each session the spider was exposed to the same stimulus ten consecutive times. The result of a session was then classified according to the spider's most active response, distinguishing between: no reaction, slight reaction and jump. A slight reaction was any movement towards the source (except a jump) for example running or twitching with one or more legs. A session was classified as jump when *Cupiennius* responded to the ten stimuli for example with three slight reactions, two jumps and five times no reaction. We let the spider rest for several minutes between the sessions.

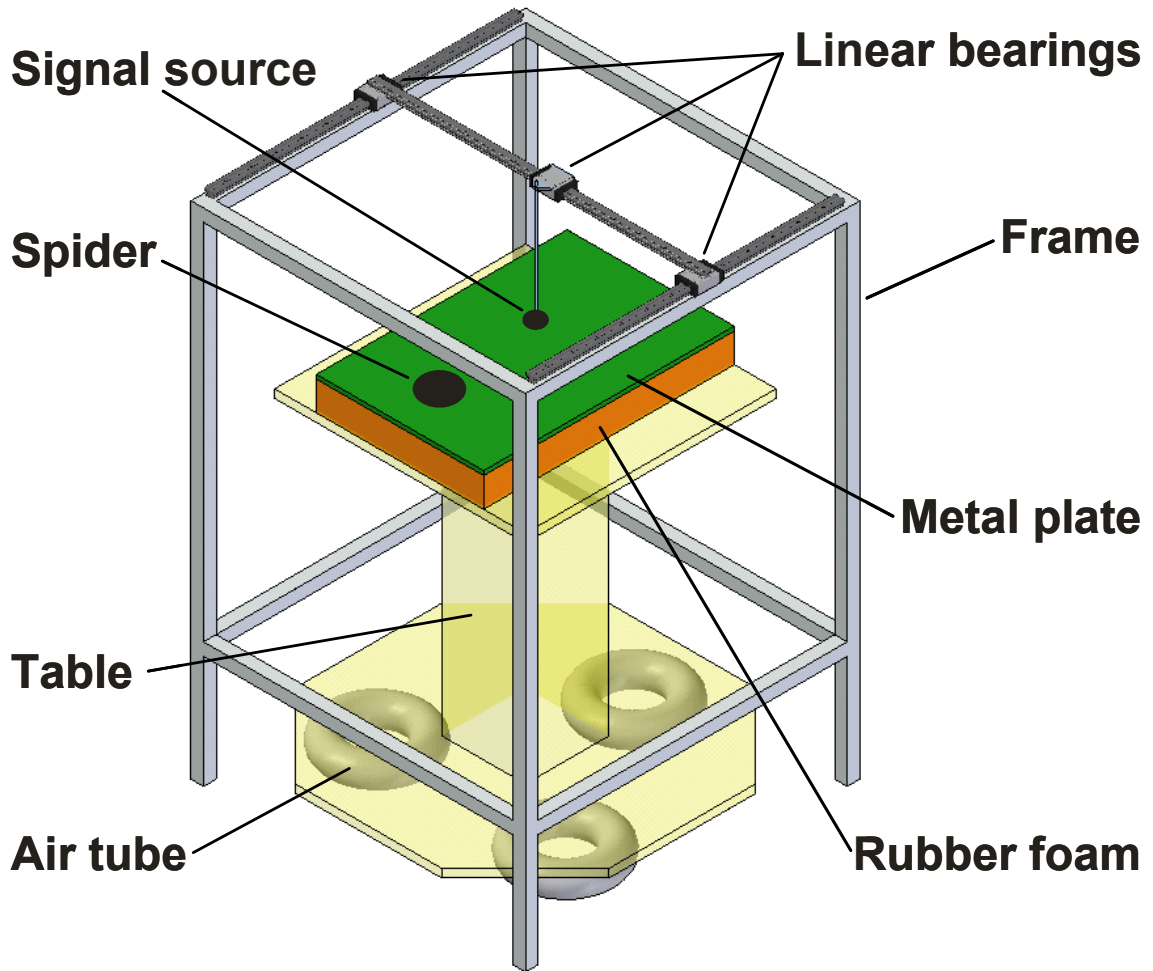


**Fig. 15** Setup used for behavioral experiments. The spider was released on a solid metal plate of approx. 20 kg ( $60 \times 40 \times 1 \text{ cm}^3$ ). Rubber foam and air tubes disconnected the metal plate from vibrations of the building. The signal source was fixed to a rod of 3 mm diameter which was connected to the frame by linear bearings and could be moved to all horizontal positions in the same plane.

## 6. Statistical tests

To evaluate and compare the experimental results two non-parametric tests were applied. The Mann-Whitney test (U test) was used to compare independent samples whereas the Wilcoxon signed-rank test served to interpret two related samples or repeated measurements on a single sample. Both tests were performed using the software XLSTAT 2009. The chosen level of significance was 5 %. The algorithms used by XLSTAT 2009 to calculate the statistical data are adapted from Wilcoxon (1945), Lehmann (1975), Siegel and Castellan (1988), Cheung and Klotz (1997) as well as Hollander and Wolfe (1999).

### III. RESULTS

#### 1. Prey capture behavior induced by flying prey: reaction to an experimentally moved humming blowfly

To learn more about the type of signals (air flow, airborne sound or substrate vibration) used by *Cupiennius* to detect, localize and catch flying prey, its motion during the hunting behavior was studied with a high-speed video camera. The main purpose was to determine the fly's position when the spider jumped towards its prey.

Therefore a fly was mounted to the setup described in chapter II.5 (Fig. 15) and moved in variable altitudes above the spiders (approx. 5 months of age). The eyes of all spiders were covered to exclude vision. In all cases of successful captures (Fig. 16) the fly was located directly above the tarsus of the leg pointing towards the approaching fly (horizontal distance:  $-0.0022 \text{ cm} \pm 1.3410 \text{ cm}$ ) when the spider started to jump (Fig. 16c). The manipulation of the natural flight characteristics by the manual pulling of the blowfly (see chapter III.3.2 and IV.4) is thought to be the reason for the comparatively large standard deviation of this value. Supposedly then the fly generates a signal (vibration, airflow or sound) informing the spider about the right time to jump when it comes close to the spider's closest leg.

For a quantitative analysis of the behavior five spiders were tested in a total of 75 sessions. The experiments were done under red light and the spider's eyes were covered to exclude vision. The spider jumped on average in 20 % of the sessions towards the fly and in 2.7 % of the sessions the fly was caught (Fig. 17). Altogether four of five spiders jumped at least once and two managed to capture at least one fly successfully. An example of a successful prey capture is shown in Fig. 18.

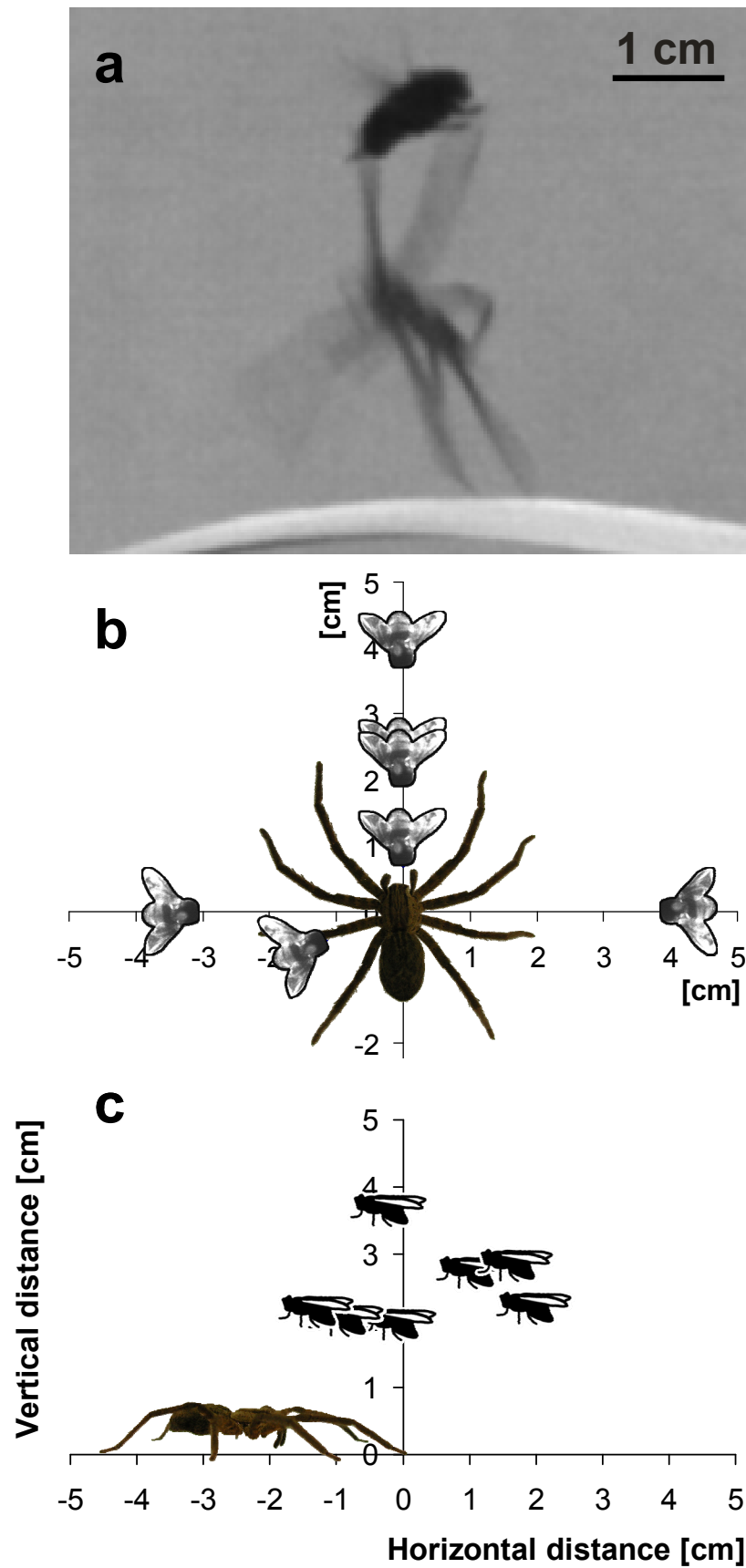


**Fig. 16** **a** High-speed video picture (approx. 220 frames  $s^{-1}$ ) showing a spider catching a blowfly. **b**, **c** Positions of flies in relation to the spider at the time of a successful jump ( $N = 6$ ,  $n = 7$ ). **b** Top view of actual horizontal positions of the flies with respect to the spider. **c** Positions from **b** in relation to the tarsus (at point of origin) of the leg pointing towards the approaching fly.

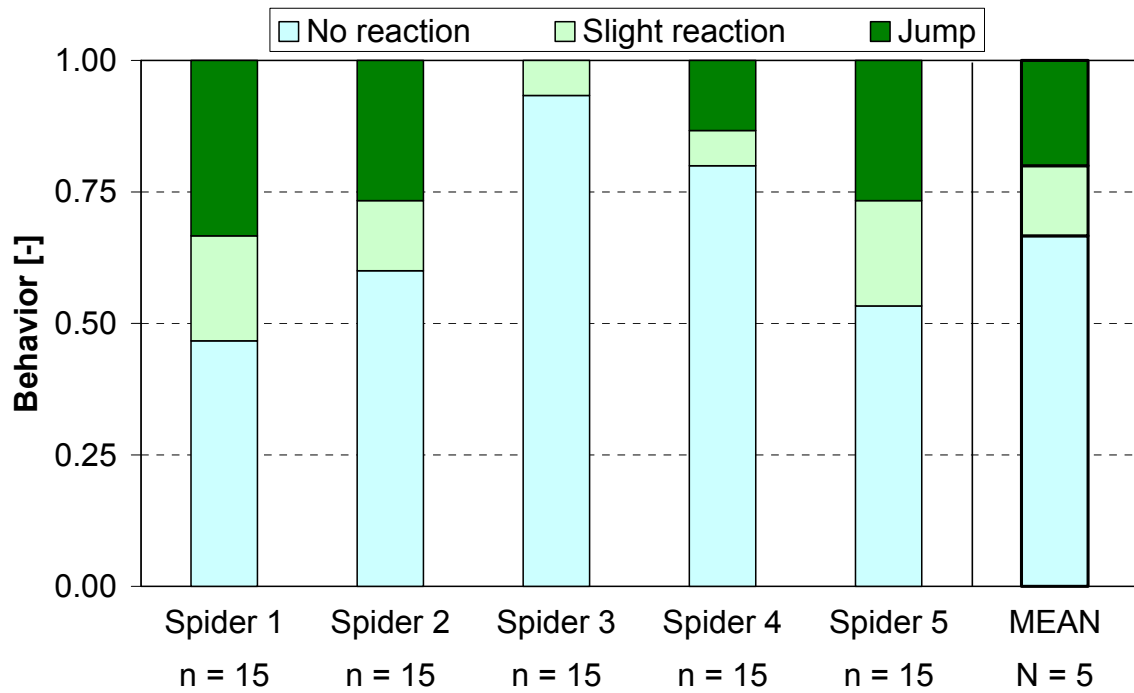


**Fig. 17** Results of behavioral experiments with tethered humming blowfly moved above spider sitting on a bromeliad leaf. Far right: mean values for five individuals shown separately on the left. Each individual was tested in 15 sessions. During a session the spider was exposed to the stimulus ten consecutive times. The session was then classified with regard to the spider's most active response. The behavioral categories were: no reaction, slight reaction and jump. The classified sessions were added and plotted in normalized form. The total number of the sessions corresponds to 1.

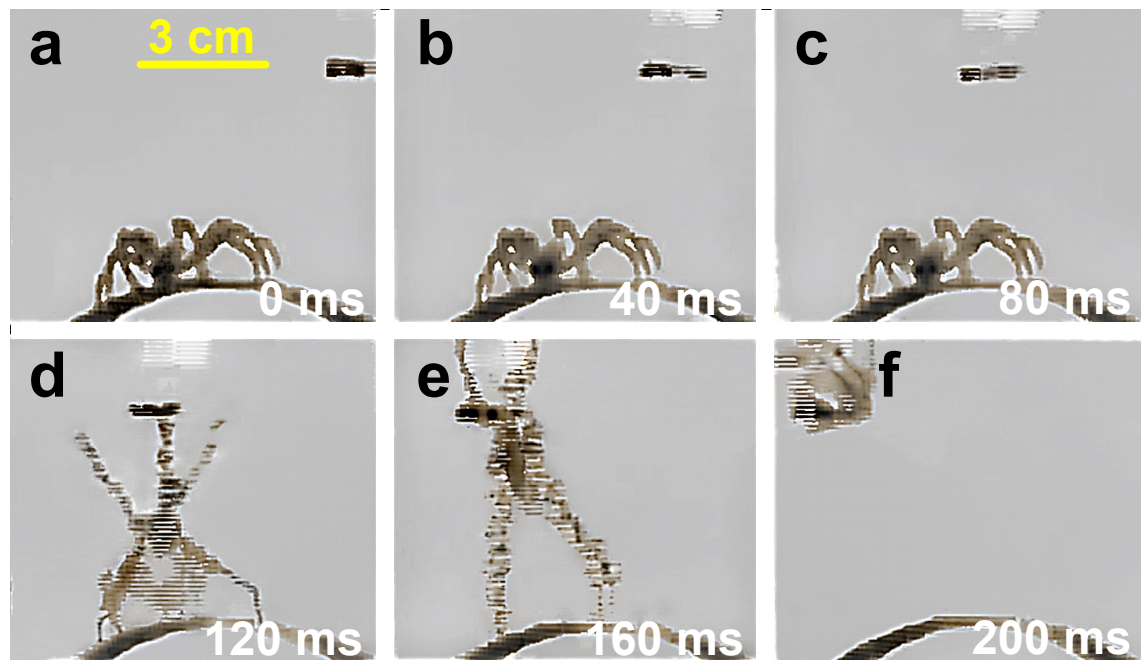


**Fig. 18 a-f** Successful jump of *Cupiennius*, sitting on a bromeliad leaf, towards a horizontally pulled humming blowfly 5 cm above the spider. The experiment was performed under red light which was filtered when preparing the figure.

## 2. On the multimodality of natural stimuli

In this chapter the actual relevance of the sensors possibly involved in the prey capture behavior (Fig. 19) is analyzed. The spider might recognize the flying prey visually and the substrate on which it sits may vibrate when a blowfly passes by so that *Cupiennius* might detect the vibrations with its slit sense organs. In addition the trichobothria may be deflected by air particle oscillations due to airborne sound and by the air flow that the fly generates.

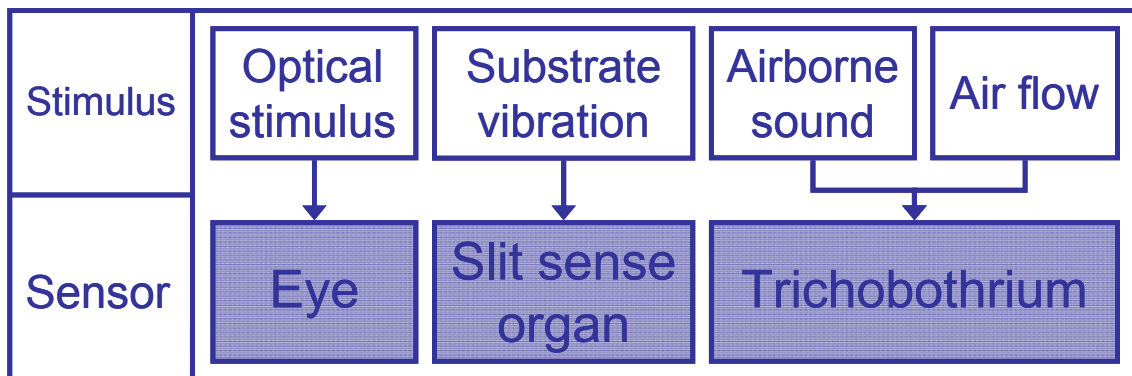


**Fig. 19** Sensors and stimuli possibly guiding prey capture behavior in *Cupiennius*.

### 2.1 Visual stimulus

Earlier work of Brittinger (1998) showed that spiders do not need vision to successfully catch flying prey. For this reason vision is not under investigation in the present study. The eyes of the spider were covered in all behavioral experiments.

### 2.2 Substrate vibration

Barth and Geethabali (1982) showed that *Cupiennius* has highly sensitive vibration receptors. We therefore analyzed the vibrations of a bromeliad leaf, with *Cupiennius* sitting on it, possibly induced by a humming blowfly passing over the spider. Laser-Doppler vibrometry was used to measure these vibrations in order to find out if the spider can sense the approaching fly by substrate vibrations.

The leaf oscillations were resolved in three directions perpendicular to each other (Fig. 20) with the measurement point on the leaf being directly underneath the spider (see insets Fig. 20a, b and c). Low frequency vibrations up to 50 Hz were detected in all directions considered (Fig. 20a, b and c). However, these vibrations were present both before and after the fly was pulled above the leaf (between 0.2 and 0.5 ms, Fig. 20) and therefore identified as noise due to background substrate vibrations, not useful as information about the approaching fly. While the fly was pulled over the leaf narrowband

vibrations at the fly's wing beat frequency, induced by the airborne sound of the humming blowfly, could be measured in the x- and z-direction (Fig. 20a and c). The magnitude of these vibrations was  $5.64 \text{ nm} \pm 1.15 \text{ nm}$  in the x-direction and  $7.24 \text{ nm} \pm 1.01 \text{ nm}$  in the z-direction ( $N = 5$ ,  $n = 15$ ) whereas in the y-direction no clear signal could be measured (see Fig. 20b). The second harmonic of the vibrations induced by the airborne sound of the fly (between 300 and 400 Hz) was too weak to be resolved for every direction (Fig. 20a, b and c).

The comparison (see chapter IV.1) of these results to the threshold curves of the slits in the vibration sensitive metatarsalorgan determined by Barth and Geethabali (1982) show that that *Cupiennius*, sitting on a bromeliad, is not able to detect either vertical or horizontal leaf vibrations induced by a humming blowfly which is pulled along a straight path 5 cm above the spider.

As substrate vibrations due to their smallness must be assumed not to play a role in the detection of flying blowflies (see IV.1) the spider should be able to still catch flying prey successfully when sitting on a stiff and heavy plate excluding vibrations. A metal plate resting on a mechanically damped table (Fig. 15) ensured that no vibrations were induced by the flying fly as verified by measuring vibrations vertically to the plate's plane with a laser-Doppler vibrometer (Fig. 22). As seen from Fig. 21 the spider successfully captures a manually pulled flying blowfly even when sitting on the heavily damped heavy and stiff plate.

All five individuals investigated jumped towards the prey and three of them caught at least one fly (Fig. 23). There was no significant difference between the percentage of jumps towards the prey during this experiment and that with the spider sitting on a bromeliad leaf ( $p = 0.794$ , Mann-Whitney test, null hypothesis: no difference). The spider answered on average 19.3 % of the sessions on the stiff plate with a prey capture jump whereas it was 20 % on the bromeliad leaf. Likewise the rates of successful jumps did not differ significantly ( $p = 0.762$ , Mann-Whitney test, null hypothesis: no difference).

According to these experiments the substrate on which the spider sits has no significant influence on its prey capture behavior under the given laboratory conditions.

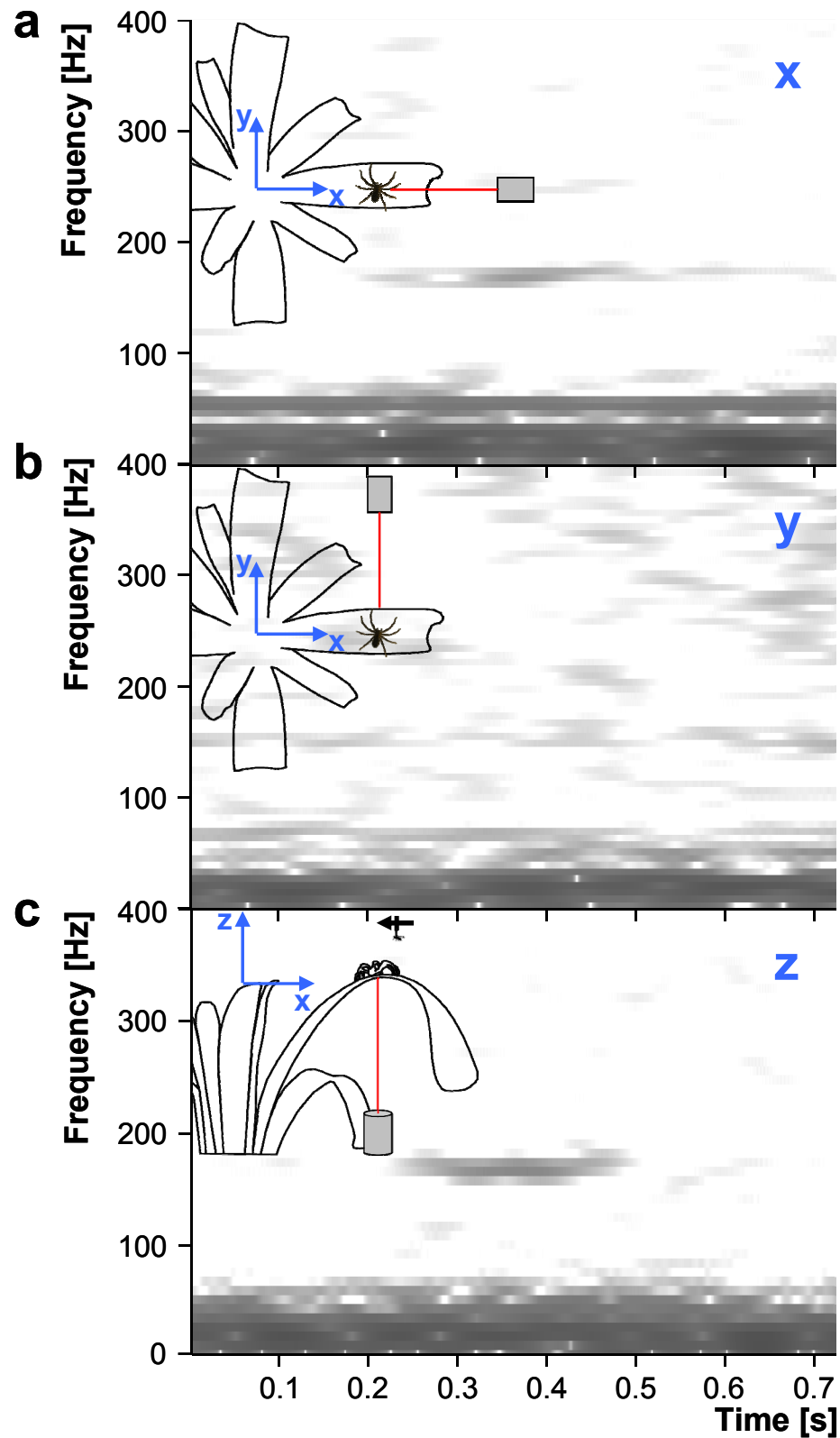


**Fig. 20 a-c** Vibrograms showing movement of a bromeliad leaf in x-, y- and z-direction when a humming blowfly was pulled along a straight line in the x-direction 5 cm above the spider (see black arrow in the inset in **c**). When the humming fly passed by the leaf (between 0.2 and 0.5 ms) the first harmonic of the fly's wing beat frequency (between 150 and 170 Hz) induced vibrations of the leaf in the x- and z-direction (**a** and **c**) ( $N = 5$ ,  $n = 15$ ). The low frequency vibrations up to 50 Hz (in **a**, **b** and **c**) were present both before and after the fly was pulled above the leaf and therefore identified as noise due to background substrate vibrations.



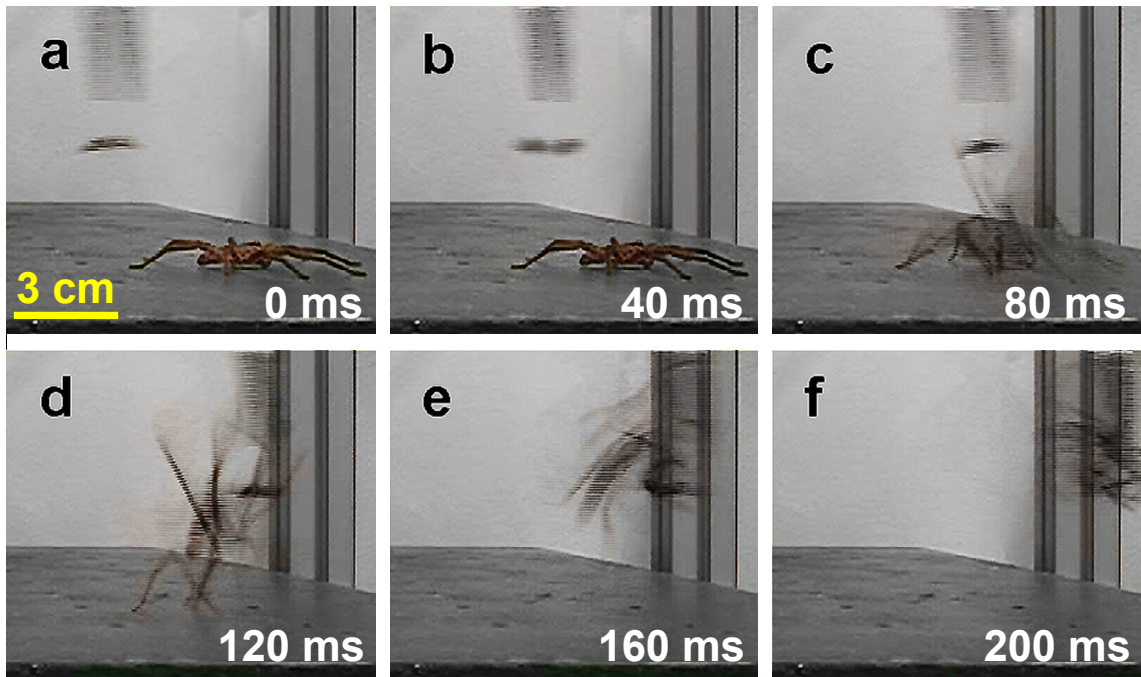


**Fig. 21 a-f** Successful capture of a humming blowfly moved manually above and over *Cupiennius* at an altitude of 5 cm above the substrate. The spider was sitting on a damped heavy metal plate (Fig. 15). For the LDV recording of the plate made during this jump see Fig. 22. The experiment was performed in red light which was filtered with picture editing when preparing the figure.

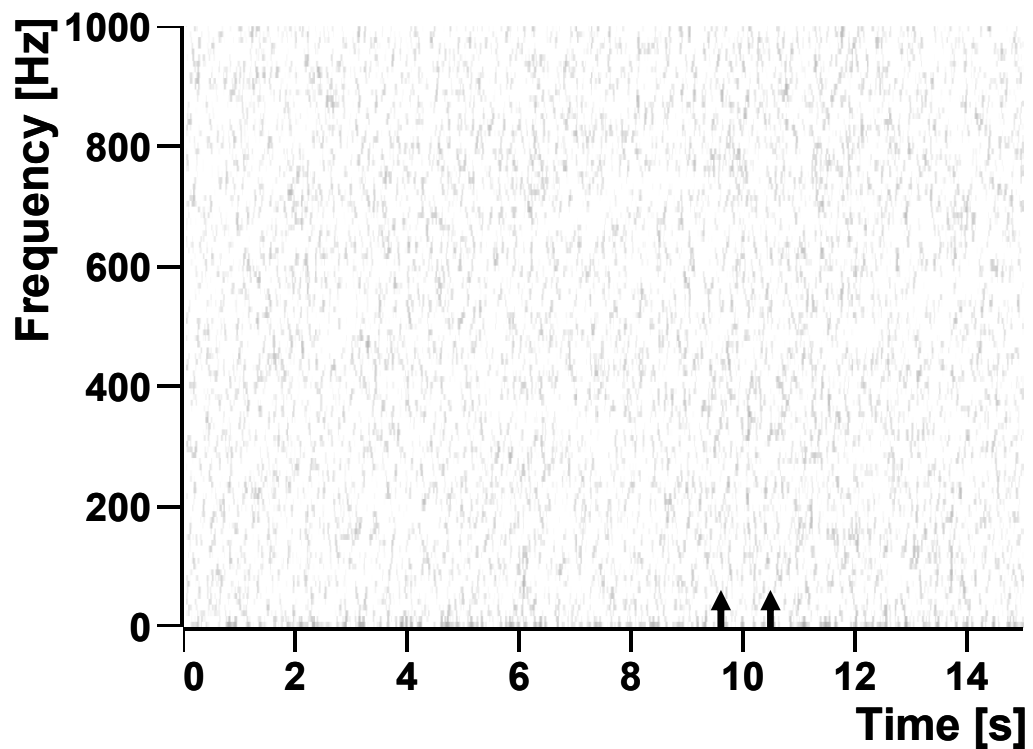


**Fig. 22** Vibrogram verifies that no fly related vibrations were measured during the successful jump of *Cupiennius* shown in Fig. 21. The fly was above the plate starting at 9.64 s. At 10.48 s the spider jumped (see arrows). The small light grey areas randomly distributed in the vibrogram are due to electrical noise.

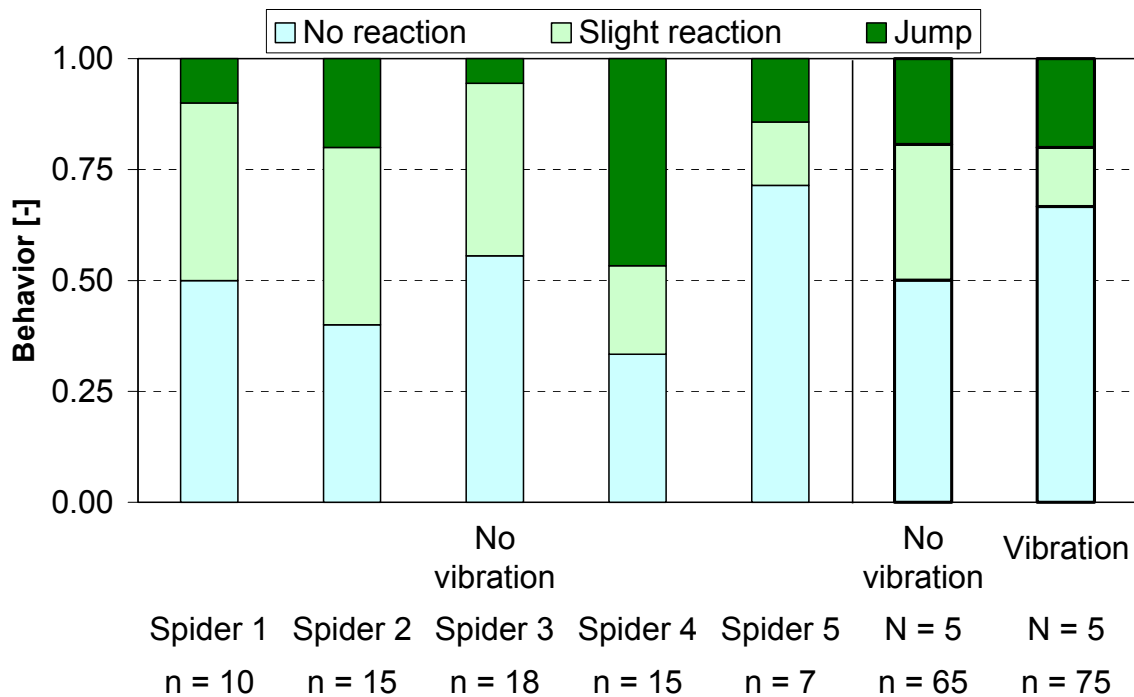


**Fig. 23** Behavioral experiment with a humming blowfly moved over a damped stiff and heavy metal plate avoiding substrate vibrations. The sixth column from the left displays the mean values obtained from five individuals (first five columns from left). During each session the spider was exposed to the stimulus ten consecutive times. The session was then classified with regard to the spider's most active response. The behavioral categories were: no reaction, slight reaction and jump. The classified sessions were added and plotted in normalized form (total number of the sessions equals 1). The mean values ("no vibration") are compared to those of Fig. 17 with the fly pulled over a bromeliad leaf ("vibration", column on far right) to evaluate the potential influence of the substrate.

## 2.3 Airborne sound

When the flying blowfly passes over the spider its wing beat causes airborne sound (Kanmiya 2005). As *Cupiennius* is able to recognize the sound particle velocity induced by such pressure fluctuations with its trichobothria they were also called "auditory hairs" by Dahl 1883 (Barth 2002). The main question of this chapter is: Does the sound particle velocity induced by the airborne sound generated by the fly reach the electrophysiological threshold so that the spider can detect the fly with its trichobothria?

### 2.3.1 Sound pressure

The acoustic measurements were performed with three flies of different age and sex (two males and one female) with their wing beat frequency varying between 130 Hz and 200 Hz. The larger wing area of both freshly eclosed and female flies correlates with a lower humming frequency (see Sueur et al. 2005). However, there are no indications that the spider distinguishes between age and sex of prey.

The frequency content of the fly's sound signal is displayed in Fig. 24. Apart from the first harmonic at wing beat frequency the second and to a clearly lesser degree the third, fourth and fifth harmonics show up. They are all characterized by a frequency band only 20 Hz wide. The two relatively small peaks seen at 20 and 50 Hz are caused by noise present even in the absence of the humming fly. The third, fourth and fifth harmonics were too weak to be resolved and therefore only the first and the second harmonics are evaluated for the pressure field around the fly.

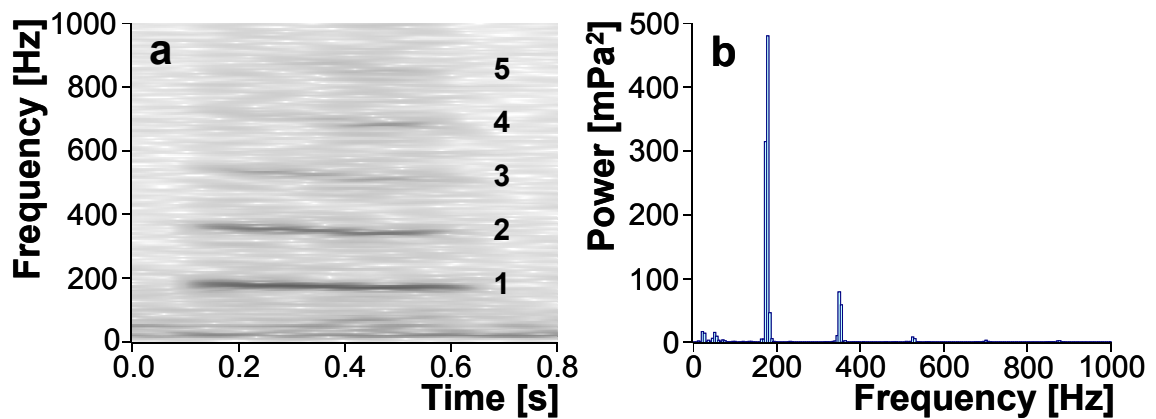


**Fig. 24** Sonogram (a) and FFT (b) of sound measured in the humming fly's symmetry plane 10 mm below and 25 mm ahead of it.

The pressure of the first harmonic ranges from 63.6 dB SPL (at  $x = 0$  mm,  $y = 0$  mm,  $z = 10$  mm) to 25.1 dB SPL (100, 0, 70) (Fig. 25). The values for the second harmonic measured at the identical grid points are in-between 51.3 dB SPL and 17.2 dB SPL (Fig. 26). They are significantly lower ( $p < 0.0001$ , Wilcoxon signed-rank test, null hypothesis: no difference) than those of the first harmonic. The pressure levels of the first and second harmonic in both horizontal planes form a symmetric pressure field regarding the symmetry axis of the fly with no significant difference between the values on each side ( $p = 0.784$  for the first harmonic and  $p = 0.985$  for the second harmonic, Wilcoxon signed-rank test, null hypothesis: no difference).

In summary the sound of the first harmonic was radiated in a dipole-like pattern (Fig. 25) whereas the shape of the second harmonic was more rounded like a monopole (Fig. 26). These results of the sound pressure around the blowfly are compared to those around *Lucilia sericata* (Sueur et al. 2005) in chapter IV.3.

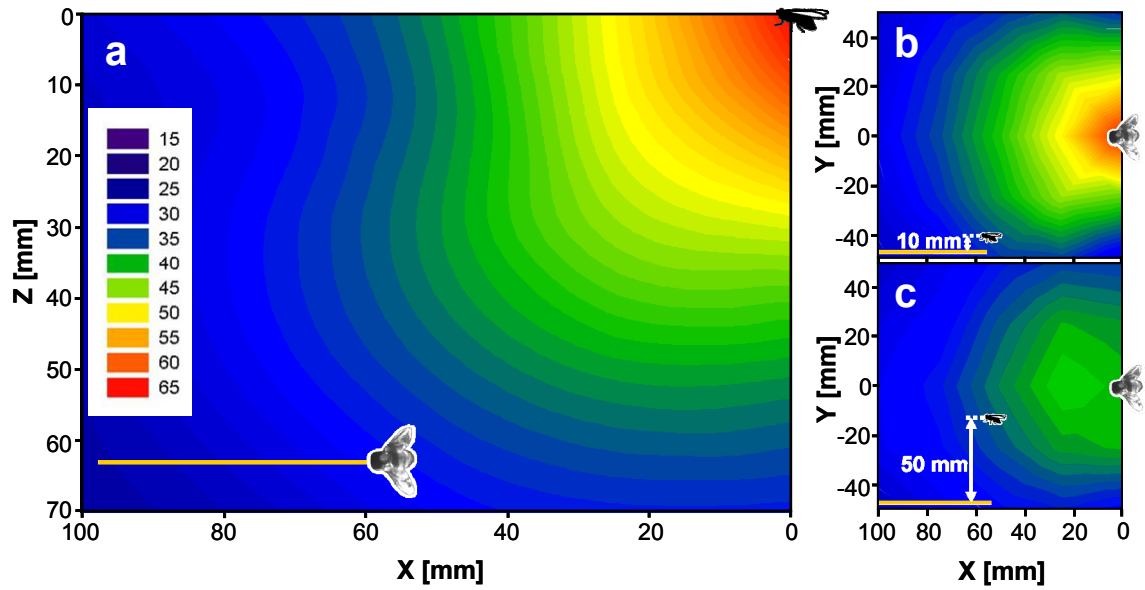


**Fig. 25** Color coded pressure fields in dB SPL of the first harmonic (wing beat frequency) around a stationary humming blowfly ( $N = 3$ ,  $n = 15$ ). **a** Vertical symmetry plane of the fly (x-z-plane). **b**, **c** Pressure field in the horizontal planes (x-y) 10 mm (**b**) and 50 mm (**c**) below the fly's thorax.

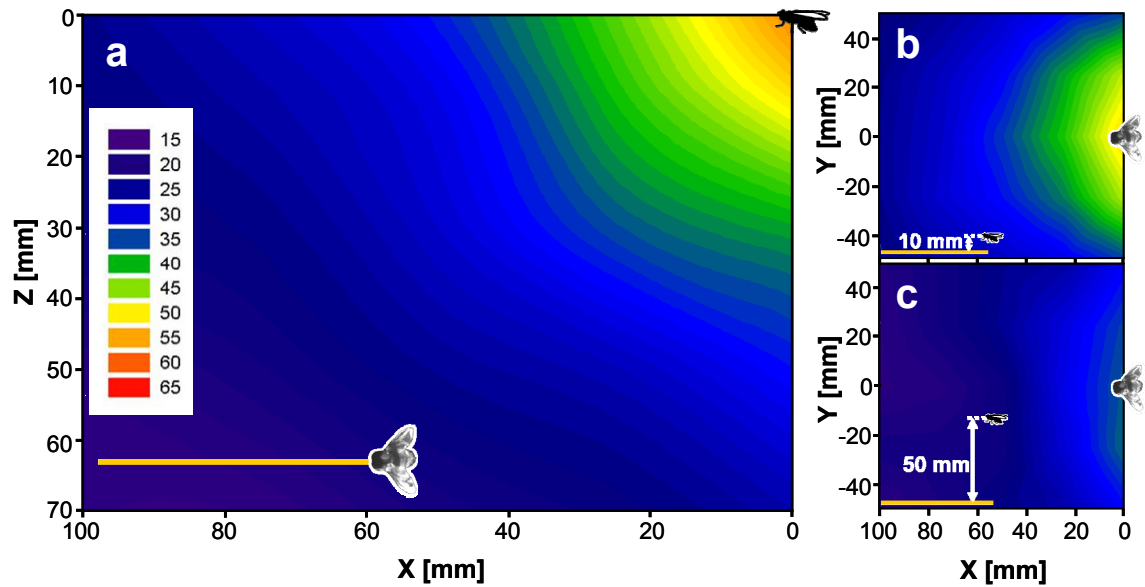


**Fig. 26** Color coded pressure fields in dB SPL of the second harmonic (double wing beat frequency) around a stationary humming blowfly ( $N = 3$ ,  $n = 15$ ). **a** Vertical symmetry plane of the fly (x-z-plane). **b**, **c** Pressure field in the horizontal planes (x-y) 10 mm (**b**) and 50 mm (**c**) below the fly's thorax.

### 2.3.2 Movement of trichobothrium due to sound

As the trichobothria are not sound pressure but particle velocity sensitive it is important to measure the mechanical response of the trichobothria on a living animal to the sound radiated from a blowfly directly and to then judge its physiological response. In a first

step the tarsal trichobothria were illuminated, their deflection examined under a microscope and the mechanically most sensitive trichobothrium selected for detailed analysis. The trichobothrium which was deflected most was 750  $\mu\text{m}$  long. This coincides quite nicely with the literature (Barth et al. 1993) as this length is the most sensitive to frequencies in the range of the first harmonic of a humming blowfly. The angular deflection and angular velocity of this hair were measured with the LDV and then compared with the physiological threshold curves provided by Barth and Höller (1999).

A sample “sonogram” containing the harmonics of the angular deflection and angular velocity due to the humming fly signal up to 1000 Hz is shown in Fig. 27. Similar to the sound radiation of the blowfly the first harmonic contains larger deflection and velocity values than the other harmonics and its frequency ranges between 130 Hz and 200 Hz with a bandwidth of around 20 Hz.

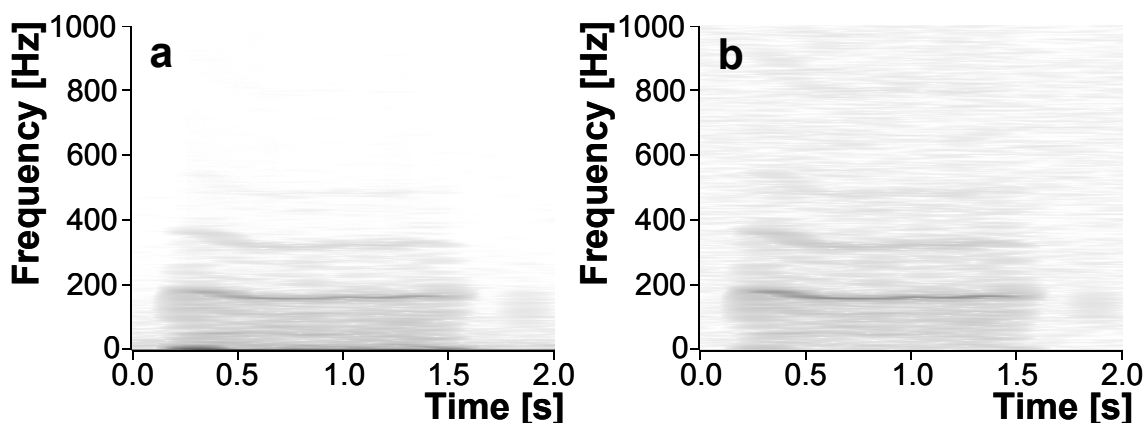


**Fig. 27** “Sonogram” of angular deflection (a) and angular velocity (b) of a trichobothrium (length 750  $\mu\text{m}$ ) on the tarsus of a living spider in response to a humming blowfly located 30 mm ahead and 10 mm above the trichobothrium.

The evaluation of the first harmonic reflecting the wing beat frequency of the trichobothrium’s movement is shown in Fig. 28. At most positions of the fly both the deflection magnitude and the angular velocity are quite far below its electrophysiological threshold. Only deflection values in the rectangular area of the vertical symmetry plane within 20 mm below and 30 mm in front exceed the threshold, which means that only in this area the spider is able to detect the fly due to its airborne sound (Fig. 28a). The size of the rectangular area (also in the vertical symmetry plane) in which the spider can sense the fly as judged from the trichobothrium’s angular velocity is even a little less (18 mm below and 28 mm in front, Fig. 28b).

The behavioral experiments in chapter III.1 and III.2.2, where the fly was caught successfully, were performed with the blowfly located 50 mm above the spider. At this

altitude both the mean values of the deflection and the angular velocity reach just 8 % and 6 %, respectively, of the physiological threshold values (Fig. 29). It is concluded that the spider was not able to sense the fly by the sound it emitted (first harmonic) under the conditions of our behavioral experiments.

As the deflection magnitude as well as the angular velocity of the second and larger harmonics were less than those of the first harmonic at all measured positions and the trichobothrium's physiological threshold increases for frequencies above 200 Hz (Barth and Höller 1999) we conclude that the second and higher harmonics of the sound generated by a humming blowfly could not be sensed by the spider either under the conditions of our behavioral experiments.

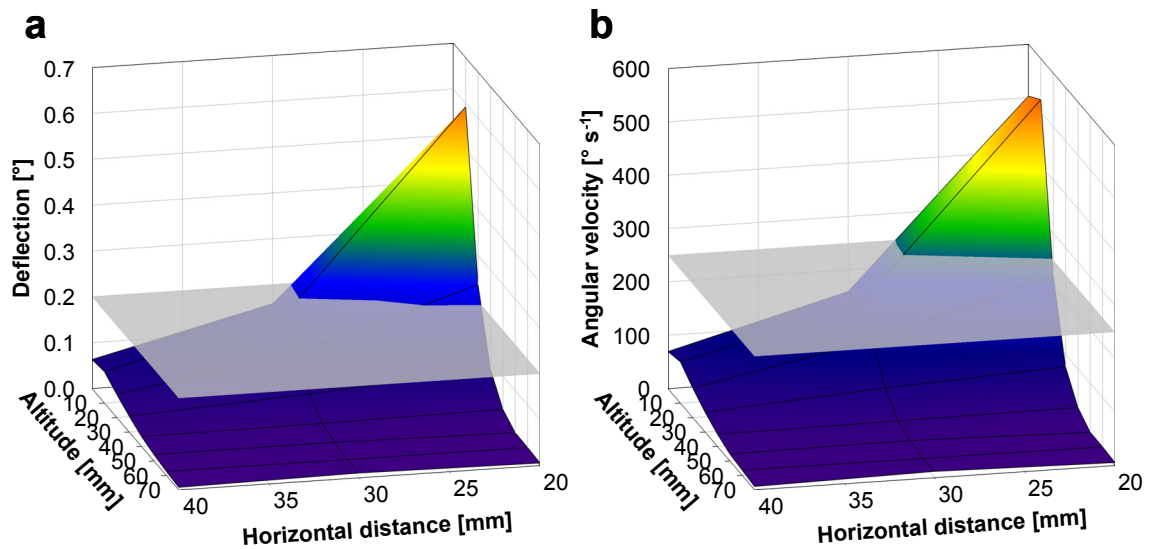


**Fig. 28 a** Angular deflection and **b** angular velocity of a trichobothrium (length 750  $\mu\text{m}$ ) on the tarsus due to sound (first harmonic) radiating from a humming blowfly. The fly was positioned at various altitudes above and horizontal positions in front of the measured trichobothrium. The grey horizontally orientated planes represent the angular deflection (**a**) and angular velocity thresholds (**b**) previously determined electrophysiologically (Barth and Höller 1999).



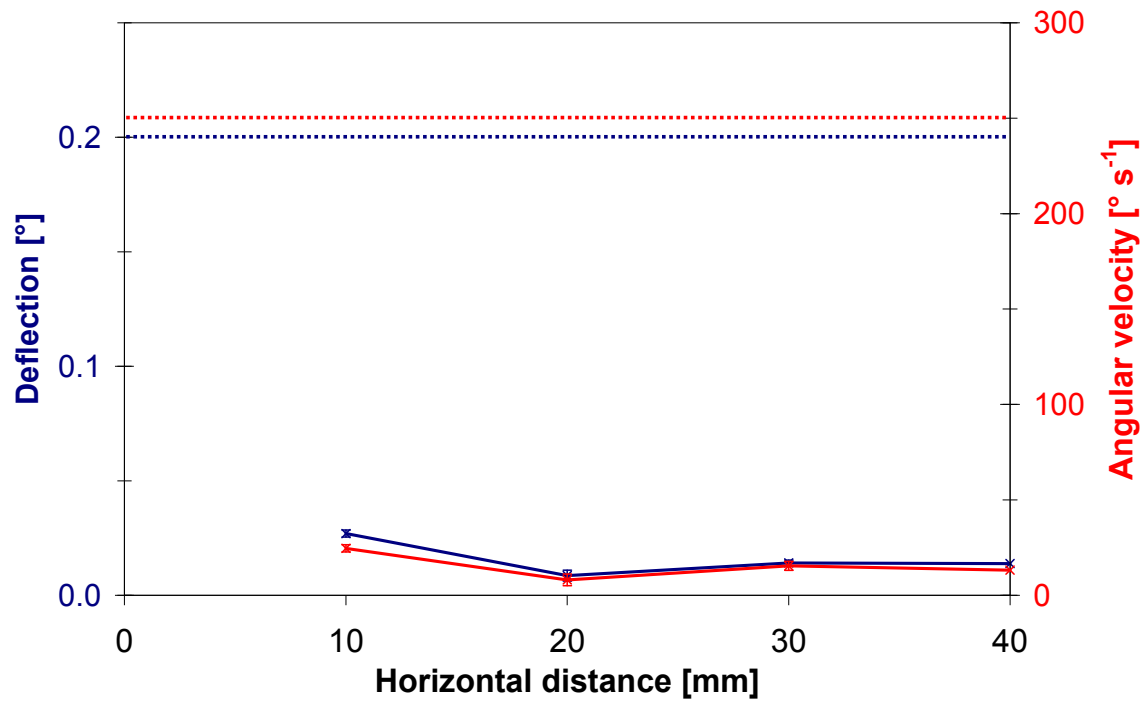


**Fig. 29** Angular deflection and angular velocity taken from Fig. 28 with the fly at an altitude of 50 mm ( $N = 8$ ,  $n = 40$ ) as in the behavioral experiments described in chapter III.1 and III.2.2 and eliciting successful prey captures. The dotted lines represent the trichobothrium's thresholds which have to be reached to elicit a physiological response (action potentials) (Barth and Höller 1999).

## 2.4 Air flow

As known from several works (Brittinger 1998; Barth and Höller 1999) air flows are an important source of information for *Cupiennius*. It has indeed been found earlier that the removal of the air flow sensors (trichobothria) abolishes the prey capture response of *Cupiennius* (Brittinger 1998). We therefore took a closer look at the air flows generated by a blowfly.

## 3. Flow field around the blowfly and above the spider

The flow field around the blowfly was determined in three steps. First the humming fly was kept stationary (chapter III.3.1), second it was artificially moved at a biological meaningful speed (chapter III.3.2) and finally the flow field around a completely freely flying blowfly was analyzed (chapter III.3.3).

### 3.1 Stationary tethered blowfly

To simplify the complex task of measuring the flow field around a freely flying blowfly moving above a spider, we first measured the flow field around a stationary tethered humming blowfly (chapter III.3.1.1). In addition we determined the flow field around

*Cupiennius* which was located on a substrate below the stationary tethered fly (chapter III.3.1.2).

### 3.1.1 Flow field around stationarily flying blowfly

The flow field around a stationary fly, located 5 cm above the substrate, was measured using horizontal and vertical planes. Fig. 30 shows the flow field in a horizontal plane 5 mm below the attachment point of the wings to the fly's thorax. In the wake of the humming blowfly the velocity vectors were directed backwards from the fly and the velocity magnitude reached values of up to  $65 \text{ cm s}^{-1}$ . In addition the air close to the wake region was flowing towards the wake. Following the conservation of mass, the air in front of the fly was sucked towards the wings with a velocity magnitude of up to  $23 \text{ cm s}^{-1}$ .

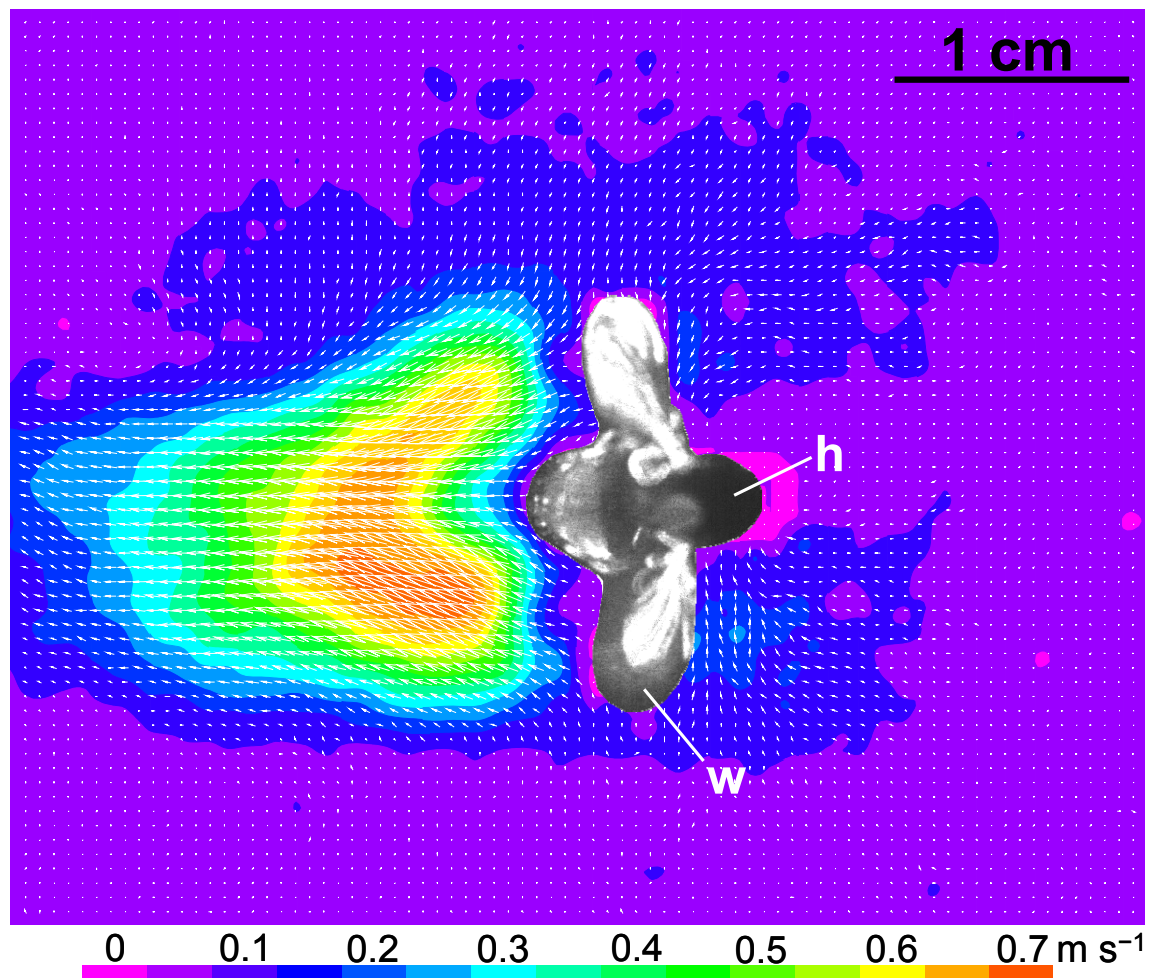


**Fig. 30** Flow field around a stationarily flying blowfly in a horizontal plane 5 mm below the level where the wings are attached to the fly's thorax. A horizontally orientated Perspex plate ( $30 \times 15 \text{ cm}^2$ ) was located 5 cm below the fly (see chapter II.3.1). The vector map presented here shows the calculated mean of 150 individual velocity fields (measurement duration 0.15 s). Colors refer to different velocity magnitudes (see scale). *w* wing, *h* head.

Velocity vectors were also measured in the vertical symmetry plane of the fly (six individuals,  $n = 19$ ). The general observation was that the velocity vectors in the wake (in agreement with Barth and Höller 1999) are pointing downwards and backwards from the fly (Fig. 31). The fly uses the impulse of the wake to move forward and upward against gravity. As seen in Fig. 30 air gets also sucked towards the fly from the front following the principle of mass conservation. The corresponding velocity vectors are directed towards the wings. By placing a horizontally orientated substrate 5 cm below the fly the cone-shaped flow in the vertical symmetry plane of the fly was divided into two components parallel to the surface of the substrate. Whereas the vectors of component one were directed backwards from the fly (bottom left in Fig. 31), the flow of component two moved forward in flight direction and formed a vortex rotating counter-clockwise ahead of the fly (bottom right in Fig. 31).

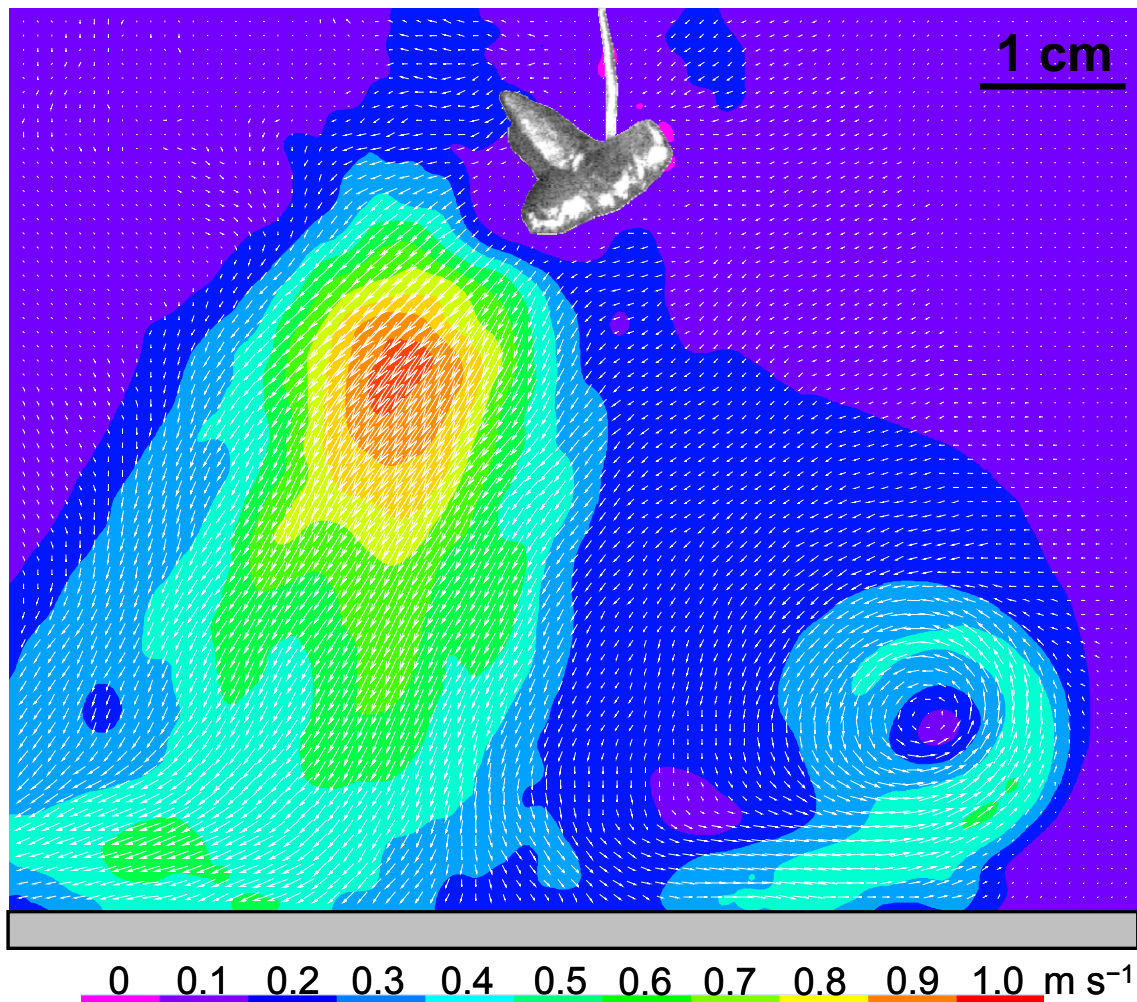


**Fig. 31** Flow field around a stationary flying blowfly in the vertical symmetry plane of the fly. A horizontally orientated Perspex plate (indicated by the grey bar) was located 5 cm below the fly taking “ground effects” from the substrate into account (see chapter II.3.1). This vector map is the calculated mean of 150 individual velocity fields (measurement duration 0.15 s). Colors refer to different velocity magnitudes (see scale).

Fig. 32 shows the flow velocities along the central axis of the cone-shaped wake region as a function of the distance from the fly's abdomen. The general shapes of the curves are similar (Fig. 32). Close to the fly the velocity increases abruptly and reaches a maximum 10 to 30 mm behind the fly. The maximum velocities are around  $1 \text{ m s}^{-1}$  (except one fly, which reached  $2.4 \text{ m s}^{-1}$ ) and decay slowly after having reached their maximum.

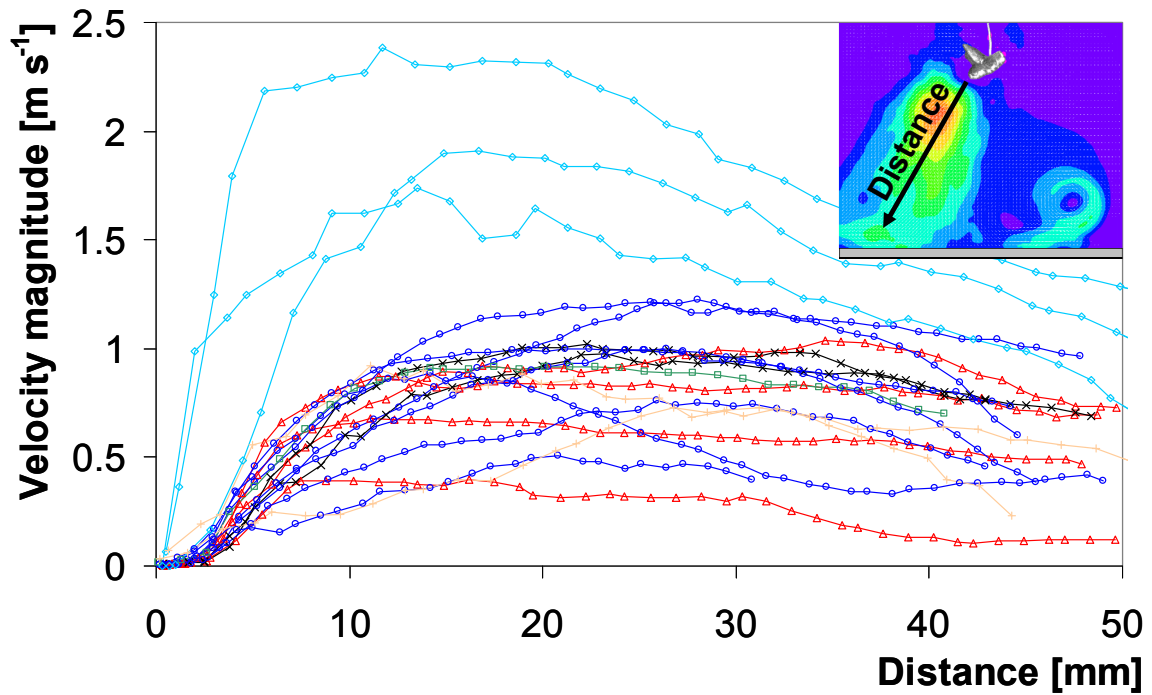


**Fig. 32** Velocity magnitude along the central axis of the cone-shaped wake region behind a stationary humming (flying) blowfly ( $N = 6$ ,  $n = 19$ ). The x-axis corresponds to the distance from the rear end of fly's abdomen along the central axis of the cone (see inset).

The question remains what the flow around the fly looks like (especially the suction flow towards the wings) when the fly is experimentally moved along a straight line simulating its natural forward motion? This will be investigated in chapter III.3.2.

### 3.1.2 Flow field around *Cupiennius*

The spider rested on a horizontally orientated Perspex plate ( $30 \times 15 \text{ cm}^2$ ). 10 cm above ground in the symmetry plane of the spider there was a stationary blowfly. The position of the fly was shifted along the x-axis during the experiments (see setup shown in Fig. 6)

$X = -10 \text{ cm}$ : Simulates the situation when a fly approaches the spider from behind. In this case a uniform flow was found above the spider that was sucked (compare Fig. 30 and Fig. 31) towards the fly (Fig. 33a, b and Fig. 34a). The mean velocity magnitudes in this flow ranged from  $1.74 \text{ mm s}^{-1} \pm 0.13 \text{ mm s}^{-1}$  above leg 1 to

$2.94 \text{ mm s}^{-1} \pm 0.29 \text{ mm s}^{-1}$  above leg 4 (Fig. 34c) and the frequency contained in the signal spectrum reached its peak at 11 Hz. As the trichobothria are in particular sensitive to air flow velocity changes (Barth and Höller 1999) the angular variation of the velocity vectors is an important parameter. The values ranged from  $148^\circ \text{ s}^{-1}$  to  $505^\circ \text{ s}^{-1}$ .

$X = -5 \text{ cm}$ : With the fly still behind but closer to the spider, the flow became much more irregular (Fig. 33c and Fig. 34b). Immediately behind the spider, especially, the instantaneous velocity vectors varied greatly both in terms of magnitude (range from 0 to  $22 \text{ mm s}^{-1}$ ) and direction (angular variation per second up to  $1400^\circ \text{ s}^{-1}$ ). The fly's wake (compare Fig. 30 and Fig. 31) is pointing downwards from the fly at an angle of about  $25\text{--}45^\circ$  in a cone like region (Barth and Höller 1999). The redirection of this flow by the Perspex substrate is thought to be the reason for the increased turbulence intensity, defined as  $I = U' / \bar{U}$  ( $U'$  root mean square of the velocity magnitude,  $\bar{U}$  mean velocity magnitude), for this case (Fig. 34d). This effect also is to be expected under natural conditions with *Cupiennius salei* sitting on large and mechanically strong leaves like those of a bromeliad.

Because the trichobothria are particularly sensitive to fluctuations of air flow velocity (Barth and Höller 1999) rms-values and turbulence intensity were measured. Above the tarsi of walking legs 3 and 4 the instantaneous velocity magnitudes were not as constant as in the preceding case with the fly at position  $x = -10 \text{ cm}$  (Fig. 34a to d). The mean rms-velocity magnitudes above leg 3 and leg 4 were higher ( $1.45 \text{ mm s}^{-1}$  and  $2.82 \text{ mm s}^{-1}$ ) for the fly at  $x = -5 \text{ cm}$  than that at  $x = -10 \text{ cm}$  ( $0.72 \text{ mm s}^{-1}$  and  $0.86 \text{ mm s}^{-1}$ ). This also resulted in a higher turbulence intensity, especially above leg 3 and leg 4 (77 % and 97 %). In comparison with the fly at  $x = -10 \text{ cm}$  the turbulence intensities were 23 % above leg 3 and 29 % above leg 4 (Fig. 34d). The difference between the turbulence intensities at fly positions  $x = -5 \text{ cm}$  and  $x = -10 \text{ cm}$  was significant for all walking legs (leg 1:  $p = 0.0005$ , leg 2:  $p = 0.002$ , leg 3:  $p = 0.0005$ , leg 4:  $p = 0.0005$ , Mann-Whitney test, null hypothesis: no difference). Furthermore the leg with the highest rms-velocity (leg 4) pointed towards the fly. Similar to the turbulence intensity the mean velocities (with the fly at  $x = -5 \text{ cm}$ ) above the legs increased with decreasing distance to the humming blowfly with its largest value again above the leg pointing towards the blowfly (leg 4) (Fig. 34c). In addition the peak velocities were higher with the fly at  $x = -5$ . The averaged peak velocity above leg 4 was  $13.84 \text{ mm s}^{-1}$  for  $x = -5 \text{ cm}$  ( $N = 3$ ,  $n = 9$ ) but only  $5.11 \text{ mm s}^{-1}$  for  $x = -10 \text{ cm}$  ( $N = 2$ ,  $n = 5$ ).

$X = 0 \text{ cm}$ : When the fly was directly above the spider its wake has moved further towards the spider (Fig. 33d).

$X = +5 \text{ cm}$ : This effect is even more pronounced with the fly in this position. Fig. 33e gives an impression of the complex character of the flow generated by the fly, as inter-



cepted and affected by the spider. The velocity magnitudes increased to values of up to  $185 \text{ mm s}^{-1}$  and the mean vorticity, with vorticity defined as  $\zeta = \partial U_y / \partial x - \partial U_x / \partial y$  ( $U_x$  velocity in  $x$ -direction,  $U_y$  velocity in  $y$ -direction), ranged from  $-18.9 \text{ s}^{-1}$  to  $5.6 \text{ s}^{-1}$ .

In a next step the flow field induced by a tethered flying blowfly artificially moved forward along a straight path was examined around the fly.

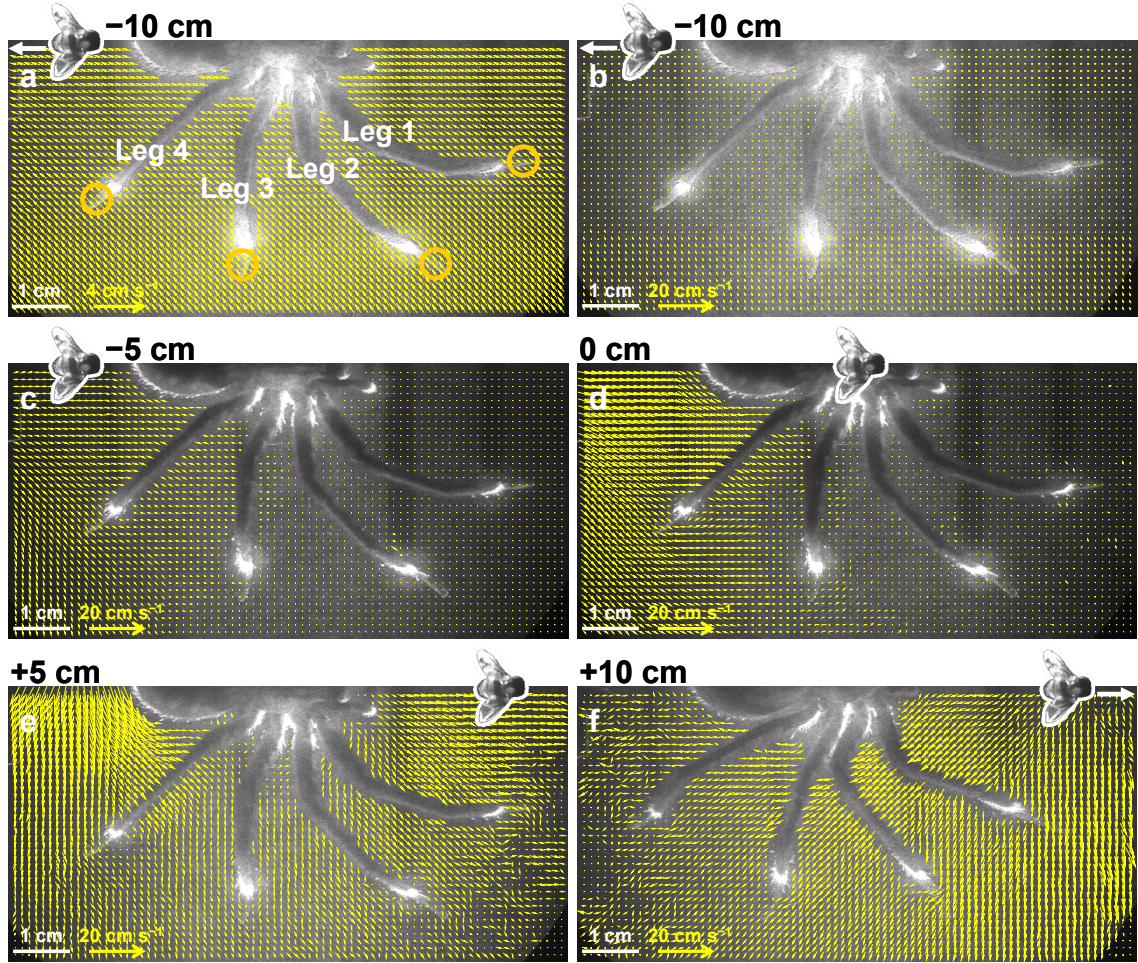


**Fig. 33** Vector maps of the flow field around the spider close to the leg tips generated by a stationary flying blowfly placed at  $x = -10 \text{ cm}$  (**a** and **b**),  $x = -5 \text{ cm}$  (**c**),  $x = 0 \text{ cm}$  (**d**),  $x = +5 \text{ cm}$  (**e**) and  $x = +10 \text{ cm}$  (**f**) relative to the spider prosoma (for further explanation see Fig. 6). The horizontal laser sheet was positioned immediately above the spider's tarsi. With the fly 10 cm behind the spider a uniform flow field towards the fly developed (**a** and **b**). **a** and **b** are the same plots except a difference in scaling. The scaling in **b** is identical to that of **c** to **f**. As the fly comes closer (**c**) the suction flow in front and towards the fly is superposed by the much stronger wake hitting the plate and spreading in all horizontal directions (compare Fig. 31). As the fly is moved step by step over and past the spider (**d** to **f**) the wake moves along with the fly. Orange circles in **a** indicate sites chosen for the measurements shown in Fig. 34.



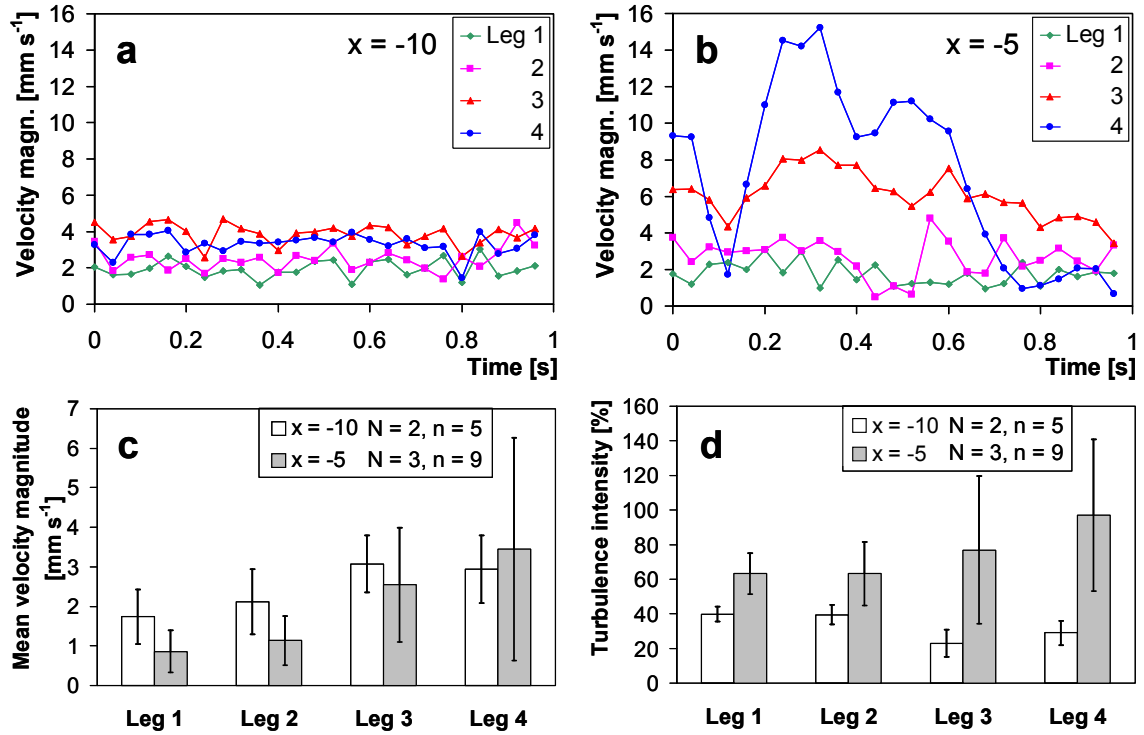


**Fig. 34** **a, b** Velocity magnitude plotted as a function of real time at locations immediately above the tarsi of each walking leg for a fly at positions  $x = -10$  cm (**a**) and  $x = -5$  cm (**b**) and 10 cm above the spider platform in both cases. **c** Mean velocity magnitude and mean rms-values for the cases shown in **a** and **b**. **d** Turbulence intensity for the cases shown in **a** and **b**.  $N$  and  $n$  represent the number of different flies and the number of measurements, respectively.

### 3.2 Tethered flying blowfly moved forward

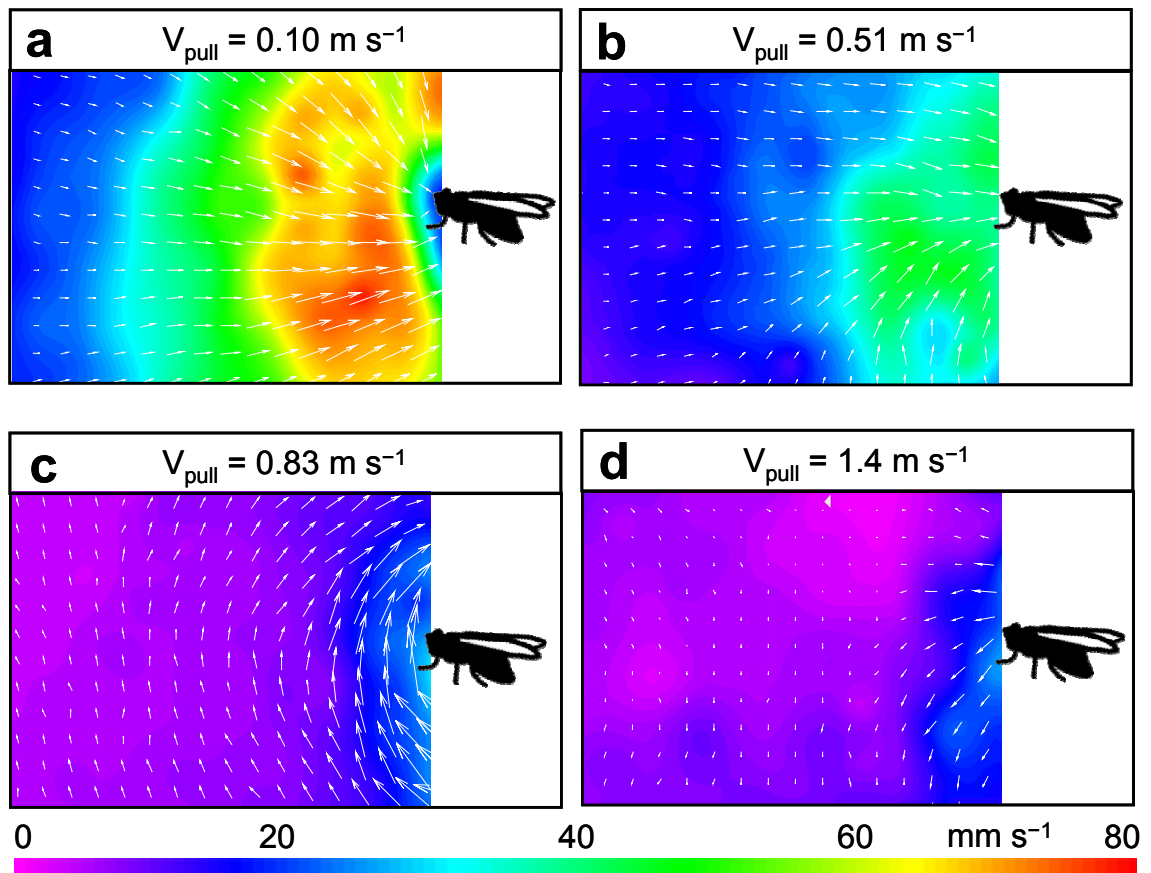
In a next step towards the description of the flow field around a naturally flying blowfly the humming fly was manually pulled over the spider (see chapter II.3.1). The specific goal was to find out whether the manual pulling of the fly is an appropriate way to measure the flow field generated by a freely flying blowfly around the spider.

Fig. 35 shows the outcome of experiments in which the blowfly was pulled at various velocities. According to Schilstra and van Hateren (1999) the horizontal velocity of a freely flying blowfly is up to  $1.2 \text{ m s}^{-1}$  and the mean velocity is  $0.5 \text{ m s}^{-1}$ . At unnaturally low fly velocities ( $V_{\text{pull}} = 0.10 \text{ m s}^{-1}$ ) the fly sucks air towards itself (Fig. 35a) whereas at unnaturally high velocities ( $V_{\text{pull}} = 1.4 \text{ m s}^{-1}$ ) air is pushed away from the fly (Fig. 35d). These results show that the flow field around a humming blowfly is strongly influenced by the pulling speed ( $V_{\text{pull}}$ ) applied manually.

Within the range of possible flight velocities as determined by Schilstra and van Hateren (1999) the shape of the flow field around the fly changes significantly (compare air flows for flight velocities of  $0.51 \text{ m s}^{-1}$  and  $0.83 \text{ m s}^{-1}$ ; Fig. 35b and c). This is most likely due to differences between the pulling speed ( $V_{\text{pull}}$ ) and the velocity the fly would

have when flying freely ( $V_{\text{free}}$ ), defined as  $\Delta V = V_{\text{pull}} - V_{\text{free}}$ . However as the flow field around a freely flying blowfly does not qualitatively change with horizontal speeds ranging from 13 to 81  $\text{cm s}^{-1}$  (see Fig. 36 and Tab. 1 in chapter III.3.3) manual pulling of a humming blowfly is inappropriate when determining the flow field around a spider. Consequently the flow field generated by a fly and around a spider can only be measured correctly using a completely freely flying blowfly.

As the circulation around the fly which occurs at  $V_{\text{pull}} = 0.83 \text{ m s}^{-1}$  (Fig. 35c) was also found in front of a freely flying blowfly in all measurements described in chapter III.3.3.1 (Fig. 36) it is expected that in this case the pulling speed was identical to the speed the fly would have assumed in free flight ( $\Delta V = 0$ ).



**Fig. 35 a-d** Velocity field in front of a fly pulled manually at various velocities ( $V_{\text{pull}}$ ). Air flow velocity magnitude is color coded (see scale at bottom). The velocities of  $0.51 \text{ m s}^{-1}$  (**b**) and  $0.83 \text{ m s}^{-1}$  (**c**) used to artificially move the fly forward were in the range of those of a freely flying blowfly (Schilstra and van Hateren 1999) whereas  $0.10 \text{ m s}^{-1}$  (**a**) was unnaturally low and  $1.4 \text{ m s}^{-1}$  (**d**) unnaturally high. The horizontally orientated Perspex plate was located 5 cm below the manually pulled fly.

### 3.3 Freely flying blowfly

What does the flow field generated by a freely flying blowfly look like and how does it affect the flow around *Cupiennius*? What information does the flow signal contain which might be used by the spider to perform a successful prey capture jump? To answer these important questions the flow field close to the trichobothria generated by a freely flying blowfly was investigated.

#### 3.3.1 Flow field around freely flying fly

The velocity field in the vertical symmetry plane of the freely flying blowfly differs from that of the stationary tethered as well as from that of the experimentally moved fly. In addition to the backwards and downwards pointing wake of the tethered blowfly there is a “downwash” behind the wake because the wake is now moved together with the fly and air is sucked into the “preceding wake area”. As the wake moves with the fly, it also pushes the air underneath the fly forward. In combination with the “downwash” a circulating flow around the front half of the fly is generated (Fig. 36). The flow field in front of the freely flying fly is similar in shape to that found in the experiment where the fly was pulled manually (Fig. 35c). In the latter experiment the pulling velocity was in the range of the flight velocity of the blowfly (Fig. 41 and Fig. 43) and in good agreement with the findings of Schilstra and van Hateren (1999). The corresponding flows above the spider legs (see orange circles in Fig. 36a) of 26 individual flights were quantified as seen in Fig. 37 to Fig. 44. The velocity information was evaluated in search of the characteristic features in the flow which the spider might use to detect, localize and catch flying prey.

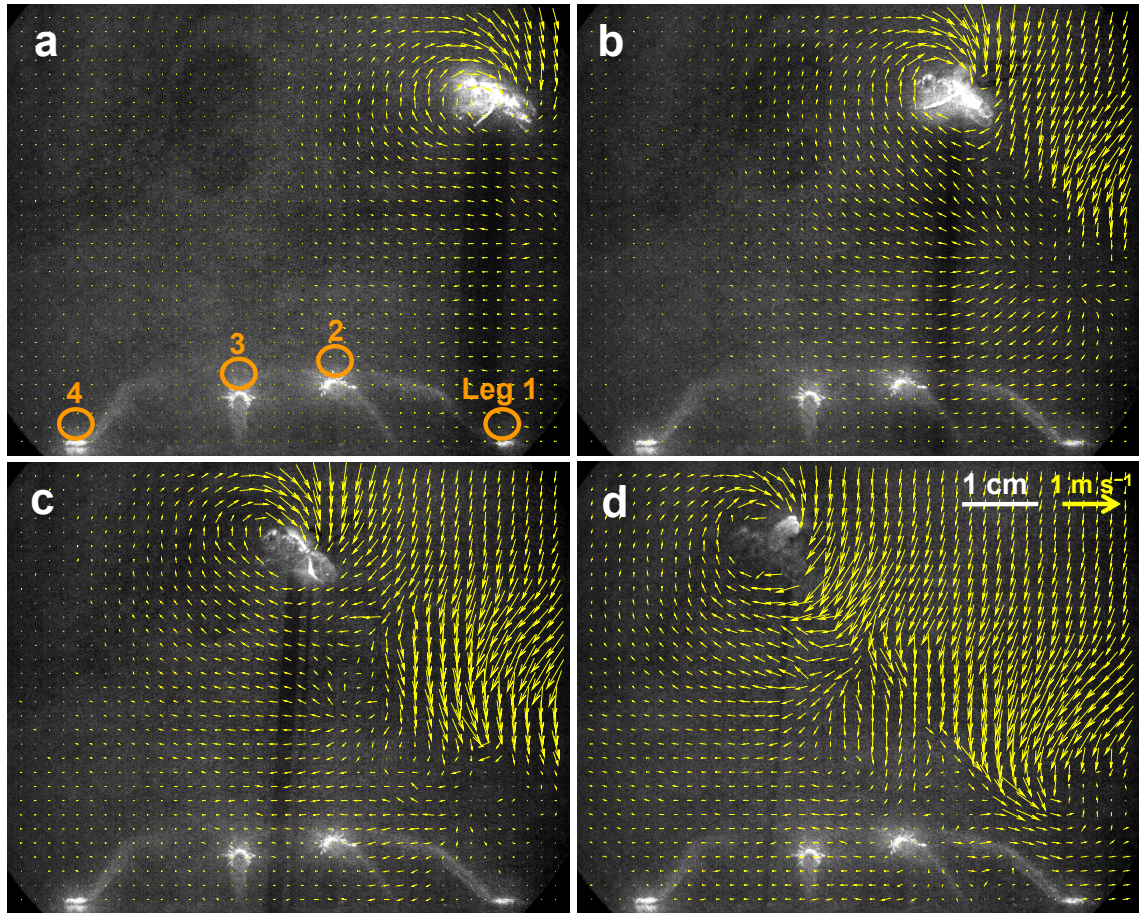


**Fig. 36 a-d** Temporal sequence (time intervals: a-b: 27 ms, b-c: 22 ms, c-d: 28 ms) of vector maps showing the flow field around a freely flying blowfly approaching from the right. The illumination of the fly indicates that it flew directly within the measurement plane (laser light sheet). All four legs on the right side of the spider were cut by the laser light sheet providing measurement points above the tarsus of legs 1 and 4 and above the tibia of legs 2 and 3 (orange circles in a, see also Fig. 7). The flow fields evaluated for 26 flights of freely flying blowflies all showed the same general pattern.

### 3.3.2 Flow signal generated by fly above spider legs

The air flow signal which a freely flying blowfly caused when flying over a spider leg (Fig. 37a) consists of three characteristic phases.

**Phase I:** When the approaching fly is still around 4 cm ( $3.84 \text{ cm} \pm 0.56 \text{ cm}$ ,  $N = 19$ ,  $n = 31$ ) away from of the spider's closest leg the velocity signal first started above the tarsus of this leg and increased exponentially due to the circulating flow in front of the fly (Fig. 36). The fly's horizontal distance at the air flow signal start was independent of the fly's altitude in all 19 flights (Fig. 38, for explanation see chapter IV.5.2) which allows the spider to detect the fly always roughly at the same horizontal distance (see chapter IV.5.2). The exponential coefficients, describing the increase of the flow velocity of these air flows, varied between  $16$  and  $79 \text{ s}^{-1}$  ( $N = 20$ ,  $n = 74$ ) and increased linearly with the horizontal flight velocity (Fig. 43). The rms-values (fluctuations in Tab. 1)

around the exponential fit (see Fig. 42) were  $0.014 \text{ m s}^{-1} \pm 0.007 \text{ m s}^{-1}$  ( $N = 20$ ,  $n = 62$ ) and the relative fluctuations (fluctuations/mean in Tab. 1) were  $33 \% \pm 17 \%$  ( $N = 20$ ,  $n = 62$ ). The maximum velocity ratios simultaneously measured between the different legs (measurement sites are shown in Fig. 36) for each flight range from 2.2:1 to 6.5:1 (mean:  $4.04 \pm 1.32$ , 20 flights).

The transition of the flow field from phase I to phase II occurred when the fly was slightly ahead of the tarsus closest to the approaching fly ( $0.096 \text{ cm} \pm 0.550 \text{ cm}$ ,  $N = 20$ ,  $n = 60$ ).

**Phase II:** When the fly was directly above the tarsus its trichobothria were abruptly exposed to the highly fluctuating flow of the fly's wake (Fig. 37a). This causes an increase ( $p < 0.0001$ , Wilcoxon signed-rank test, null hypothesis: no difference) of the rms-values by an order of magnitude ( $0.113 \text{ m s}^{-1} \pm 0.050 \text{ m s}^{-1}$ ,  $N = 20$ ,  $n = 62$ ) compared to phase I. The rms-values of phase II were determined relative to its mean value. Based on the mean value of each phase the relative fluctuations of phase II ( $70 \% \pm 23 \%$ ,  $N = 20$ ,  $n = 62$ ) are more than twice as large as those of phase I. In Fig. 37b the frequency spectra of the phase I and II flows are shown. Each phase features one characteristic spectrum peak. Averages of the peak frequencies (68 measurements, 20 flights) are significantly higher ( $p < 0.0001$ , Wilcoxon signed-rank test, null hypothesis: no difference) for phase II ( $17.92 \text{ Hz} \pm 4.49 \text{ Hz}$ ) than for phase I ( $8.16 \text{ Hz} \pm 1.62 \text{ Hz}$ , Tab. 1). In addition the standard deviation indicates that the peak frequencies of phase I vary less than half as much than those of phase II. In contrast to phase I (upper frequency limit:  $84.4 \text{ Hz} \pm 33.0 \text{ Hz}$ , Tab. 1), phase II contains frequencies up to  $250 \text{ Hz}$  (upper limit of measurement range) showing several smaller peaks between  $100$  and  $250 \text{ Hz}$  (Fig. 37b).

**Phase III:** When the blowfly was located about  $3 \text{ cm}$  ( $2.98 \text{ cm} \pm 0.74 \text{ cm}$ ,  $N = 19$ ,  $n = 31$ ) beyond the spider's tarsus the signal decayed again.

The flow velocity within all three phases was larger than  $1 \text{ mm s}^{-1}$  and therefore above the detection threshold of the trichobothria (Barth and Höller 1999).



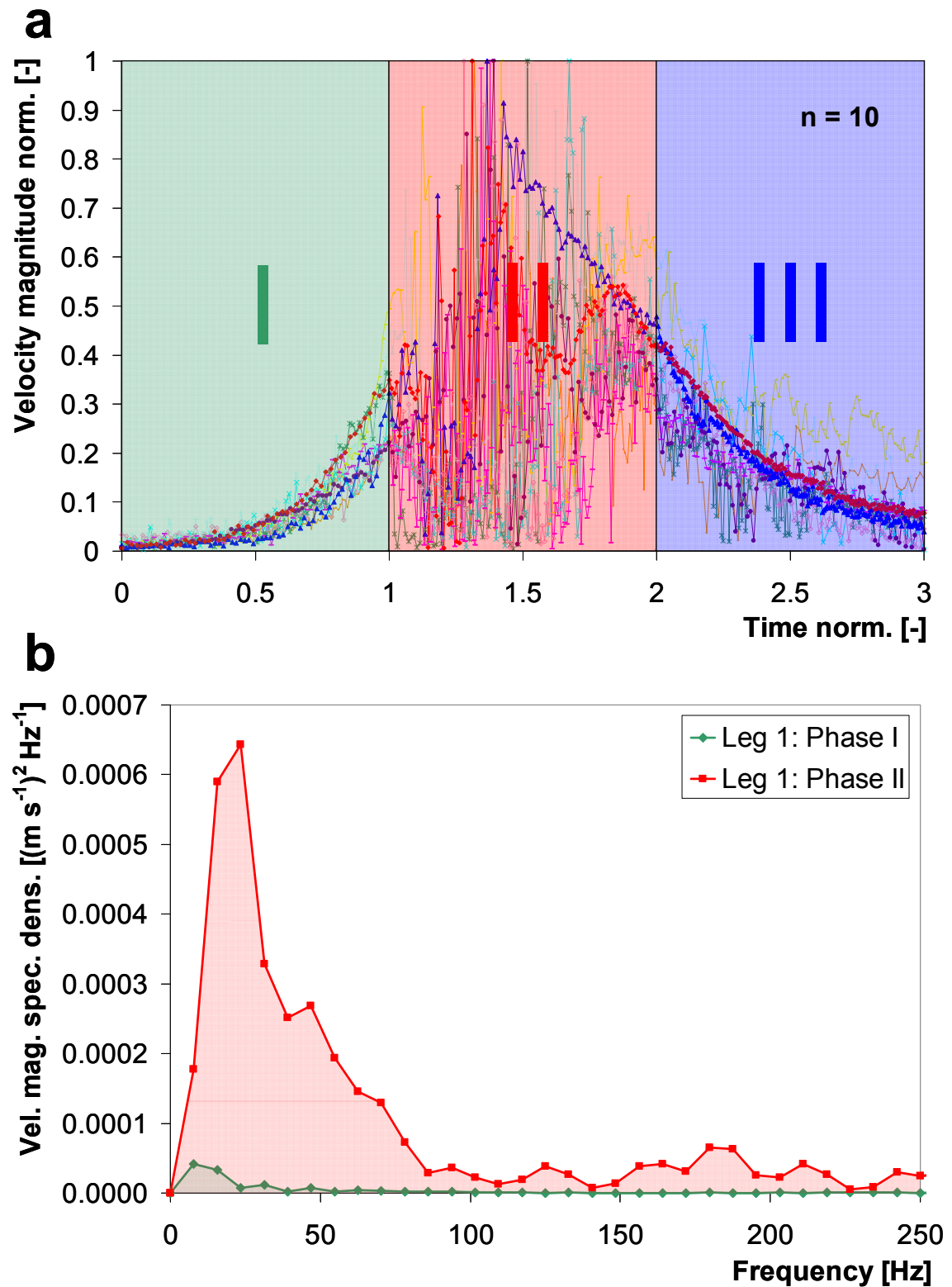


**Fig. 37 a** Velocity magnitude of the air flow signal generated by a freely flying blowfly at the location of the trichobothria (see orange circles in Fig. 36a) when it passes above the spider ( $N = 5$ ,  $n = 10$ ). Each velocity signal is normalized, its maximum representing 1, in order to allow the comparison between different experiments. The time regarding the three phases is normalized as well with phase I ranging from 0 to 1, phase II from 1 to 2 and phase III from 2 to 3. A complete flight in real-time of a blowfly above a spider and passing by its legs 1 to 4 is illustrated In Fig. 40. **b** Spectral density of the velocity magnitude (Vel. mag. spec. dens.) of phases I and II of the fly generated flow



above the tarsus of leg 1 (see orange circle in Fig. 36a). The values on the y-axis are equivalent to the squared velocity magnitude relative to the spectrum's bin width. In each of the 68 experiments ( $N = 20$ ) both the peak frequency of and the energy contained in phase II were larger than those of phase I.

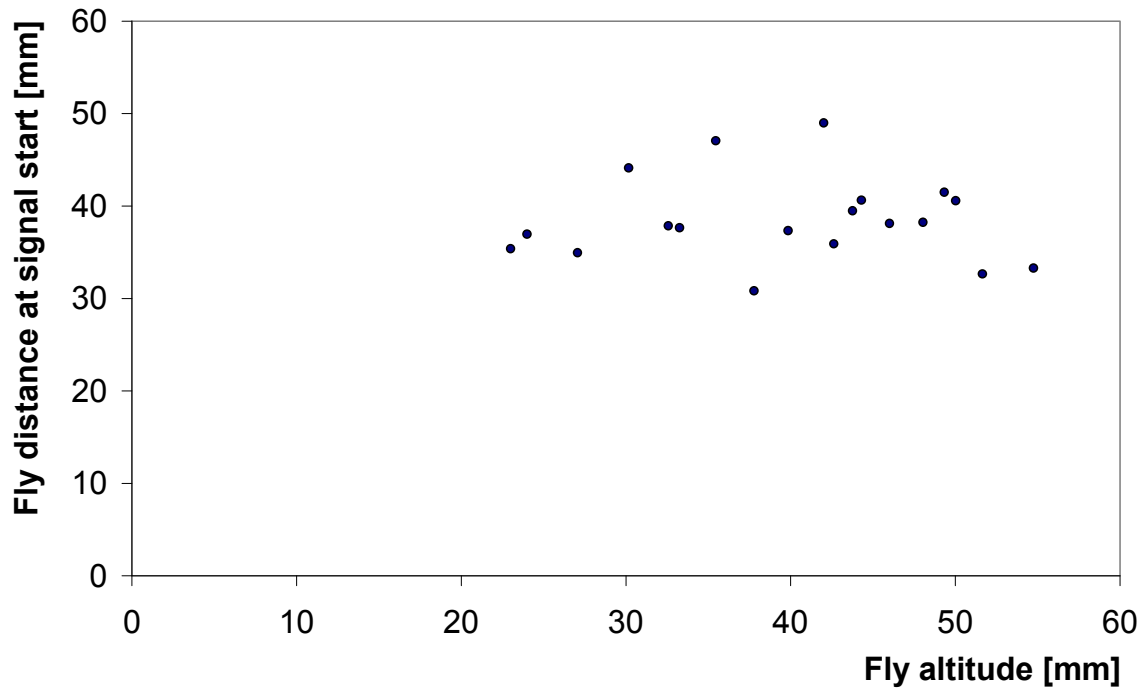


**Fig. 38** Horizontal distance of the approaching fly to the tarsus of the spider's closest leg at signal start in relation to the fly's altitude in 19 flights.

As the flow velocity is measured in a plane the flow vector is composed of a horizontal and a vertical component in a Cartesian coordinate system. These velocity components of the individual phases in Fig. 37a are shown separately in Fig. 39a and b. In phase I the horizontal velocity component contributes more to the flow than the vertical velocity component because of the circulating flow below the fly which is predominantly horizontal. In phase III the vertical velocity components are larger than the horizontal ones due to the almost vertical "downwash" behind the fly (Fig. 36). During phase II the influence of the horizontal component decreased whereas that of the vertical component increased.

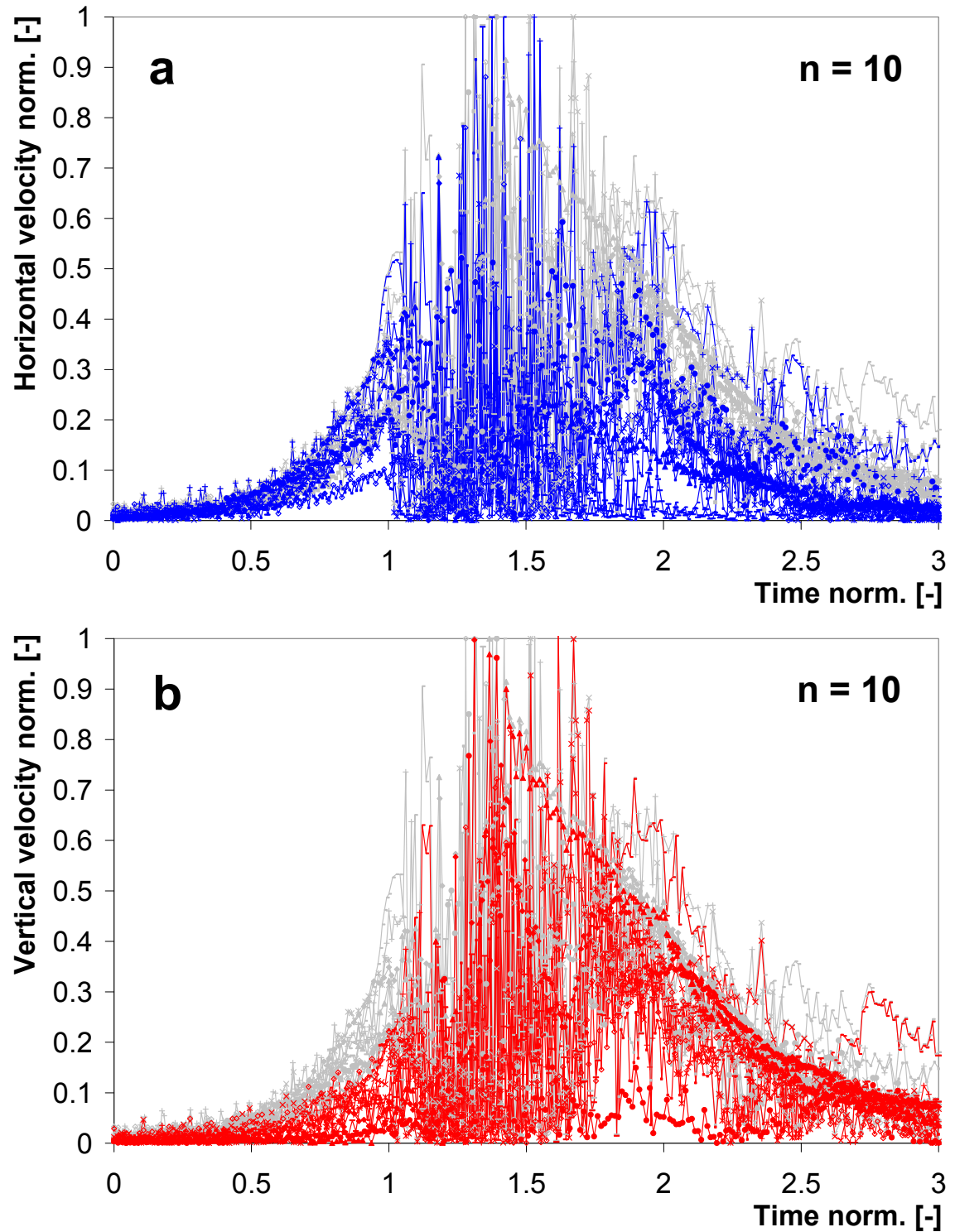


**Fig. 39** Comparison of the horizontal velocity component in blue (**a**) and the vertical component in red (**b**) to the composite velocity magnitude in grey. Flow induced by a freely flying blowfly and also shown in Fig. 37a.

In Fig. 40 the complete flight of a blowfly above a spider and passing by its legs 1 to 4 is illustrated. The air flow signal generated by the fly first started above the leg closest to the approaching fly and then moved with the fly across the spider. The time differences ( $\Delta t$ ) between the air flow signal onsets above leg 1 and leg 4 vary from 0.038 s to

0.108 s (Tab. 1). As seen in Fig. 41  $\Delta t$  decreases with increasing velocity (horizontal component) at which the fly flies as one would expect. However the linear dependency between  $\Delta t$  and the horizontal component of the fly's velocity as shown in Fig. 41 is only valid within the range of velocities shown (13 cm s<sup>-1</sup> and 81 cm s<sup>-1</sup>). Outside this range the curve is a negative power function with  $\Delta t \rightarrow \infty$  for the fly velocity  $\rightarrow 0$  and  $\Delta t \rightarrow 0$  for the fly velocity  $\rightarrow \infty$ . The potential use of the differences in time of the air flow signal arrival for prey localization will be discussed in chapter IV.7.

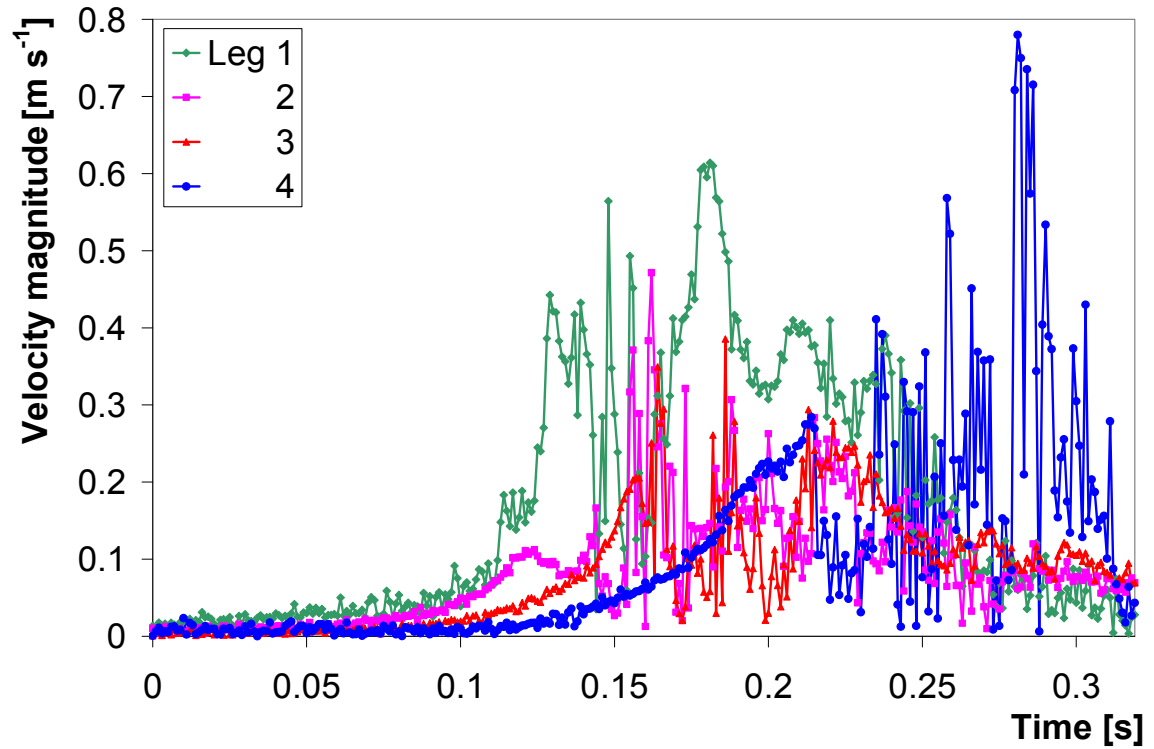


**Fig. 40** Time resolved velocity magnitude of the fly induced air flow above all four legs on one side of the spider (measuring points see circles in Fig. 36a). Here the fly approached the spider from in front (from the right in Fig. 36) of the spider with its trajectory parallel to the spider's symmetry axis.

The exponential coefficients of phase I measured for 20 flights (determined as indicated in Fig. 42) increased linearly with increasing horizontal fly speed (Fig. 43). In addition the fluctuation of the velocity magnitude around the exponential fit also depended linearly on the fly's altitude above the spider (Fig. 44).

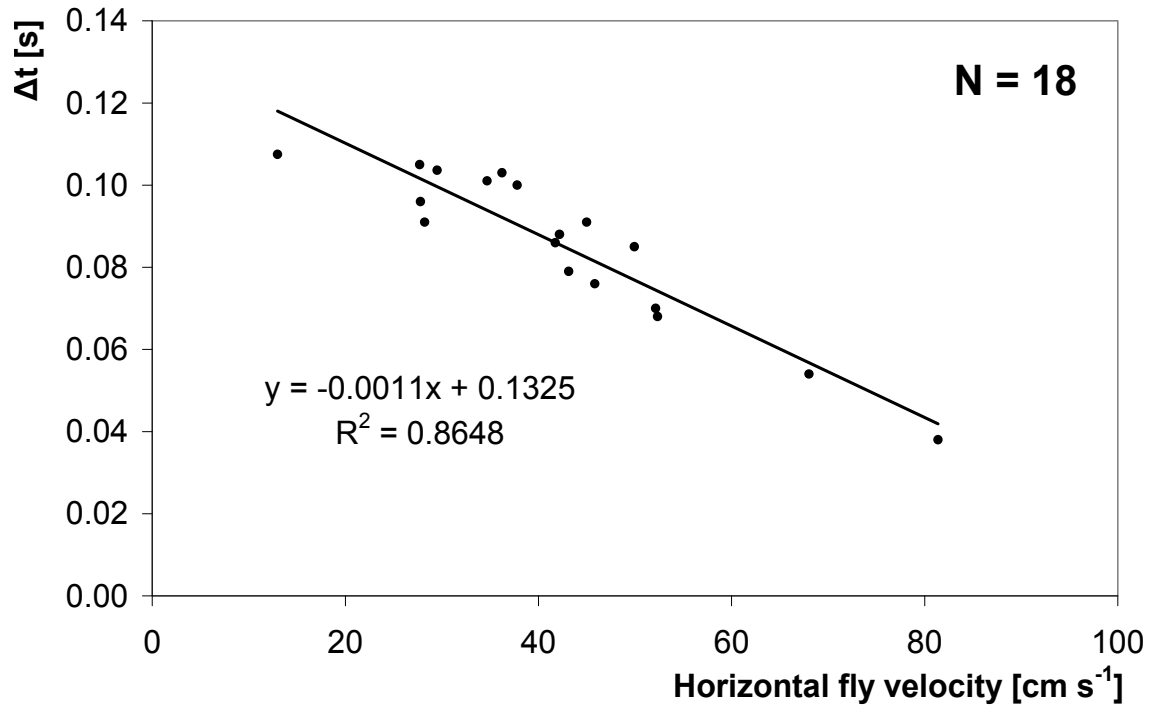


**Fig. 41** Time differences ( $\Delta t$ ) resulting from the delayed onset of the air flow signal generated by the blowfly at legs 1 and 4 (measured at the two outermost circles in Fig. 36a).

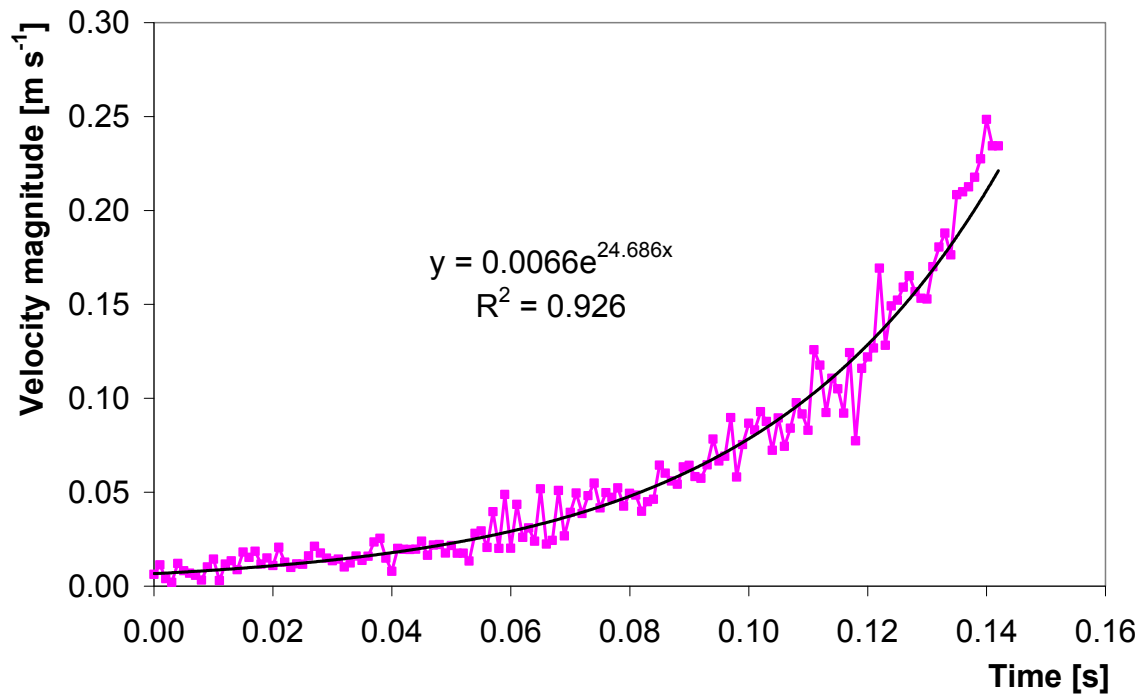


**Fig. 42** Exponential increase of the velocity magnitude during phase I above the tarsus of leg 2. The black curve displays the exponential fit using a coefficient of  $24.686 \text{ s}^{-1}$  (coefficient of determination = 0.926). Based on this fit the rms-values were calculated to determine the fluctuations of phase I shown in Fig. 44.

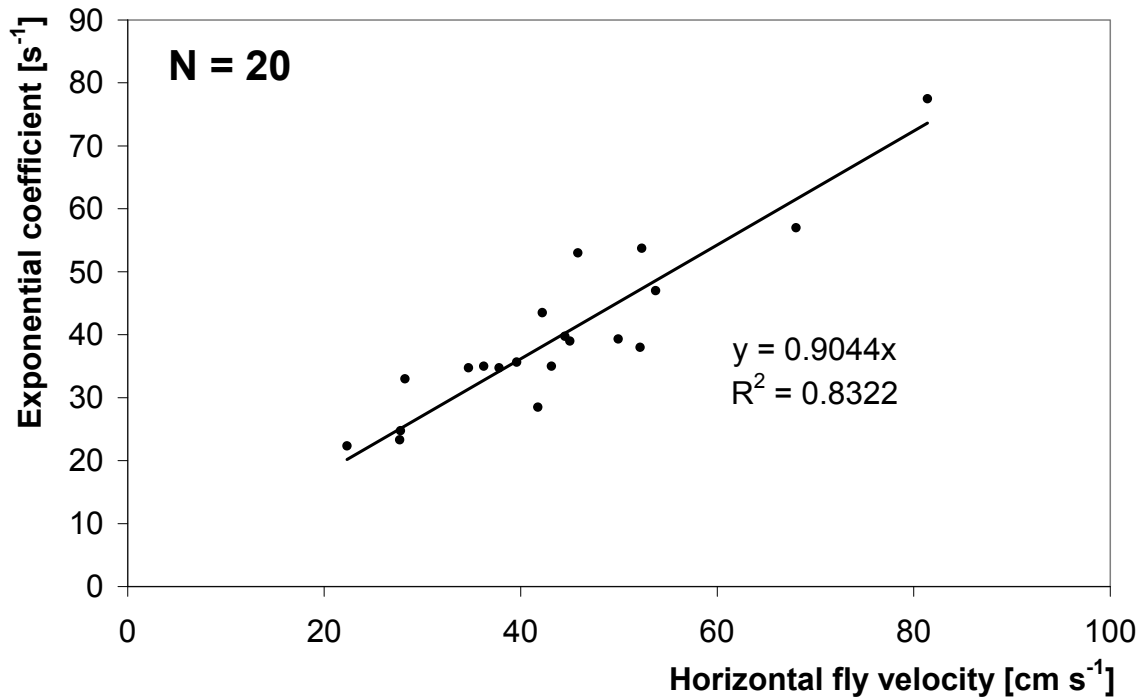


**Fig. 43** The coefficient of the exponential increase of the absolute flow velocity in phase I increases linearly with the fly's horizontal flight velocity.

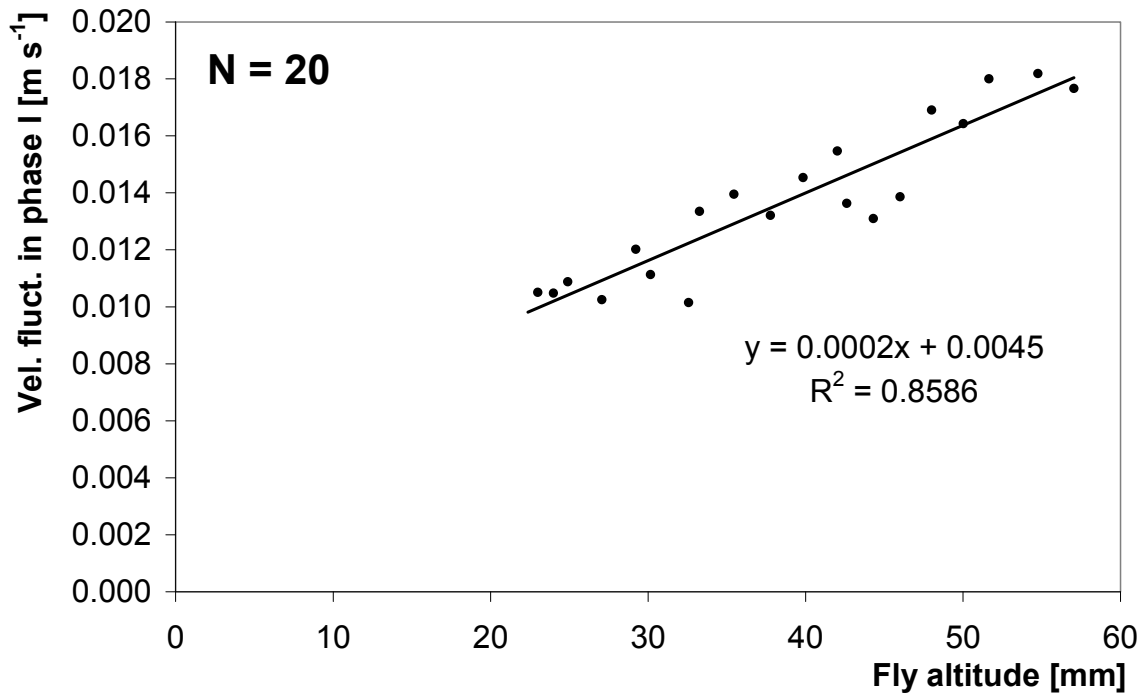


**Fig. 44** The fluctuations of the velocity magnitude in phase I increase linearly with the fly's altitude above the substrate, on which the spider sits. The velocity fluctuations were calculated as rms-values around the exponential fit (see Fig. 42).

**Tab. 1** Summary of important parameters evaluated by DPIV measurements of the airflow above *Cupiennius* and generated by a freely flying blowfly. The mean and rms, the minimum and the maximum value of each parameter were evaluated from  $n$  measurements of  $N$  flights. **Max. velocity** indicates the maximum velocity magnitude in phases I and II.  **$\Delta t$  leg 1-4** is the time difference of the arrival of the velocity signal between leg 1 and leg 4 (Fig. 36 and Fig. 41). The maximum velocity ratios between neighboring legs during phase I are described in the line **Max. intensity ratio**. The peak frequency of the power spectrum in each signal phase is plotted in the row **Spectrum peak** (see Fig. 37b). The **Upper frequency limit** describes the frequency range between 0 Hz and the upper limit. The row **Fluctuations** summarizes the fluctuations of the velocity magnitude around the exponential fit of the signal in phase I (Fig. 42 and Fig. 44) and around the mean in phase II. In **Fluct./mean** the fluctuations from above are based on the mean value of each phase. The values of exponential coefficients, described in Fig. 42, are noted as **Velocity gradients**. The bottom two rows document the **Horizontal velocity** and the **Altitude** above the spider of all analyzed flights (see also Fig. 41, Fig. 43 and Fig. 44)

		Fly generated flow			N	n
		Mean $\pm$ Rms	Min	Max		
<b>Max. velocity [m s<sup>-1</sup>]</b>	<b>Phase I</b>	0.164 $\pm$ 0.051	0.080	0.300	25	25
	<b>Phase II</b>	0.639 $\pm$ 0.218	0.134	1.046	25	25
<b><math>\Delta t</math> leg 1- 4 [s]</b>	<b>Start Ph I</b>	0.086 $\pm$ 0.019	0.038	0.108	18	18
<b>Max. intensity ratio</b>	<b>Phase I</b>	4.0 $\pm$ 1.3	2.2	6.5	20	20
<b>Peak of spectrum [Hz]</b>	<b>Phase I</b>	8.2 $\pm$ 1.6	7.8	15.6	20	68
	<b>Phase II</b>	17.9 $\pm$ 4.5	15.6	31.3	20	68
<b>Upper frequency limit [Hz]</b>	<b>Phase I</b>	84.4 $\pm$ 33.0	23.0	156.0	20	68
	<b>Phase II</b>	247.7 $\pm$ 11.5	164.0	250.0	20	68
<b>Fluctuation [m s<sup>-1</sup>]</b>	<b>Phase I</b>	0.014 $\pm$ 0.007	0.005	0.037	20	62
	<b>Phase II</b>	0.113 $\pm$ 0.050	0.018	0.248	20	62
<b>Fluct./mean [%]</b>	<b>Phase I</b>	33 $\pm$ 17	8	85	20	62
	<b>Phase II</b>	70 $\pm$ 23	23	125	20	62
	<b><math>\Delta</math>Phases</b>	37 $\pm$ 26	-8	109	20	62
<b>Velocity gradient [s<sup>-1</sup>]</b>		40.297 $\pm$ 14.592	16.000	79.000	20	74
<b>Horizontal velocity [cm s<sup>-1</sup>]</b>		41.32 $\pm$ 16.04	12.98	81.40	26	26
<b>Altitude [mm]</b>		38.76 $\pm$ 10.88	22.37	57.04	26	26



## 4. Prey capture behavior induced by synthetic air flows

In the preceding chapter (III.3.3) the flow field generated by a freely flying blowfly was examined close to the trichobothria. To prove, that the air flow velocities are a sufficient stimulus to elicit prey capture, behavioral experiments exposing the spider to synthetic flows were carried out. A simple mechanical device consisting of a rotating cylinder and a fender (Fig. 8) was used to simulate the natural stimulus (chapter III.4.1).

As previous results had suggested that the fluctuating flow pattern contained in phase II is eliciting the spider's prey capture jump, the spider was exposed to a synthetic air flow signal without these fluctuations as well (see chapter III.4.2).

### 4.1 Complete signal

To simulate the flow velocity signal generated by a freely flying blowfly close to the spiders' trichobothria a mechanical device was developed which is described in chapter II.4.1.

Fig. 45a shows the similarity of the artificial fly-like air flow measured above the spider leg to the natural air flow. As seen from a comparison of the frequency spectra of the fly signal (Fig. 37b) with that of the synthetic signal (Fig. 45b) the structures of phase I and II are very similar indeed in both cases. In both signals phase I consistently reaches its maximum at 8 Hz, with a spectral density below  $0.0001 \text{ (m s}^{-1}\text{)}^2 \text{ Hz}^{-1}$ . In phase II the signals reach their maxima at 17.9 Hz (fly) and 15.65 Hz (synthetic), respectively, with spectral densities around  $0.0006 \text{ (m s}^{-1}\text{)}^2 \text{ Hz}^{-1}$ . In contrast to phase I, where the bulk of both signals (fly and synthetic) occur at frequencies below 20 Hz, the main part of the signals of phase II is below 70 Hz. In addition several smaller peaks could be measured up to 250 Hz in phase II of both the natural and the synthetic flow indicating a frequency content expanded as compared to that of phase I.

During the behavioral experiments the spider was stimulated by pulling the synthetic air flow generator horizontally 5 cm (measured from the lower edge of the cylinder to the floor) above the substrate (like the fly in chapter III.1 and III.2.3) with the spider. Three out of four spiders jumped during the sessions at least once (Fig. 46). The percentages of jumps towards the stimulus did not differ significantly ( $p = 0.683$ , Mann-Whitney test, null hypothesis: no difference) between experiments using the synthetic fly flow (23.3 %) and the fly (19.3 %), respectively. Due to the bigger size of the target the ratio of successful jumps (see example in Fig. 47) is more than three times higher in case of the synthetic flow (18.3 %) than in case of the natural fly signal (5.1 %). As the fly stimulus and the synthetic stimulus were answered with 49.9 % and 46.7 %, respec-

tively, by either a slight reaction or jump, the spider is equally attracted ( $p = 0.556$ , Mann-Whitney test, null hypothesis: no difference) to both types of flow.

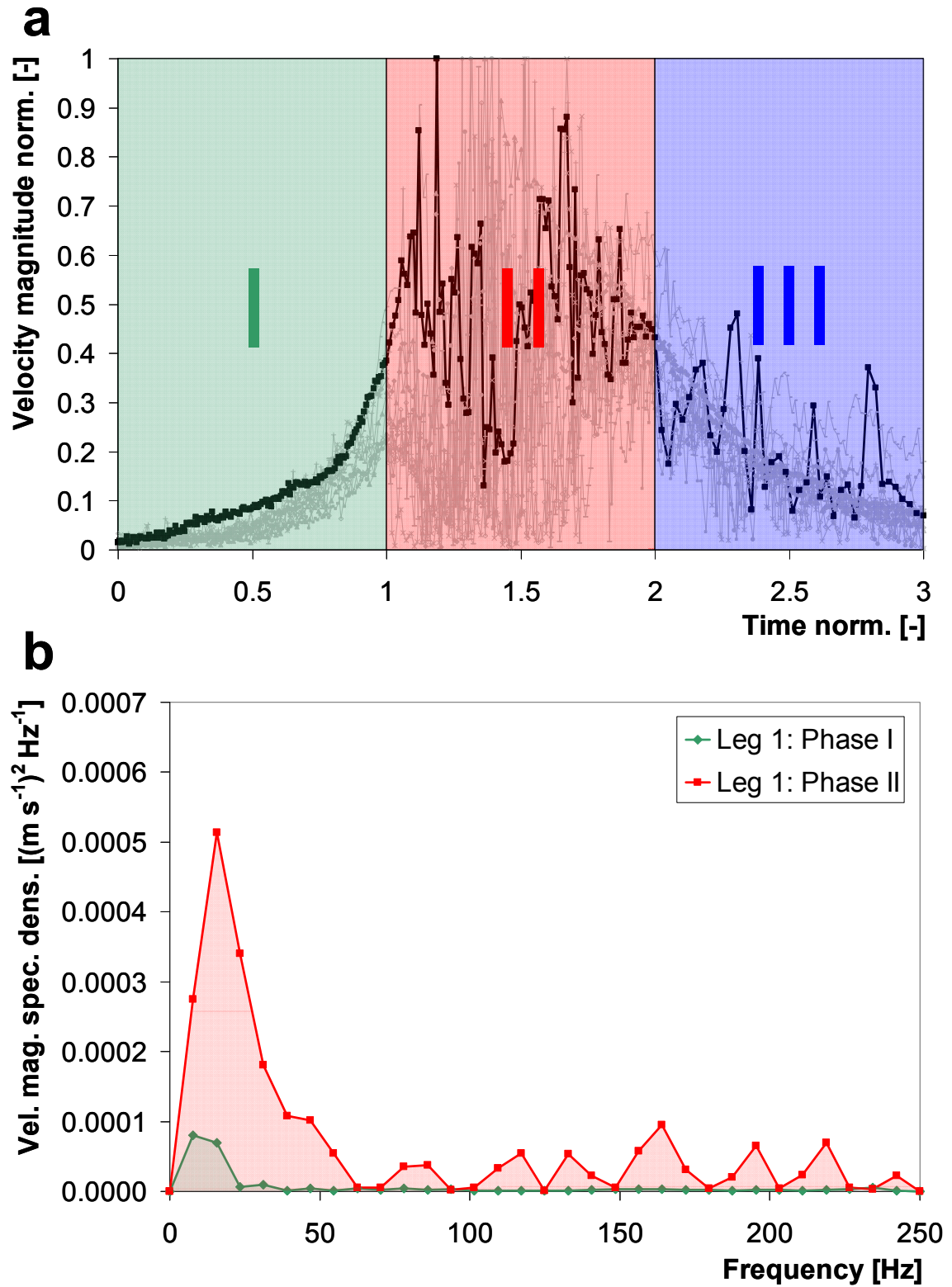


**Fig. 45** **a** Normalized velocity magnitude of the artificial air flow signal generated by the “fly flow generator” (black line) at the location of the trichobothria (measurement areas see orange circles in Fig. 36a) when pulled over the spider at fly-like velocities ranging from  $13 \text{ cm s}^{-1}$  to  $81 \text{ cm s}^{-1}$  (Tab. 1). The results of the ten flights of the freely flying blowfly from Fig. 37a are plotted in grey for

comparison. The graphs are normalized as in Fig. 37a. **b** Spectral density of the velocity magnitude (Vel. mag. spec. dens.) of phases I and II obtained for one measurement of the synthetic fly flow above the tarsus of leg 1 (see orange circle in Fig. 36a). The values on the y-axis are equivalent to the squared velocity magnitude relative to the spectrum's bin width.

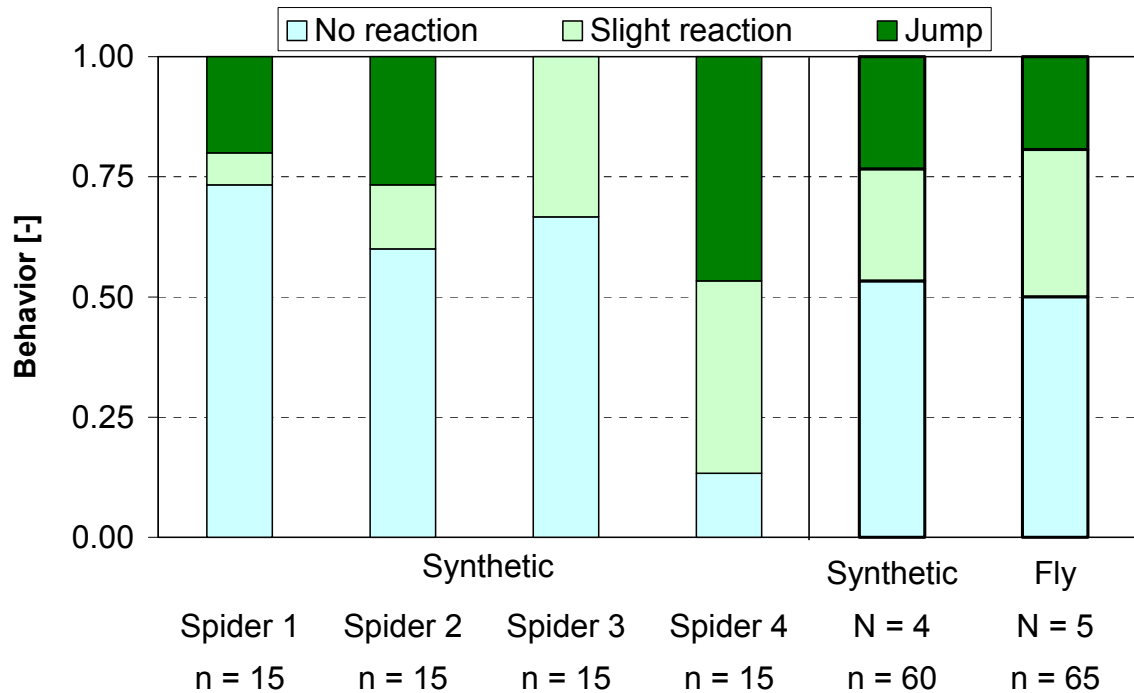


**Fig. 46** Results of behavioral experiments using the synthetic fly flow generator moved over the spider sitting on a damped, stiff and heavy metal plate (Fig. 15). The fifth column from the left displays the mean values for four individuals (first four columns from the left). In each session the spider was exposed to the stimulus ten consecutive times. The session was then classified with regard to the spider's most active response. The behavioral categories were: no reaction, slight reaction and jump. The classified sessions were added and plotted in normalized form the total amount of the sessions corresponding to the value 1. These mean values ("synthetic") are compared to the ones shown in Fig. 23 resulting from the experiment with the tethered blowfly pulled manually over the damped stiff plate ("fly", column on the right).

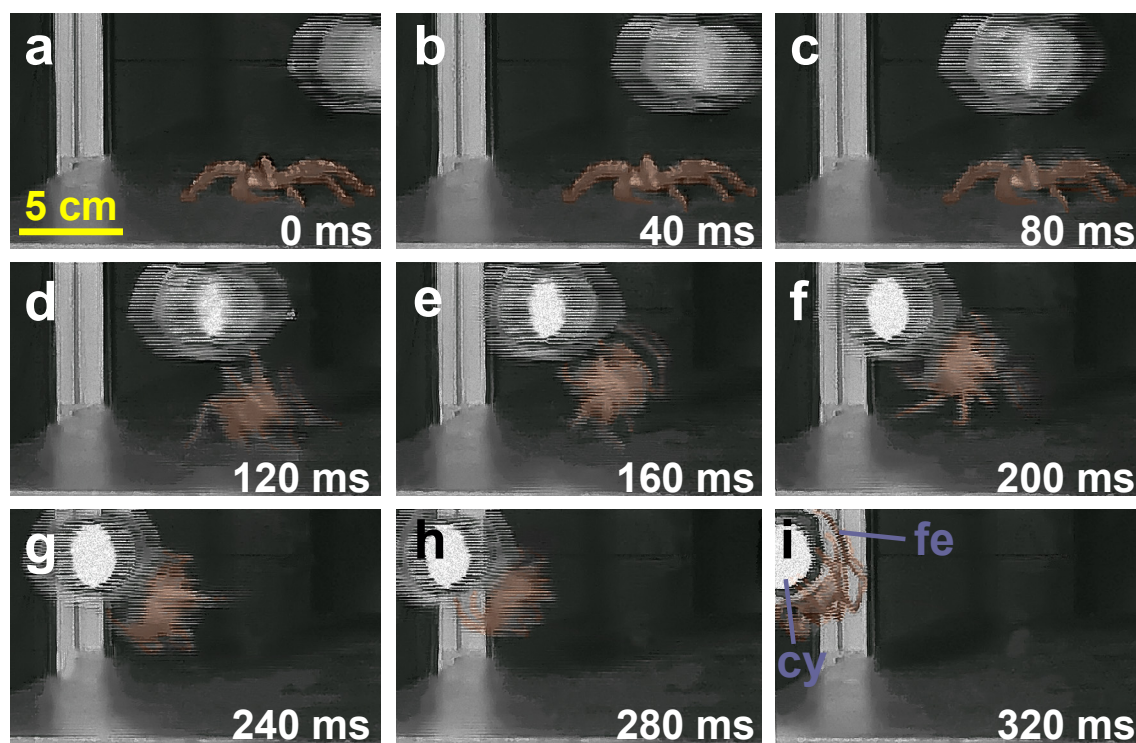


**Fig. 47 a-i** Sequence of pictures showing the successful “capture” of the rotating cylinder (cy) with the fender (fe) attached which was used to simulate the fly-generated natural air flow. The stimulus source was horizontally moved at 5 cm (measured from the lower end of the cylinder) above the spider which sat on a stiff and heavy metal plate (Fig. 15) to exclude substrate vibrations induced by the stimulus. When the stimulus was pulled over the spider it raised both first legs on each side and transferred its center of gravity backwards (**d**). Afterwards the spider released the jump mostly by extending legs 4 on both sides and “caught” the device. The experiment was performed under red light which was filtered when editing the photographs for the figure.

## 4.2 On the significance of phase I

In the quasi-natural situation the spider jumped towards the fly when it was directly above the tarsus of the spider leg closest to it (see chapter III.1). At this point in time the flow sensors on the tarsus were exposed to the transition of the airflow from phase I to phase II (see chapter III.3.3.2). Therefore the onset of phase II may well be responsible for triggering the jump. To decide on this hypothesis we investigated the reaction of the spider towards a stimulus simulating only phase I of the fly signal and not containing the fluctuations typical of phase II. The absence of a jump of the spider towards the artificial “phase I only” stimulus would support the hypothesis.

In addition to the setup shown in Fig. 8 an airflow deflector was mounted to the rear end of the rotating cylinder (Fig. 13) in order to get rid of the wake which causes the fluctuations during phase II of the fly signal (see chapter II.4.2 for detailed description). This velocity signal (black line) is displayed in Fig. 48a. Phase I was still reasonably similar to that of the natural fly flow signal (grey lines). The frequency content of the

velocity increase (phase I) (Fig. 48b) still nicely imitated that of the naturally generated fly flow (Fig. 37b) and that of the complete synthetic fly-like air flow (Fig. 45b) as did the structure, peak frequency and the spectral density of the velocity magnitude. At the end of phase I (transition to phase II) the frequency content of the velocity signal did not change (Fig. 48b) as it would in the natural (Fig. 37b) and also in the complete synthetic fly-like air flow (Fig. 45b). This is important as our intention was to examine the effect of the (missing) flow fluctuations on the behavior. During phase III, which follows phase II, the signal decays again. As the spider jumps not later than during phase II, phase III of the natural fly signal does not influence the prey capture behavior of the spider. Therefore it is important that the fluctuations which occur during the natural fly signal (grey lines in Fig. 48a) are also excluded during phase III of the synthetic flow signal with the wake deflected (black line in Fig. 48a).

When exposing the spider to the flow signal shown in Fig. 48 its behavior changes significantly in regard to the occurrence of jumps ( $p < 0.0001$  Mann-Whitney test, null hypothesis: no difference) (Fig. 49). Without the fluctuations of phase II no prey capture jump could ever be elicited in 75 sessions (second column from right in Fig. 49) whereas on average in 23.3 % of the sessions prey capture jumps were recorded when exposing the spider to the complete synthetic fly-like airflow (column on the right in Fig. 49). But there is no significant difference ( $p = 0.968$ , Mann-Whitney test, null hypothesis: no difference) between the percentage of slight reactions (exclusive jumps) towards the complete synthetic fly-like airflow (23.3 %) and those towards the stimulus of only phase I (25.3 %) of the synthetic fly-like air flow (Fig. 49).

By analyzing the motion sequences extracted from video film recordings of all 32 slight reactions triggered by the flow stimulus contained in phase I (example shown in Fig. 50) it could be observed that in all cases the reaction was directed towards the approaching device. Furthermore in 16 out of 32 cases the spider twitched with those legs first which were closest to (and pointed towards) the approaching device (see Fig. 50). During the remaining 16 slight reactions the spider responded also in direction towards the stimulus but it twitched with more than one leg during the same time period of 40 ms between two frames of the video recording.

In 73.3 % of the sessions exposing the spider to the synthetic fly flow with the wake deflected the spider showed no reaction. As only in 53.3 % of the sessions offering the complete synthetic fly stimulus no reaction was observed the spider reacted almost significantly more towards this stimulus ( $p = 0.056$ , Mann-Whitney test, null hypothesis: no difference) which it additionally answers with a prey capture jump.

Further detailed interpretation of the behavior concerning detection, recognition, localization and prey capture jump will be given in the discussions (chapter IV.5 to IV.8.)

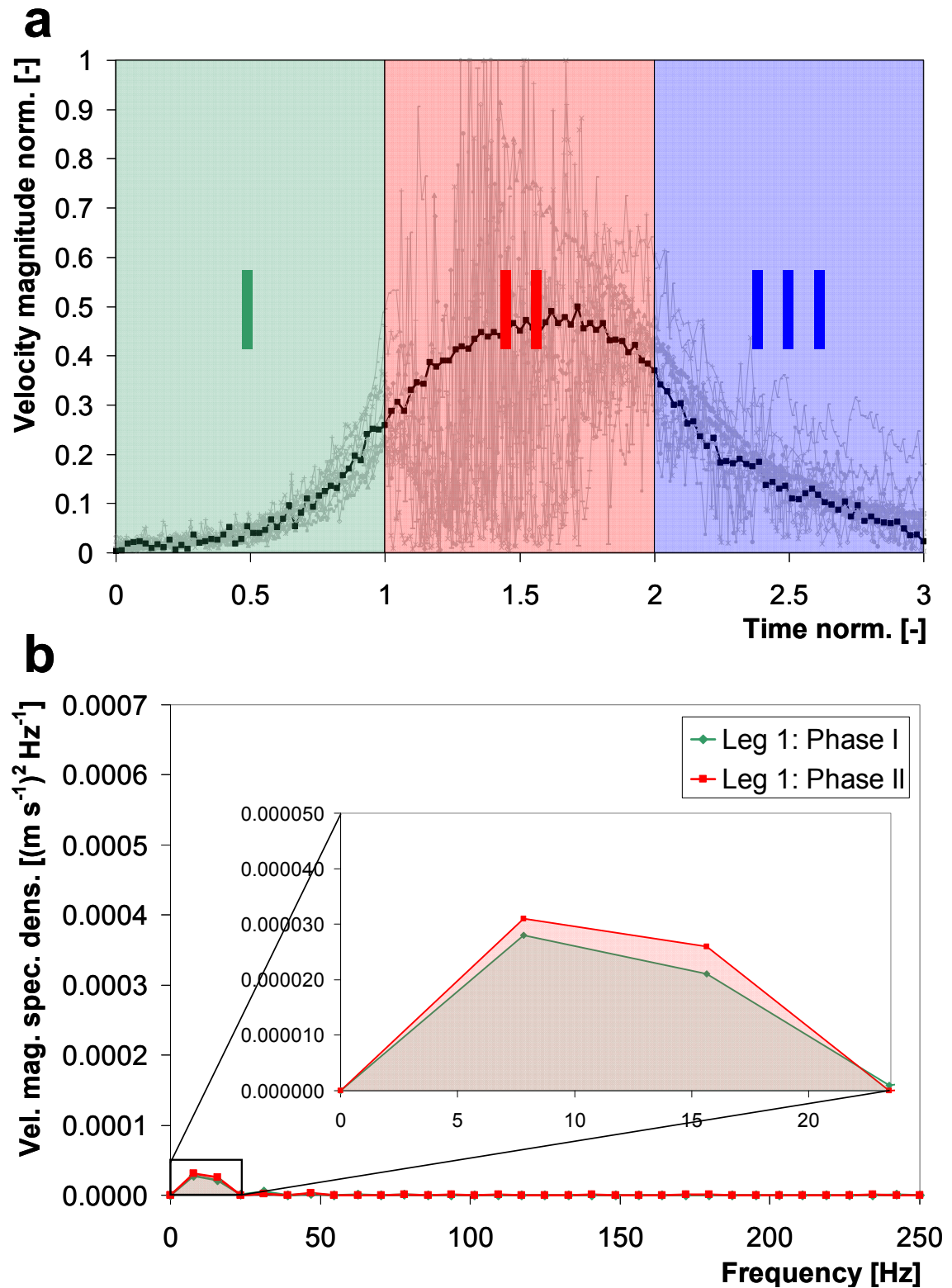


**Fig. 48 a** Velocity magnitude of the air flow signal generated by the fly flow generator with the deflector attached in order to exclude the fluctuating phase II (black line) of the natural fly flow signal (grey lines). Flow measurement at the location of the spider's sensors (see orange circles in Fig. 36a) when the flow source was pulled over the spider. Values for ten flights of the freely flying blowfly from Fig. 37a are plotted in grey for comparison. The graphs are normalized in the same way as in Fig. 37a. **b** Spectral density of the velocity magnitude (Vel. mag. spec. dens.) of phases I and II shown in **a**. The values on the y-axis are equivalent to the squared velocity magnitude relative to the spectrum's bin width.



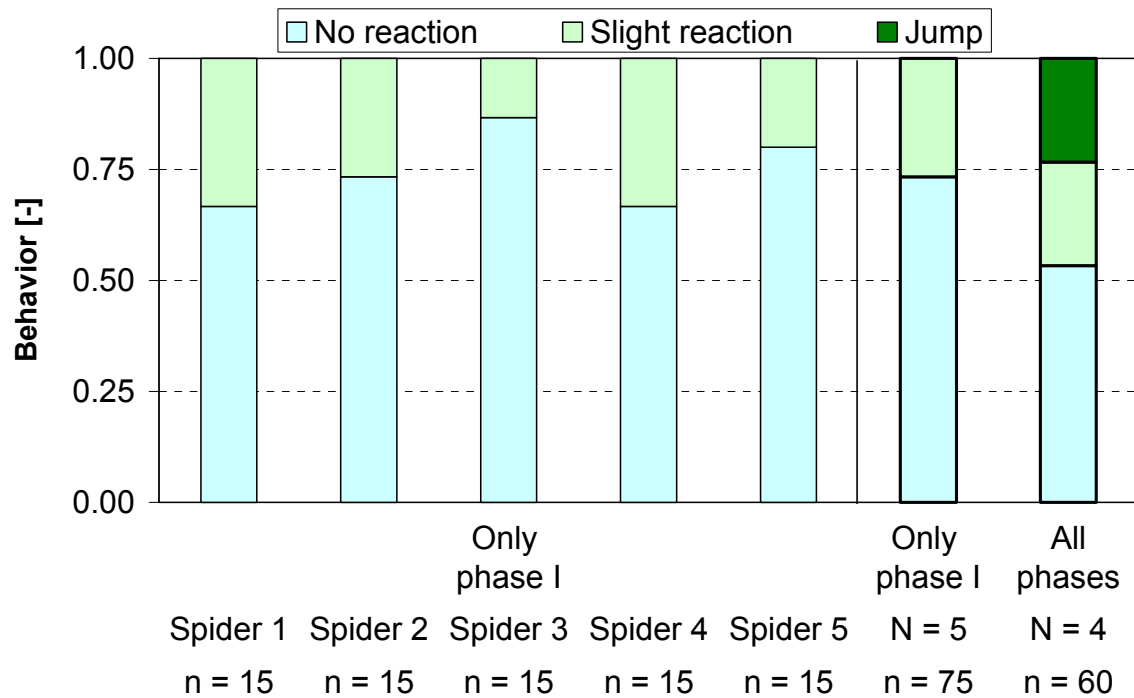


**Fig. 49** Behavioral experiments using the synthetic flow of phase I only (see Fig. 48). The spider sat on a damped stiff and heavy metal plate to avoid substrate vibrations (Fig. 15). The sixth column from the left displays the mean values of the behavioral reactions of five individuals (first five columns from the left). During each session the spider was exposed to the stimulus ten consecutive times. The session was then classified with regard to the spider's most active response. The behavioral categories were: no reaction, slight reaction and jump. The classified sessions were added and plotted in normalized form. The total amount of the sessions corresponds to 1. These mean values ("only phase I") are compared to the ones of Fig. 46 where the entire signal was used as stimulus ("all phases", column on the right).

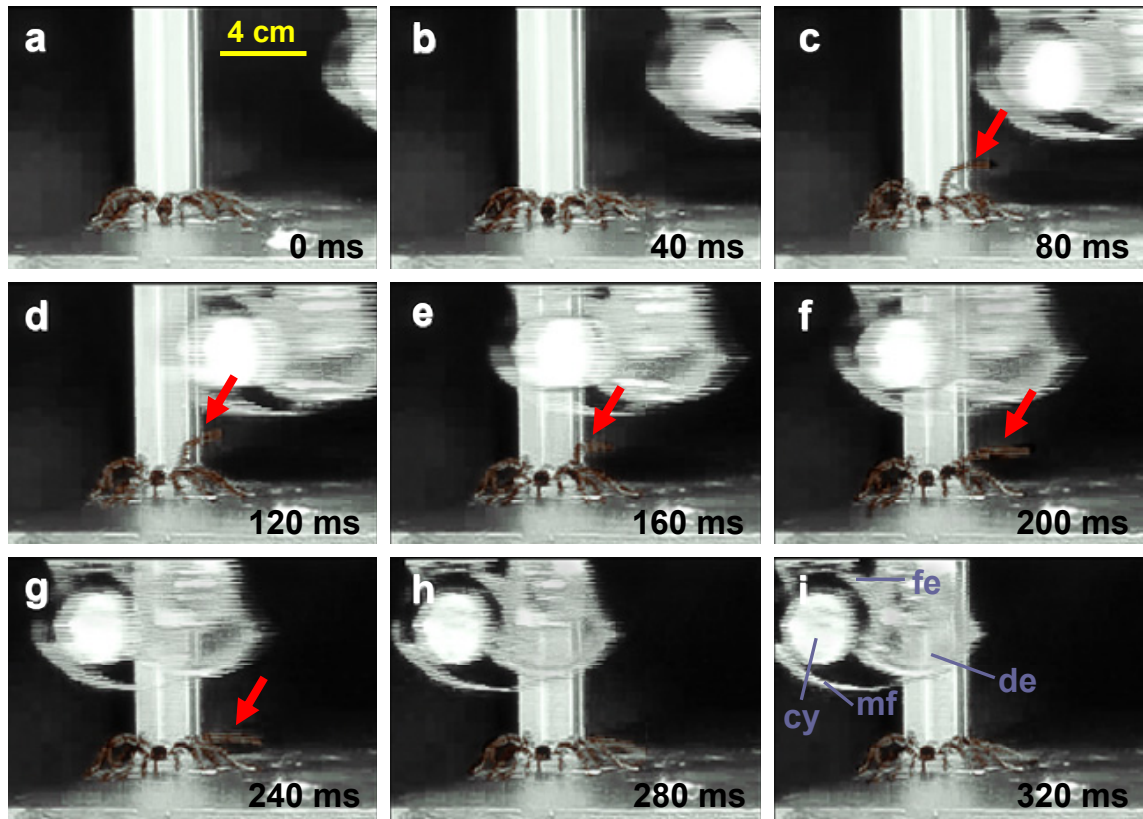


**Fig. 50 a-i** Sequence of pictures showing a slight reaction but no jump of a spider when exposed to the air flow generated artificially by a rotating cylinder (cy) with deflector (de) which excluded phase II of the natural flow. The spider twitched first with the leg closest to (and pointing towards) the approaching stimulus (see arrow). The experiment was performed under red light which was filtered afterwards when preparing the figure. *fe* fender, *mf* meshed fence.

### 4.3 Control experiment

To ensure that the spiders' reactions were elicited by the synthetic air flow signal only the fly flow generator was pulled over the spider with the rotating cylinder turned off. Although the pulling itself of such a device causes airflow with velocities of up to  $0.025 \text{ m s}^{-1}$  at the spiders' sensors the flow pattern characteristic of the fly is absent and therefore the spider should not react to it. In addition the control experiment also explores whether the spider can sense the device in another way (substrate vibration, vision or airborne sound e.g. induced by the linear bearing when the stimulus was pulled horizontally).

In general, when *Cupiennius* receives a prey signal it immediately takes its characteristic hunting position and waits motionless in this position (typical for sit-and-wait hunter) to attack the prey when it is close enough. This behavior could be observed during the experiments with both the natural (chapter III.1 and III.2.2) and artificial (chapter III.4.1 and III.4.2) fly flow. By contrast during the control experiments the spider did

not take its characteristic hunting position but was undirected wandering around. Obviously the presented stimulus in the control experiment did not reach its attention

None of the four animals tested ever jumped. During the control experiment significantly fewer slight reactions were observed than during exposure to phase I of the synthetic flow stimulus ( $p = 0.009$ , Mann-Whitney test, null hypothesis: no difference) (Fig. 51). However two of four tested animals showed reactions in altogether 2 of the 60 sessions which were directed away from the signal source. In contrast, the slight reactions elicited by the artificial “phase I only” airflow were directed towards the stimulus (Fig. 50). This leads to the conclusion, that the spider senses the device but due to the absence of the characteristic flow pattern it identified it as “non prey”.

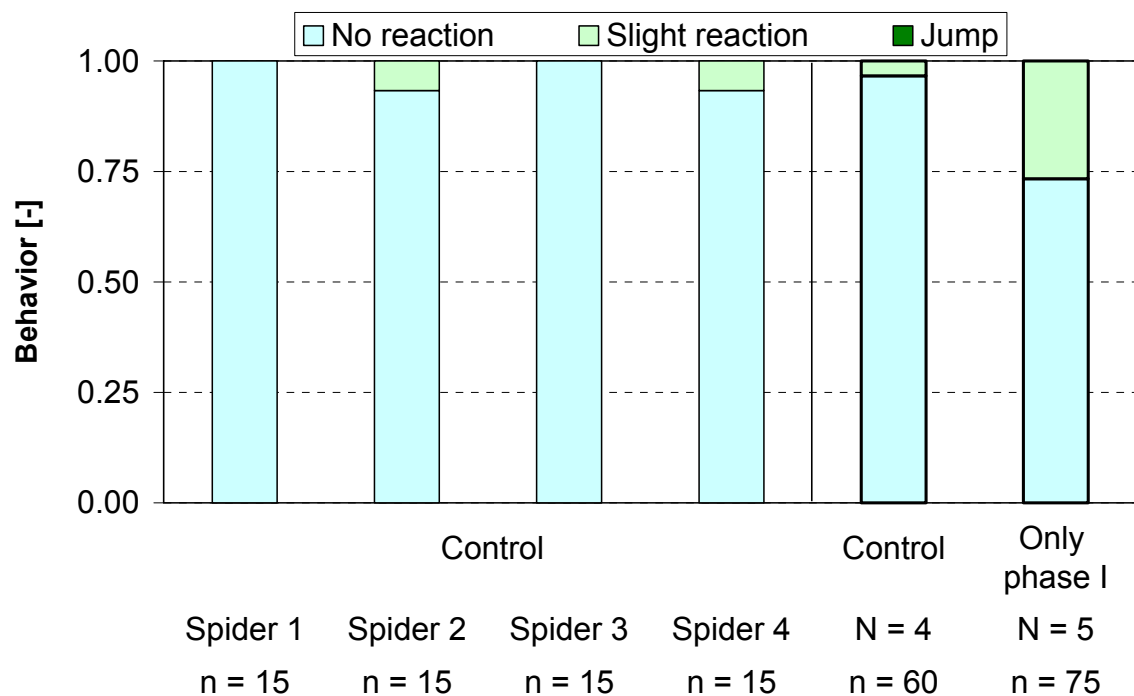


**Fig. 51** Control experiment with the fly flow generator moved over the spider but the rotating cylinder turned off. The fifth column from the left displays the mean values of the behavioral reactions of four individuals (first four columns from the left). During each session the spider was exposed to the stimulus ten consecutive times. The session was then classified with regard to the spider’s most active response, distinguishing between: no reaction, slight reaction and jump. The classified sessions were added and plotted in normalized form. The total amount of the sessions corresponds to 1. These values (“control”) are compared to the ones of Fig. 49 obtained when using the rotating cylinder but deflecting the wake (“only phase I”, column on the right). In both experiments there were no jumps at all.

## IV. DISCUSSION

The following discussion of the results is divided into three parts.

First the **influence of the substrate** (chapter IV.1) as well as the **influence of the number of repeated identical sessions** (chapter IV.2) on the spider's behavior are discussed. In addition the differences between the **sound pressure fields** around *Lucilia sericata* and *Calliphora erythrocephala* (chapter IV.3) are explained.

Second the flow fields around the fly in three different arrangements, **stationary tethered** (see chapter III.3.1), **manually moved forward** (see chapter III.3.2) and **freely flying** (see chapter III.3.3), are discussed. The conclusion is that only freely flying blowflies ensure a relevant description of the flow field.

The third part deals with the basic questions of orientation. How might the spider use the flow information to **detect** (chapter IV.5), **recognize** (chapter IV.6) and **localize** (chapter IV.7) flying prey and what elicits the **jump** towards it (chapter IV.8)?

### 1. Influence of the substrate on the capture of flying prey

Behavioral experiments in chapter III.1 showed that *Cupiennius*, sitting on a bromeliad leaf, is able to successfully capture a humming blowfly which was pulled horizontally 5 cm above it. In chapter III.2.2 leaf oscillations, simultaneously recorded during these behavioral experiments, were evaluated (see Fig. 20) to find out if the spider is able to sense the blowfly through these vibrations. Therefore these oscillations are compared to the threshold curves of the slits in the vibration sensitive metatarsalorgan for both dorsoventral and lateral deflections of the tarsus determined by Barth and Geethabali (1982).

The mean thresholds for dorsoventral deflections at the fly's mean wing beat frequency of 160 Hz range between 70 nm (slit 3) and 300 nm (slit 7). These thresholds are 10 and 42 times higher, respectively, than our mean value of the leaf's vertical deflection due to the humming fly. Even the smallest threshold value for dorsoventral deflections (50 nm) is still 5.4 times higher than the largest vertical leaf deflection (9.18 nm). As the horizontal leaf vibrations induced by the fly only occur in the direction of the leaf axis (x-direction) the tarsus is at most deflected when it is aligned perpendicular to the leaf axis (y-direction). With the tarsus in this arrangement the thresholds for stimulation by lateral deflection, which range from 100 nm (slit 6) to 300 nm (slit 5), are between 18 and 53 times higher than the measured leaf displacements.

Moreover, the thresholds determined by Barth and Geethabali (1982) just describe the movement of the tarsus' tip relative to the metatarsus. These thresholds can only be directly compared with the leaf deflections in case the spider's metatarsus is not deflected with the leaf. However as the metatarsus (and the whole spider) oscillates to some extent with the leaf the deflection of just the tarsal tip is always less than the leaf deflection. This implies that the deflection thresholds determined by Barth and Geethabali (1982) between the tarsal tip and the metatarsus are not yet reached when the leaf is deflected with those threshold amplitudes.

The overall conclusion is that *Cupiennius*, sitting on a bromeliad, is not able to detect the blowfly by the leaf vibrations it induces when it is pulled along a straight path 5 cm above the spider.

This conclusion is proven as *Cupiennius* was able to successfully capture the blowfly under the same conditions as in chapter III.1 (apart from the substrate) when sitting on a damped heavy and stiff metal plate (chapter III.2.2).

This indicates that the substrate on which *Cupiennius* sits does not influence the prey capture of flying prey.

## **2. Influence of the number of repeated identical sessions on the spider's willingness to jump**

Therefore every set of 15 identical sessions of each spider during an experiment was divided into three categories: first (sessions 1 to 5), middle (sessions 6 to 10) and last (sessions 11 to 15). Although most of the jumps were recorded during the first sessions (21) the difference was not significant ( $p = 0.3651$ , Mann-Whitney test, null hypothesis: no difference) to the amount of jumps recorded during the last sessions (11). Furthermore during the middle sessions the spider elicited the lowest amount of jumps (8).

Therefore we can conclude that the willingness to jump is neither constantly increased (learning effect) nor constantly decreased (stimulus less attractive) when the sessions are repeated.

## **3. Differences between the sound pressure fields around *Calliphora erythrocephala* and *Lucilia sericata***

In chapter III.2.3.1 the sound pressure field around the blowfly (*Calliphora erythrocephala*) was determined. The sound of the first harmonic was radiated in a dipole-like pattern (Fig. 25) whereas the second harmonic's shape was more rounded like that of a

monopole (Fig. 26). These results are in good agreement with those of Sueur et al. (2005) who determined similar shapes by evaluating the first and second harmonic for *Lucilia sericata*. As the pressure levels around *Calliphora erythrocephala* of the first harmonic were significantly higher than those of the second harmonic at all measured positions this result differs from that of Sueur et al. (2005) who stated that the first harmonic is only larger in front of the fly whereas the second harmonic is dominant on the sides. Both horizontal planes of the sound pressure field around the blowfly show a symmetric pressure field regarding the symmetry axis of the fly whereas Sueur et al. (2005) had slightly asymmetric results for *Lucilia sericata*.

#### 4. Differences between the flow fields generated by a stationary tethered, a manually moved and a freely flying blowfly

The flow field around the fly differed for all three cases studied.

(i) When flapping its wings a stationary fly generates a wake pointing downwards and backwards. The resulting impulse serves to move the fly forward and upwards against gravity (Fig. 31). Following the conservation of mass the surrounding air is sucked towards the front side of the wings (Fig. 30 and Fig. 31), a phenomenon reminiscent of a stationary ventilator which blows out air on one side and sucks air in at the other side.

Barth and Höller (1999) already reported this wake and measured mean air flow velocities of up to  $1 \text{ m s}^{-1}$  inside its cone-shaped volume. This value agrees well with the present measurements in five of six flies (up to  $1.2 \text{ m s}^{-1}$ ). One animal reached values of up to  $2.4 \text{ m s}^{-1}$ .

(ii) The flow field changed when the fly was manually moved forward at various horizontal velocities (Fig. 35). The changes depended on the velocity difference  $\Delta V$ , defined as  $\Delta V = V_{\text{pull}} - V_{\text{free}}$ , between the pulling speed ( $V_{\text{pull}}$ ) and the velocity the fly would have when flying freely ( $V_{\text{free}}$ ). As  $V_{\text{free}}$  could not be measured two pulling velocities ( $V_{\text{pull}}$ ) outside the flying speed range of the blowfly (determined by Schilstra and van Hateren 1999) were chosen to reach negative ( $V_{\text{pull}}$  clearly smaller than  $V_{\text{free}}$ ) and positive values ( $V_{\text{pull}}$  clearly larger than  $V_{\text{free}}$ ) for  $\Delta V$ . In this way it was possible to qualitatively determine the effects. As long as  $V_{\text{pull}}$  is definitely smaller than  $V_{\text{free}}$  ( $\Delta V$  negative) air is still sucked towards the wings from in front (Fig. 35a) as it is the case for a stationary tethered fly. The velocity of the suction flow increases with the absolute value of the negative  $\Delta V$  (compare Fig. 35a and b). When the fly is moved definitely faster than  $V_{\text{free}}$  ( $\Delta V$  positive) the air in front of the fly is pushed ahead of it (Fig. 35d) because more air is pushed away by the manually moved fly than the fly sucks by its wing beat to generate the wake.



The change of the flow field by pulling the fly with a velocity differing from  $V_{\text{free}}$  also affects the results of the behavioral experiments with a manually moved fly (chapter III.1 and III.2.2). This effect explains both the comparatively low jumping rates by the spider during the behavioral experiments and the comparatively large standard deviation of the fly's horizontal distance to the spider at the time of the prey capture jump (see chapter III.1).

How does the flow field around other insects look like when they are manually moved? To our knowledge no data exists in the literature where blowflies or other insects were manually moved forward as described above. Instead stationary tethered insects were exposed to laminar background flow in a wind tunnel. This situation can be compared to that of the tethered flying blowfly moved forward when the camera would be pulled at the same speed as the manual pulled blowfly. Therefore the stationary position of the camera in our experiment is compensated by subtracting the pulling velocity from the resulting velocity field afterwards which makes our results comparable to the following.

Dickinson and Götz (1996) investigated the flow field around the fruit fly *Drosophila melanogaster* whereas Barth et al. (1995) measured that around a blowfly. In both cases the fly was stationary and tethered in a wind tunnel which generated a laminar flow. A cone-shaped region pointing downwards and backwards from the fly which is directed more horizontally with increasing background flow (Barth et al. 1995). At background flow velocities of  $0.12 \text{ m s}^{-1}$  the flow velocities inside this cone were up to  $1 \text{ m s}^{-1}$  (Barth et al. 1995). Our results show as well cone-shaped region of increased velocities of up to  $1.5 \text{ m s}^{-1}$  when the fly is pulled at  $0.10 \text{ m s}^{-1}$ . Also the wake's angle with regard to the horizontal plane is increased at higher background velocities. Also Dickinson and Götz (1996) detected a similar shaped wake region with increased velocities of up to  $0.7 \text{ m s}^{-1}$  behind the fruit fly *Drosophila melanogaster* in the wind tunnel (background flow:  $0.2 \text{ m s}^{-1}$ ). The smaller velocities compared to the blowfly are due to the smaller size and weight of the fruit fly which needs less lift to overcome gravity than the blowfly. In addition the formation of a wake during the tethered flight of the hawkmoth *Manduca sexta* at various background velocities (Willmott et al. 1997) shows that also bigger sized insects (wingspan of about 10 cm) produce a wake pointing downwards and backwards to overcome gravity and move forward.

(iii) When the blowfly is flying freely, air is circulating around its front half as the wake now moves with the fly (see detailed description in chapter III.3.3.1). At various horizontal speeds between  $13$  and  $81 \text{ cm s}^{-1}$  the structure of the flow field did not qualitatively change during all 26 analyzed flights. This differs from the flow field around a tethered flying blowfly manually moved forward which changes considerably with the speed at which the fly is pulled forward. As mentioned above the reason for this discrepancy are differences between the pulling speed ( $V_{\text{pull}}$ ) and the velocity the fly would have when flying freely ( $V_{\text{free}}$ ) even when  $V_{\text{pull}}$  is in the range of  $V_{\text{free}}$  (Fig. 35b). The

conclusion is that only a freely flying blowfly can be used to properly investigate the flow around the flow sensors of *Cupiennius* generated by a fly.

As the circulating flow, investigated in front of the freely flying blowfly, could also be measured once in front of a blowfly manually moved forward (Fig. 35c) we assume that during this experiment the pulling speed was equal to the velocity the fly would have when flying freely ( $\Delta V = 0$ ).

The circulation around the blowfly increases the pressure below and causes a pressure drop above the fly. This leads to an additional lift (see wing theory).

Unfortunately, to our knowledge there are no other quantitative data in the literature describing the flow field around freely flying insects.

## 5. Detection of the blowfly

Before *Cupiennius* is able to successfully catch flying prey like a blowfly the victim must first be detected. To this end the signal must contain characteristic air flow patterns different from those of the background noise and the signal intensity must be above the sensory threshold.

### 5.1 Detection of a stationary humming blowfly

The air flow velocity generated by the humming of a stationary tethered blowfly 10 cm above the spider, differs from the background noise measured in the natural habitat (Barth et al. 1995) regarding its frequency content and fluctuations independent of the fly's horizontal position (from  $x = -10$  cm to  $x = +10$  cm; see Fig. 6). The background wind noise contains low frequencies up to 3 Hz with its peak at 0.05 Hz (Barth et al. 1995). The frequency content of the airflow generated by the humming of a stationary tethered blowfly was larger at all fly positions examined (from  $x = -10$  cm to  $x = +10$  cm; see Fig. 6). Even with the fly at position  $x = -10$  cm, where the lowest frequencies were found in the flow above the spider, the peak frequency was at 11 Hz. In addition the wind fluctuations (rms) are  $< 15\%$  with values around 2-3 % typical for unperturbed background flow (Barth et al. 1995). The fluctuations induced by a stationary tethered fly (Fig. 34) consistently exceeded these values. Even at the positions  $x = -10$  and  $x = -5$ , when the approaching fly is still behind the spider and therefore the spider is not directly exposed to the fluctuating wake of the fly, the values range between 23 % (above leg 3,  $x = -10$ ) and 97 % (above leg 4,  $x = -5$ ) (chapter III.3.1.2).

The trichobothria of *Cupiennius* detect air flow velocities between  $1 \text{ mm s}^{-1}$  and  $1 \text{ m s}^{-1}$  (Barth and Höller 1999). The air flow velocities generated by a stationary tethered blowfly (10 cm above the spider) are within that range at all horizontal distances of the fly examined (from  $x = -10$  cm to  $x = +10$  cm; see Fig. 6). In addition the air flow

around the spider was measured with the fly at  $x = -13.2$  cm (the largest horizontal distance where measurements in this setup could be taken). Even with the fly at this position the velocities above the spider's tarsi were as large as  $2.65 \text{ mm s}^{-1}$  above leg 4 and decreased to  $1.5 \text{ mm s}^{-1}$  above leg 1. Therefore action potentials occurring in all legs have to be expected (Barth and Höller 1999). Barth et al. (1995) determined the maximal horizontal distance of a stationary tethered humming blowfly positioned 10 cm above the spider where hunting behavior could be elicited to be 19 cm. However, different from our experiments, where the fly's front side was pointing towards the spider, in the study of these authors the fly pointed towards the spider with its abdomen which makes a direct comparison difficult.

## 5.2 Detection of a freely flying blowfly

Under more natural conditions with the blowfly flying freely the flow velocity at the sensor exceeds the physiological threshold (start of phase I) when the approaching fly is still at a horizontal distance of 4 cm (chapter III.3.3.2). This distance was independent of both the fly's horizontal flying speed and its altitude above the spider in all 19 flights ranging from 23 mm to 55 mm above the spider's tarsus (Fig. 38). When the freely flying blowfly passes above the horizontal substrate a characteristic flow field around the fly develops (Fig. 36). The flow velocities below the blowfly right above the substrate, where the spider's sensors are located, were above the physiological threshold (ca.  $1 \text{ mm s}^{-1}$ ) at all measured altitudes. Therefore the approaching fly's horizontal distance to the spider at the signal start is independent of the fly's altitude in between the measured values ranging from 23 mm to 55 mm. But this is certainly not generally the case for every altitude. For example with the fly located at an altitude of 1 m above the spider the flow velocities at the spider's sensors would not reach the physiological threshold at any horizontal distance of the fly.

By averaging the fly's horizontal velocity ( $41 \text{ cm s}^{-1}$ ) in 26 flights (Tab. 1) it takes 98 ms from beginning of the stimulation (onset of phase I) of the tarsal trichobothria of the leg pointing towards the fly until the fly is directly above this leg's tarsus (start of phase II) when the jump is generated. To decide if this time span is sufficient for the spider to start the jump in time, it is compared with latency experiments by Brittinger (1998) in which spiders were stimulated with a synthetic air flow source that elicited prey capture behavior. For subadult spiders the time between the turning-on of the stimulation source (positioned 0.5 cm away from the stimulated trichobothria) and the onset of a behavioral response was 88 ms (Brittinger 1998). As the time difference between the turning-on of the stimulus source and the arrival of the air flow at the trichobothria (0.5 cm away from the source) was measured to be 50 ms (Ungersböck 2004) the latency between the arrival of the flow signal at the trichobothria and the onset behavioral response was 38 ms. This implies that the time span of 98 ms between the

onset of stimulation (start of phase I) of the trichobothria on the tarsus and the beginning of the jump (at the start of phase II) is sufficient for the spider to elicit the prey capture jump in time, that is when the fly is above it.

Although under field conditions the background noise contains flow velocities typically below  $0.1 \text{ m s}^{-1}$  (Barth et al. 1995), which are in the range of the velocity signal generated by a flying fly (phase I: 0 to  $0.16 \text{ m s}^{-1}$ , Tab. 1), it differs regarding its time dependent progression, frequency content and fluctuations (rms) from that of the freely flying blowfly. The characteristic exponential velocity increase during phase I of the flow signal induced by an approaching blowfly (Fig. 37a) differs from the much more steady background wind (Barth et al. 1995). In addition the frequency spectrum of the background wind noise contains low frequencies up to 3 Hz with a peak at 0.05 Hz whereas frequencies up to 50 Hz with a mean frequency peak at 8.2 Hz characterize the velocity signal of phase I. However, the peak frequencies of phase I and phase II (17.9 Hz) are not in the pronounced tuning range between 50 and 120 Hz measured by Barth and Höller (1999). There are also differences in the degree of fluctuation of both air flows. Unperturbed background flow fluctuates by 2-3 % (Barth et al. 1995) whereas fluctuations around the exponentially increasing velocity signal are 33 % rms by referring to the mean velocity of phase I. As the trichobothria are very sensitive to flow accelerations (Barth and Höller 1999) more action potentials will be generated with increasing flow fluctuations. Therefore the spider is more attracted to the higher fluctuating flow velocities of the blowfly than compared to the low fluctuating background flow. This leads to the conclusion that the spider is able to detect the blowfly with its trichobothria in the presence of background wind noise.

In addition behavioral experiments, in which the spider was stimulated with the flow signal contained in phase I, showed reactions of the spider towards the approaching stimulus (chapter III.4.2). This is taken as evidence that the spider detects the blowfly during phase I.

No further statements regarding the sensory response to the background noise and fly signal can be made as there are no electrophysiological threshold measurements of the trichobothria available below 10 Hz. The exponential increase of the threshold from 100 Hz to 10 Hz (compare Barth and Höller 1999, Fig. 9) suggests a continuing exponential increase for lower frequencies than 10 Hz. This would be reasonable in the context of background noise filtering.

## 6. Recognition of the blowfly

As the jump is elicited at the start of phase II (chapter III.3.3.2) *Cupiennius* must be able to recognize the flying blowfly as prey either during phase I or at the transition between phases I and II. In contrast to the mere detection of a source, following from any reac-

tion of the spider at the right time, we could not precisely determine the point in time of recognition nor the flow pattern which is responsible for it (e.g. as prey or predator). However, behavioral experiments with flow patterns contained in phase I (chapter III.4.2) often showed a directed reaction towards the approaching source, when the leg closest to the approaching source twitched or was lifted. Although this is not an explicit evidence this reaction may indicate a successful recognition as it is directed towards the approaching source when the source is located above the tarsus of the closest leg. At this point in time the spider usually jumps towards the approaching blowfly.

Additional to be above threshold and differ from background noise, as it is important for detection, the velocity signal of the prey must contain at least one parameter which differs from the flow signal of nonprey in the habitat for a successful recognition. The decisive parameter regarding substrate vibrations eliciting attack or escape behavior of *Cupiennius* are frequency and amplitude of the vibration (Hergenröder and Barth 1983a). With both increasing frequency and amplitude the probability of an escape behavior increases (Hergenröder and Barth 1983a). Likewise the back swimmer *Notonecta glauca* L. (Lang 1980), the surface-feeding fish *Aplocheilichthys lineatus* (Bleckmann 1980) and the semi-aquatic spider *Dolomedes triton* (Bleckmann and Barth 1984) distinguish between prey and nonprey using the frequency content of the vibrations received. Both amplitude and frequency (fluctuations) might be also decisive for the discrimination of air flow signals.

Comparisons with air flows produced by other animals in the habitat of *Cupiennius* are difficult due to the lack of data in the literature. A comparison to air flows generated by predators of *Cupiennius salei* would be of particular interest because most likely they are detected by the trichobothria as well (Barth 2002). The caterpillar *Barathra brassicae* uses its filiform hairs to escape from the parasitic wasp *Dolichovespula media* by simply dropping down from the leaf it sits on (Tautz and Markl 1978).

So far predatory wasps (*Pompilidae*), parasitic Neuroptera (*Mantispidae*), a bird (*Oropendola*) and some reptiles are known to catch *C. salei* (Barth 2002). *Pompilidae* paralyze the spider and use it as food for their larvae (Barth 2002). Larvae of *Mantispa viridis* invade the egg sac of *Cupiennius* (Milliron 1940) either during its construction or when the spider is already carrying it around with the eggs in it (Roble 1986). They feed from the spider eggs till they hatch as adults (Bruchwein et al. 1992). *Oropendola* approaches the shelter of *Cupiennius* between leafs and uses its solid bill to widen the narrow spaces between the leaves where the spider hides in order to catch it (Barth pers. comm.).

How do those predators approach *Cupiennius* and what flows are induced by the predators? Unfortunately there is no explicit literature available. The larvae of *Mantispa viridis* approach the egg sac by creeping and the day active *Oropendola* uses its bill while

sitting on a leaf or branch to catch *Cupiennius*. Reptiles approach the spider by running. As there is no literature from which to know whether the predatory wasp (*Pompilidae*) approaches the spider by running or flying (rather running, Barth pers. comm.) most of the predators – if not all – seem to approach on the ground.

An animal that moves on the ground causes airflow. The shape of this flow field will certainly differ from that generated by flying animals. The maximum air flow velocity in the range of some  $\text{cm s}^{-1}$  occurs directly in front of the approaching animal and decays exponentially with increasing horizontal distance (Gnatzy and Kämper 1990; Dangles et al. 2006; Casas et al. 2008). The air flow velocity in front of a running wolf spider (*Pardosa lugubris*) decays within a distance of only 3 mm by 50 % and at a distance of 15 mm the velocity signal is reduced to  $1 \text{ mm s}^{-1}$  (sensory threshold of *Cupiennius*) (Casas et al. 2008). The digger wasp (*Liris niger*) induces peak air particle velocities of  $1\text{--}2 \text{ cm s}^{-1}$  close to its body when approaching its prey (crickets) (Gnatzy and Kämper 1990). Only frequency components below 50 Hz could be measured, with increasing intensities towards lower frequencies, especially below 10 Hz (Gnatzy and Kämper 1990). In the concentrated wake region of the freely flying blowfly the flow field with highly fluctuating flow velocities of up to  $1 \text{ m s}^{-1}$  markedly differs from that of a running animal where the maximum flow velocities are in the range of some  $\text{cm s}^{-1}$  only (Gnatzy and Kämper 1990; Dangles et al. 2006; Casas et al. 2008). However, most likely *Cupiennius* detects running predators first by the plant vibrations they produce. These propagate much faster (e.g. between 5 and  $55 \text{ m s}^{-1}$  on *Agave Americana*, Wirth 1984). In addition the spider can detect them at a larger distance than the low velocity air flow signal. For example the average attenuation of bending waves is  $0.35 \text{ dB cm}^{-1}$  on a banana plant (Barth et al. 1988) which corresponds to a 50 % decrease of the deflection at a distance of 17 cm whereas the air flow rapidly decreases within a cm or two.

Regarding prey *Cupiennius* is relatively unselective (Barth 2002). It captures everything which it can overcome (flies, cockroaches, earwigs, crickets, grasshoppers and moths). Occasionally it could be observed eating frogs and lizards (Barth 2002). The prey of *Cupiennius* mostly consists of animals that walk on the ground. It is detected first by plant vibrations and after that by its air movements when the prey animal is within 1–3 cm of a spider leg (Barth 2002). Although cockroaches, earwigs, crickets, grasshoppers are able to fly they are mostly walking on the ground where they are captured by *Cupiennius*. Moths are the only prey, beside flies, that rather fly than walk. Therefore a comparison between the airflow around these two insects is of major interest. The only moth around which the flow field is described is the hawkmoth *Manduca sexta* (Willmott et al. 1997). Although *Manduca sexta* is not known as prey of *Cupiennius* (Barth pers. comm.) as well as it is bigger than moths which *Cupiennius* captures, the general morphology of both is similar. Despite a wing span 5 times larger, a mean flying speed



4.4 times higher (Stevenson et al. 1995) and a wing beat frequency 6 times smaller (Heinrich 1971) than for a blowfly, the moth also generated a wake of increased velocity pointing downwards and backwards from its abdomen (Willmott et al. 1997) which is qualitatively alike to that of the blowfly (Barth et al. 1995; chapter III.3.1 and III.3.2). Therefore it is most likely that also the flow field around a freely flying hawkmoth contains the same three phases that are induced by a freely flying blowfly when passing above the spider (see chapter III.3.3). Especially phase I and the transition to phase II of the flow might be the stimulus which is important to for a recognition as the spider jumps when the trichobothria of the leg closest to the approaching fly detect the onset of phase II.

## 7. Localization of the flying blowfly

After the fly has been detected and recognized the spider must be able to exactly localize it to time the prey capture jump successfully. In addition to the fly's position its velocity provides extra problems and therefore information on the speed of its approach must be determined by the spider as well to warrant a successful prey capture.

### 7.1 Position

When *Cupiennius* is ready for prey capture it lifts the body slightly above the substrate and keeps its legs in typical positions forming uniformly distributed radii of a full circle (Hergenröder and Barth 1983b; Brittinger 1998). The spatial threshold from where a fly can be detected by the spider only depends on distance and is independent from direction (Barth et al. 1995; Brittinger 1998). Or in other words: the spider can detect flies in every horizontal direction equally well (Barth et al. 1995).

#### 7.1.1 Horizontal distance

*Cupiennius* is able to sense the approaching blowfly when the fly is still around 4 cm in front of the tarsus of the spider's closest leg (chapter III.3.3.2). When the blowfly passes above the spider the fly generates a characteristic air flow signal close to the trichobothria which is composed of three phases (Fig. 37a). The occurrence of the three phases corresponds to the horizontal position of the fly relative to the spider. The start of the flow signal (phase I) as well as the transition between phases I and II are independent of both the fly's altitude and horizontal speed. As the spider starts its prey capture jump when the fly is directly above the tarsus of the leg pointing towards the approaching fly it must be able to measure and evaluate the horizontal distance of the prey at this location. Behavioral experiments (chapter III.4.2) show that the spider reacts to but does not jump towards the source of the flow of phase I. So the spider must at least be able to sense that during phase I the fly is approaching but not close enough for a

jump. Receiving the distance-dependent signal at over 900 individual sensors spread over a circular area of up to 12 cm in diameter the spider has a big redundancy and refinement of the distance information.

Also fish evaluate the velocity information of flow fields in water to localize prey (Coombs 1999; Kanter and Coombs 2003). Franosch et al. (2005) and Goulet et al. (2008) present a model in which fish are able to predict the horizontal distance of prey by evaluating the positions at the lateral line canal where either extreme values (minimum and maximum) or zero crossings of the flow velocities occur. The distance to the prey is linearly dependent on the distance between the positions at the lateral line canal where these values appear. The air flow around *Cupiennius* generated by a freely flying blowfly features indeed extreme values and zero crossings in its wake region. However, as these values only appear temporally and spatially erratic at the trichobothria the distances between these positions are not linearly dependent on any distance of the flying prey. Consequently *Cupiennius* is not able to evaluate the horizontal distance of the flying prey by this mechanism.

### 7.1.2 Direction

Behavioral experiments described in chapter III.4.2 show that *Cupiennius* is able to sense the direction from which the fly is approaching. By exposing the spider to the air flow contained in phase I it twitches with those legs first which point into the direction of the approaching stimulus. Most likely the spider either uses time differences of the signal start or intensity differences of the flow velocities between different sensors located on different legs. A combination of both strategies is possible as well.

#### 7.1.2.1 Time differences

Due to the dispersed arrangement of the sensors all around the spider body, differences in the time of signal arrival at the different legs (and possibly even at different positions at one leg) (Fig. 40) can be used by *Cupiennius* to identify the azimuth to the signal source (Brittinger 1998; Barth 2002). If the time difference of the signal arrival between different legs is  $\geq 50$  ms the spider turns significantly more often to that leg which receives the signal first (Brittinger 1998). But even at differences of 10 ms the spider turns more often towards the leg stimulated first (Brittinger 1998). When a freely flying blowfly passes above a *Cupiennius* of 7.5 cm leg span, between leg 1 on one and leg 4 on the opposite side, the time difference of the arrival between the tarsi of leg 1 and 4 on the same side (5.8 cm horizontal distance) is  $86 \text{ ms} \pm 19 \text{ ms}$  (chapter III.3.3.2). This time span suffices to enable the spider to turn significantly more often into the direction of the first stimulus (Brittinger 1998). Even the time delays for neighboring legs which vary from  $20 \text{ ms} \pm 4 \text{ ms}$  (leg 2 tibia  $\leftrightarrow$  leg 3 tibia) to  $34 \text{ ms} \pm 8 \text{ ms}$  (leg 1 tarsus  $\leftrightarrow$  leg 2

tibia) enable the spider to turn more often towards the direction of the first stimulus (Brittinger 1998).

Time differences also play a role for the detection of substrate vibrations. *Cupiennius* turns towards the first stimulus when different legs are stimulated with a time difference of 4 ms only (Hergenröder and Barth 1983b). According to Wirth (1984) even a time delay of 2 ms is enough for most spiders to turn towards the leg which was stimulated first.

In scorpions (*Paruroctonus mesaensis*) the time delay between the arrival of substrate vibrations at different tarsi (where the vibration sensors are located) is the most important cue for determining the direction to a distant signal source as well (Brownell and Farley 1979). Between the tarsi closest and farthest away from the source the conduction time of a surface wave in sand is about 1 ms. For this reason the scorpion has to resolve even smaller time delays than *Cupiennius*. The scorpion can detect time delays as small as 0.2 ms but it is maximally sensitive to 0.8 to 1 ms delays (Brownell and Farley 1979). Time differences are also used for orientation based on acoustic stimuli. Grasshoppers (*Chorthippus biguttulus*) turn towards the first acoustic signal at time differences as small as 0.5 ms (von Helversen and Rheinlaender 1988; von Helversen 1997) and humans can resolve acoustic time differences as small as 5  $\mu$ s (Heldmaier and Neuweiler 2003).

#### 7.1.2.2 Intensity differences

In addition to time differences intensity differences maybe used to orient towards the signal source. When simultaneously applying substrate vibrations of different intensity ratios ranging from 2:1 to 16:1 at different legs, the scorpion (*Paruroctonus mesaensis*) always turns towards the larger intensity (Brownell and Farley 1979). The turning was most accurate for amplitude ratios between 3:1 and 5:1. Intensity differences are also used for orientation to acoustic stimuli. Grasshoppers (*Chorthippus biguttulus*) turn towards the louder acoustic signal at intensity differences as small as 1 dB (von Helversen and Rheinlaender 1988; von Helversen 1997). Also humans are able to resolve acoustic intensity differences as small as 1 dB (Zenner 1994).

In contrast to the complicate spatial propagation of leaf vibrations in plants (see below) air flow velocities decrease with increasing distance from the source due to friction. Therefore they may be used by the spider to determine the direction to the source of the air flow. The maximum air flow velocity ratios simultaneously measured between different legs during phase I (freely flying blowfly passing above the spider) range from 2.2:1 to 6.5:1 (chapter III.3.3, Tab. 1). As these values are in the same range as those discussed above and below (acoustics of grasshoppers and humans as well as substrate vibrations of both scorpions and spiders) it may be quite possible, that intensity differences are used by the spider to evaluate the direction of an approaching flying prey.

To our knowledge so far no other data exists regarding air flow intensity (velocity) differences at different legs of *Cupiennius* (or any other animal). Concerning the detection of intensity differences between substrate vibrations by its slit sensilla there is only few data. By stimulating two legs with different oscillation amplitudes (ratio 3.3:1) *Cupiennius* turns towards the greatest intensity (Hergenröder and Barth 1983b). However, the vibration amplitudes, measured on leafs that *Cupiennius* favors, do mostly not decrease constantly with distance from the signal source. Complicated frequency dependent spatial patterns are formed instead (Wirth 1984) which complicate a correct determination of the direction by intensity differences. This leads to the conclusion that *Cupiennius* mainly uses time differences of leaf vibrations to determine the direction of the source whereas intensity differences of leaf vibrations due to their leaf-dependent propagation most likely only provide additional information.

### 7.1.3 Altitude

Hydrodynamic stimuli get blurred with increasing distance (Goulet et al. 2008). This is to some extend identical to visional stimuli where blur acts as a pictorial depth cue (O'Shea et al. 1997; Goulet et al. 2008). There may be a similar key for estimating the vertical distance (altitude) of a flying blowfly. In the case of air flow the parameter for blur could be the velocity fluctuation of the flow. The fluctuation contained in the velocity signal before the spider jumps (phase I) towards a freely flying blowfly increases linearly with the fly's altitude (Fig. 44). As this data is independent from the individual fly used as well as other factors like the horizontal speed of the fly and the exponential coefficient of the velocity in phase I, the velocity fluctuations of phase I contain enough information to resolve on a theoretical basis the altitude of the passing blowfly. The fact that the sensors are very sensitive to air flow fluctuations (Barth and Höller 1999) supports this hypothesis.

## 7.2 Horizontal fly velocity

Obviously catching a flying blowfly is a very difficult task necessitating a very precise localization of the prey. Furthermore as the fly changes its position fast, knowledge of the fly's velocity should be in favor of a successful prey capture. The horizontal velocity of the approaching fly is reflected by the time of arrival differences of the signal ( $\Delta t$ ) at different legs (Fig. 41). As expected  $\Delta t$  decreases linearly with increasing horizontal flight velocity. Because these time differences are larger than 50 ms *Cupiennius* is able to resolve them (Brittinger 1998). In addition the steepness of the exponential increase of the velocity in phase I increases linearly with increasing horizontal flight velocity (Fig. 43) giving the spider another possibility to resolve it. Both  $\Delta t$  and the steepness of the exponential velocity increase are independent from the

altitude and the approaching direction of the fly and so the evaluation of each of both parameters is sufficient to clearly determine the horizontal fly speed.

Fish and frogs are also thought to use their lateral line canal system to extract prey velocity. Franosch (2005) presents a theoretical model which enables *Xenopus* to resolve the prey's speed in water by evaluating the flow velocity at its lateral line canals.

## 8. Prey capture: Triggering the jump

When the spider jumps the approaching fly is located directly above the leg closest to (and pointing towards) the fly (see chapter III.1). Exactly at this point in time the flow pattern at the sensors of this leg changes from phase I to the much more fluctuating air flow of phase II (chapter III.3.3.2). The hypothesis that the jumping motion is triggered when the spider receives the fluctuating air flow signal of phase II is supported by the behavioral experiments described in chapter III.4.2. The spider does not respond anymore with a prey capture jump when phase II of the fly flow signal is missing.

Finally, the main results from this work are summarized in Fig. 52 which shows the flow parameters with which *Cupiennius* is theoretically able to detect, recognize, and localize flying prey and to trigger the jump. Basically five stimulus parameters suffice: velocity magnitude, velocity fluctuation, velocity gradient, time difference and intensity difference.

These results may also help to develop an artificial flow sensor detecting and localizing a source of air flow or water flow. It should be able to analyze each of the five flow parameters described in Fig. 52 because the basic questions for orientation (detection, recognition, localization and capturing (tracking) of a moving target) are also crucial for these sensors.

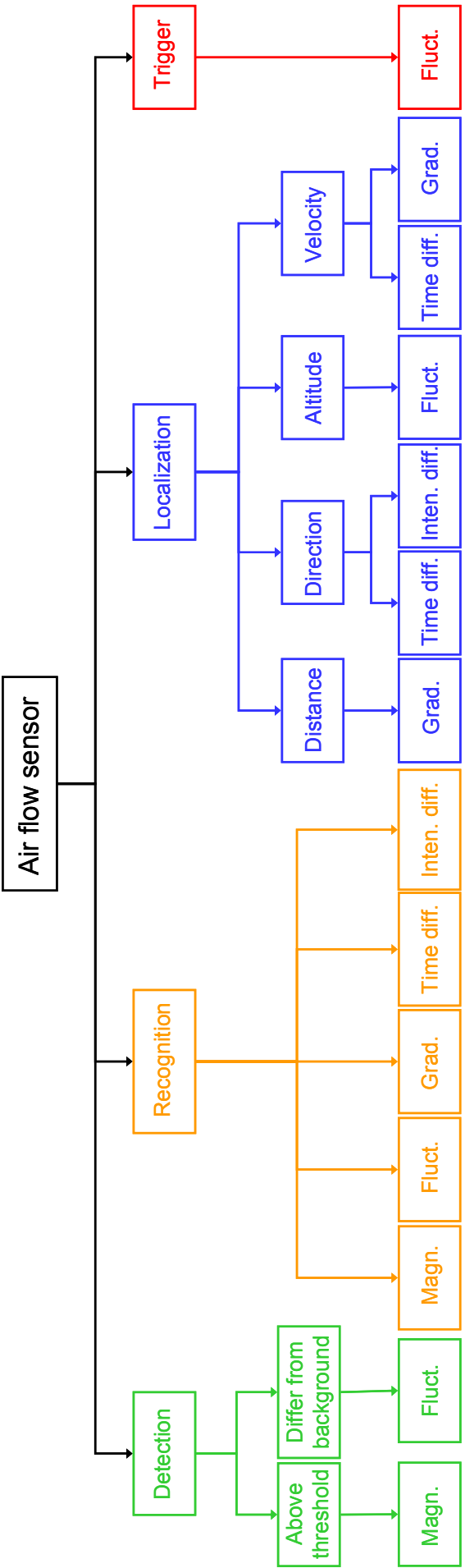


**Fig. 52** Overview of the flow parameters contained in the air flow generated by a freely flying blowfly with which the spider is thought to be able to detect, recognize and localize the fly and to finally trigger its jump towards flying prey. The flow parameters are: velocity magnitude (Magn.), velocity fluctuation (Fluct.), velocity gradient (Grad.), time difference (Time diff.) and intensity difference (Inten. diff.).



## REFERENCES

- Barth FG, Geethabali (1982) Spider vibration receptors. Threshold curves of individual slits in the metatarsal lyriform organ. *J Comp Physiol A* 148:175-185
- Barth FG, Bleckmann H, Bohnenberger J, Seyfarth E-A (1988) Spiders of the genus *Cupiennius* SIMON 1891 (Araneae, Ctenidae). II. On the vibratory environment of a wandering spider. *Oecologia* 77:194-201
- Barth FG, Wastl U, Humphrey JAC, Devarakonda R (1993) Dynamics of arthropod filiform hairs. II. Mechanical properties of spider trichobothria (*Cupiennius salei* KEYS.). *Phil Trans R Soc Lond B* 340:445-461
- Barth FG, Humphrey JAC, Wastl U, Halbritter J, Brittinger W (1995) Dynamics of arthropod filiform hairs. III. Flow patterns related to air movement detection in a spider (*Cupiennius salei* Keys.). *Phil Trans R Soc Lond B* 347:397-412
- Barth FG, Höller A (1999) Dynamics of arthropod filiform hairs. V. The response of spider trichobothria to natural stimuli. *Phil Trans R Soc Lond B* 354:183-192
- Barth FG (2002) A spider's world. Senses and behavior. Springer, Berlin Heidelberg New York
- Barth FG (2003) Sensors and sensing: a biologist's view. In: Barth FG, Humphrey JAC, Secomb TW (eds) *Sensors and sensing in biology and engineering*. Springer, Wien New York, pp 3-15
- Birch JM, Dickson WB, Dickinson MH (2004) Force production and flow structure of the leading edge vortex on flapping wings at high and low Reynolds numbers. *J Exp Biol* 207:1063-1072
- Bleckmann H (1980) Reaction time and stimulus frequency in prey localization in the surface-feeding fish *Aplocheilichthys lineatus*. *J Comp Physiol A* 140:163-172
- Bleckmann H, Barth FG (1984) Sensory ecology of a semi-aquatic spider (*Dolomedes triton*): II. The release of predatory behavior by water surface waves. *Behav Ecol Sociobiol* 14:303-312
- Bomphrey RJ, Lawson NJ, Harding NJ, Taylor GK, Thomas ALR (2005) The aerodynamics of *Manduca sexta*: digital particle image velocimetry analysis of the leading-edge vortex. *J Exp Biol* 208:1079-1094
- Brodsky AK (1994) The evolution of insect flight. Oxford University Press

- Brownell P, Farley RD (1979) Orientation to vibrations in sand by the nocturnal scorpion *Paruroctonus mesaensis*: Mechanism of target localization. J Comp Physiol A 131:31-38
- Brushwein JR, Hoffman KM, Culin JD (1992) Spider (*Araneae*) taxa associated with *Mantispa viridis* (Neuroptera: Mantispidae) J Arachnol 20:153-156
- Brittinger W (1998) Trichobothrien, Medienströmung und das Verhalten von Jagdspinnen (*Cupiennius salei* Keys.). Dissertation, Universität Wien
- Cambridge Electronic Design Limited (CED) (2004) Spike2 for Windows version 5, manual
- Casas J, Steinmann T, Dangles O (2008) The aerodynamic signature of running spiders. PLoS ONE 3(5): e2116. doi:10.1371/journal.pone.0002116
- Chapman RF (1998) The insects: structure and function. Cambridge University Press, New York
- Cheung YK, Klotz JH (1997). The Mann Whitney Wilcoxon distribution using linked lists. Statistica Sinica 7:805-813.
- Coombs S (1999) Signal detection theory, lateral-line excitation patterns and prey capture behaviour of mottled sculpin. Anim. Behav. 58:421–430
- Dahl F (1883) Über die Hörhaare bei den Arachniden. Zool Anz 6:267-270
- Dangles O, Ory N, Steinmann T, Christides JP, Casas J (2006) Spider's attack vs. cricket's escape: velocity modes determine success. Anim Behav 72: 603–610
- Dickinson MH, Götz KG (1996) The wake dynamics and flight forces of the fruit fly *Drosophila melanogaster*. J Exp Biol 199:2085-2104
- Dickinson MH, Lehmann F-O, Sane S (1999) Wing rotation and the aerodynamic basis of insect flight. Science 284:1954-1960
- Dring RP (1982) Sizing criteria for laser anemometry particles. J Fluids Eng 104:15-17
- Ellington CP, van den Berg C, Willmott AP, Thomas ALR (1996) Leading-edge vortices in insect flight. Nature 384:626 - 630
- Franosch J-MP, Sichert AB, Suttner MD, van Hemmen JL (2005) Estimating position and velocity of a submerged moving object by the clawed frog *Xenopus* and by fish—a cybernetic approach. Biol Cybern 93:231–238
- Gnatzy W, Kämper G (1990) Digger wasp against crickets. II. An airborne signal produced by a running predator. J Comp Physiol A 167: 551-556

- Goulet J, Engelmann J, Chagnaud BP, Franosch J-MP, Suttner MD, van Hemmen JL (2008) Object localization through the lateral line system of fish: Theory and experiment. *J Comp Physiol A* 194:1-17
- Heinrich B (1971) Temperature regulation of the sphinx moth, *Manduca sexta*: I. Flight energetics and body temperature during free and tethered flight. *J Exp Biol* 54:141-152
- Heldmaier G, Neuweiler G (2003) Vergleichende Tierphysiologie. Bd. 1: Neuro- und Sinnesphysiologie. Springer, Berlin Heidelberg New York
- von Helversen D, Rheinlaender J (1988) Interaural intensity and time discrimination in an unrestrained grasshopper: a tentative approach. *J Comp Physiol A* 162:333-340
- von Helversen (1997) Acoustic communication and orientation in grasshoppers. In: Lehrer M. (ed) Orientation and communication in arthropods. Birkhäuser, Basel Boston Berlin, pp 301-341
- Hergenröder R (1982) Vibratorische Signale und Beutefang bei einer Jagdspinne: zur Neurobiologie eines Verhaltens (*Cupiennius salei* Keys.). Dissertation, Frankfurt am Main
- Hergenröder R, Barth FG (1983a) The release of attack and escape behavior by vibratory stimuli in a wandering spider (*Cupiennius salei* Keys.). *J Comp Physiol A* 152:347-358
- Hergenröder R, Barth FG (1983b) Vibratory signals and spider behavior: How do the sensory inputs from the eight legs interact in orientation? *J Comp Physiol A* 152:361-371
- Hollander M, Wolfe DA (1999) Nonparametric statistical methods, Second Edition. John Wiley and Sons, New York
- Humphrey JAC, Devarakonda R, Iglesias J, Barth FG (1993) Dynamics of arthropod filiform hairs. I. Mathematical modelling of the hair and air motions. *Phil Trans R Soc Lond B* 340:423-444
- Humphrey JAC, Devarakonda R, Iglesias I, Barth FG (1998) Errata re. Humphrey et al. 1993. *Phil Trans R Soc Lond B* 352:1995
- Humphrey JAC, Barth FG, Reed M, Spak A (2003) The physics of arthropod medium-flow sensitive hairs: Biological models for artificial sensors. In: Barth FG, Humphrey JAC, Secomb TW (eds) Sensors and sensing in biology and engineering. Springer, Wien New York, pp 129-144

- Kanmiya K (2005) Communication by vibratory signals in Diptera. In: Drosopoulos S, Claridge MF (eds) Insect sounds and communication. Physiology, behaviour, ecology, and evolution. CRC Press, Boca Raton, pp 381-396
- Kanter MJ, Coombs S (2003) Rheotaxis and prey detection in uniform currents by Lake Michigan mottled sculpin (*Cottus bairdi*) J Exp Biol 206:59-70
- Klopsch C, Barth FG, Humphrey JAC (2007) The air flow generated by a flying prey insect around a wandering spider and its motion-sensing hair sensilla. Proc of the 5<sup>th</sup> International Symp Turbulence and Shear Flow Phenomena, TU Munich, August 27-29, 3:1023-1028
- Lang HH (1980) Surface wave discrimination between prey and nonprey by the back swimmer *Notonecta glauca* L. (Hemiptera, Heteroptera). Behav Ecol Socio-biol 6:233-246
- Lehmann EL (1975) Nonparametrics: statistical methods based on ranks. Holden-Day, San Francisco
- Lehmann F-O, Sane SP, Dickinson MH (2005). The aerodynamic effects of wing-wing interaction in flapping insect wings. J Exp Biol 208:3075-3092
- Melchers M (1963) Zur Biologie und zum Verhalten von *Cupiennius salei* (Keyserling), einer amerikanischen Ctenide Zool Jb Syst 91:1-90
- Melchers M (1967) Der Beutefang von *Cupiennius salei* Keyserling (Ctenidae). Z Morph Ökol Tiere 58:321-346
- Milliron HE (1940). The emergence of a neotropical mantispid from a spider egg sac. Ann Entomol Soc America 33:357-360
- Nachtigall W (2003) Insektenflug: Konstruktionsmorphologie, Biomechanik, Flugverhalten. Springer, Berlin Heidelberg New York
- O'Shea RP, Govan DG, Sekuler R (1997). Blur and contrast as pictorial depth cues. Perception 26:599-612
- Rehner N (1978) Zur Orientierung einer Jagdspinne beim Beutefang. Diplomarbeit, Goethe Universität Frankfurt am Main
- Roble SM (1986) A new spider host association for *Mantispa viridis* (Neuroptera, Mantispidae). J Arachnol 14:135-136
- Sane SP (2003) The aerodynamics of insect flight. J Exp Biol 206:4191-4208
- Schilstra C, van Hateren JH (1999) Blowfly flight and optic. I. Thorax kinematics and flight dynamics. J Exp Biol 202:1481-1490
- Siegel S, Castellan NJ (1988). Nonparametric statistics for the behavioral sciences, Second Edition. McGraw-Hill, New York

- Stevenson R, Corbo K, Baca L, Le Q (1995) Cage size and flight speed of the tobacco hawkmoth *Manduca sexta*. J Exp Biol 198:1665-1672
- Sueur J, Tuck EJ, Robert D (2005) Sound radiation around a flying fly. J Acoust Soc Am 118:530-538
- Tautz J, Markl H (1978) Caterpillars detect flying wasps by hairs sensitive to airborne vibration. Behav Ecol Sociobiol 4:101-110
- Ungersböck S (2004) Zur Ontogenie der Orientierung nach Luftströmungsreizen bei *Cupiennius salei*. Diplomarbeit, Universität Wien
- Vogel S (1966) Flight in *Drosophila*: I. Flight performance of tethered flies. J Exp Biol 44:567-78
- Vogel S (1967a) Flight in *Drosophila*: II. Variations in stroke parameters and wing contour. J Exp Biol 46:383-392
- Vogel S (1967b) Flight in *Drosophila*: III. Aerodynamic characteristics of fly wings and wing models. J Exp Biol 46:431-443
- Walla P, Barth FG, Eguchi E (1996). Spectral sensitivity of single photoreceptor cells in the eyes of the ctenid spider *Cupiennius salei* Keys. Zoological Science 13:199-202
- Wilcoxon F (1945) Individual comparisons by ranking methods. Biometrics 1:80-83
- Willmott AP, Ellington CP, Thomas ALR (1997) Flow visualization and unsteady aerodynamics in the flight of the hawkmoth, *Manduca sexta*. Phil Trans R Soc Lond B Biol Sci 352:303-316
- Wirth E (1984) Die Bedeutung von Zeit- und Amplitudenunterschieden für die Orientierung nach vibratorischen Signalen bei Spinnen, Diplomarbeit, Universität Frankfurt
- Zenner H-P (1994) Hören. Physiologie, Biochemie, Zell- und Neurobiologie. Thieme, Stuttgart

# CURRICULUM VITAE

## Persönliche Daten

Name: Christian Klopsch  
Adresse: Gschwandnergasse 42/7  
1170 Wien  
Telefon: 0650/ 527 66 88  
E-Mail: [christian.klopsch@univie.ac.at](mailto:christian.klopsch@univie.ac.at)  
Geburtstag: 29.06.1979  
Geburtsort: Regensburg  
Staatsangeh.: deutsch  
Familienstand: ledig



## Ausbildung

10.2006 – heute Doktoratsstudium der technischen Wissenschaften am Institut für Strömungsmechanik und Wärmeübertragung, Technische Universität Wien interdisziplinär mit dem Department für Neurobiologie, Universität Wien

09.2004 – 02.2005 Diplomarbeit am Lehrstuhl Windkanal/Strömungsmesstechnik, Fachhochschule Regensburg  
Titel: „Experimentelle Bestimmung des Geschwindigkeitsfeldes an einem Aneurysma-Modell“

10.2000 – 03.2005 Studium an der Fachhochschule Regensburg, Studiengang Maschinenbau, Schwerpunkt: Fahrzeugtechnik  
Abschluss: Dipl.-Ing. (FH)

1990 – 1999 Werner-von-Siemens-Gymnasium Regensburg  
Abschluss: Abitur

1986 – 1990 Gerhardinger Grundschule Regensburg

## Zivildienst

07.1999 – 06.2000 Tätigkeit im Pflegedienst der Herz-Thorax-Station, Universitätsklinik Regensburg